1-70-01787

Bell Aerospace Company DIVISION OF textron

POST OFFICE BOX 1 BUFFALO NEW YORK 14240

FINAL REPORT FOR CONTRACT NAS 12-2074

DIGITAL FLIGHT CONTROL and LANDING SYSTEM for the CH-46C HELICOPTER

REPORT NO 6200-933013

MAY 1970

By

William Cockayne
Walter Rusnak
Lionel Shub

For

NASA/Electronic Research Center

Cambridge, Mass

CONTENTS

CONTENTS (CONT)

ILLUSTRATIONS

TABLES

I INTRODUCTION

On February 27, 1969, NASA/ERC, Cambridge, Mass , awarded Contract No 12-2074 to Bell Aerospace Company to perform an analytical and hybrid simulation study of a Digital Flight Control and Landing System (DFCLS) for the CH-46 Helicopter This study was to be preliminary to the testing and demonstration of such a system aboard the CH-46C helicopter at NASA/Langley Research Center In June 1969, BAC was awarded a second contract by NASA/ERC to perform the system integration and hardware assembly required to perform the testing and demonstration of the flight control and landing system Both of these programs were part of NASA's V/STOL program designed to demonstrate the technologies required for the navigation, guidance and control of V/STOL vehicles

This report is on the first of these study programs The principal output of this study was to be a flight control system design including specifications on input data, output data and display requirements and with a definition of the control laws over the flight regime The flight control system was to be a flexible, multi-mode, experimental system suitable for evaluation by flight testing of control, display and guidance concepts related to landings of V/STOL under minimum visibility conditions The flight control system was to include a number of manual modes and their displays to investigate velocity, attitude and attitude rate controls as well as a fully automatic mode

It was an objective, to demonstrate the flight control system in automatic approach and landing In this connection, it was a secondary objective of the program to define and evaluate by simulation the guidance laws required to perform this approach and landing Included in this task was the requirement to supply displayed information suitable for the pilot to perform the landing in each of the manual flight control modes

NASA/ERC defined a base line system which included a central digital airborne computer, a strapdown navigation system, a ground based GSN-5 radar and a digital telemetry link These equipments were to be combined to form an integrated approach and landing system using the central digital computer to perform all computations However, the flight control and guidance laws developed in this study, are valid, independently of this hardware definition since these laws are specified in terms of input and output data requirements These data requirements formed the basis for specifying the hardware of the baseline system but can be used to define the hardware requirements of other possible configurations

The study was divided into tasks as follows

Item 1 Establish Data Base

The characteristics of the helicopter and its onboard flight control elements were compiled, the error models of the subsystems of the baseline system were formulated and the wind model was defined The Data Base was used to provide the data required for the remaining tasks This report discusses the Data Base in Section IV

Item 2 Flight Control Laws

A set of control laws were defined for a digital approach and landing flight control subsystem The flight control subsystem includes six manual modes with varying degrees of pilot assistance and a fully automatic mode A detailed description of these digital flight control laws is contained in BAC Report No 6200-933011 "Final Flight Control Software Package." The flight control system is discussed in Section III-B. of this report

Item 3 Guidance Laws

Guidance laws suitable for flight demonstration of the flight control system in an approach and landing under minimal visibility conditions were formulated A detailed decription of these digital guidance laws is contained in BAC Report No 6200-933012 "Final Guidance Software Package" The guidance laws are discussed in Section III-C of this report

Item 4 Simulation and Evaluation

A real time simulation using a piloted cockpit was developed as described in Section IV of this report The flight control and guidance laws were mechanized on an IBM 7090 computer in a manner similar to that in which they could be mechanized on an airborne computer Performance criteria were established and automatic and pilot runs were made These results are discussed in Section IV of this report

Item 5. System Design

A guidance and control configuration was established Subsystem requirements and interfaces were defined to the device level A system signal flow diagram was developed These results are reported in BAC Report No 6200-933033 "Systems Performance/Design Requirements Specification"

Item 6 Equipment Specification

Equipments required to mechanize the system were identified as "existing" or "to be developed" in BAC Report No 6200-933032 "Hardware Identification" The "to be developed" items were specified in the systems performance/design requirements specification

Item 7 Technical Presentations

Presentations were made as required by the contract at facilities and dates set by agreement between BAC and NASA/ERC

II SUMMARY AND CONCLUSIONS

A SUMMARY DESCRIPTION OF THE DFCLS

The Digital Flight Control and Landing System (DFCLS) may be depicted in a simplified diagram as shown in Figure II-1 This is an abstraction of the original baseline system proposed by NASA/ERC which is illustrated in Figure III-1 of Section III

In the guided modes, position data of the vehicle is obtained with respect to an orthogonal coordinate system ANF defined with a horizontal axis along the desired approach heading, a second axis along the local vertical and the origin at the desired touchdown point In Figure II-1, the position vector X = x, y, z, is the position coordinate of the helicopter with respect to this coordinate system This data may be obtained by inertial means, radar measurements, combinations of these or by any method which gives the position with the accuracy required This information is processed by the airborne digital computer using the guidance laws For the experimental system, two sets of laws have been specified, one set developed during the course of this study and a second set to be developed independently for purposes of comparison In the figure these are identified as Guid 1 and Guid 2

In the guided modes, using appropriate update algorithms and optimal filtering techniques, if required for precision, the position information (rate of change of this information) is used to update and refine the vehicle velocity coordinates The vehicle velocity again may be obtained by any sensing technique which has the required accuracy

The velocity data (to be used in both guided modes and in unguided modes where velocity control modes have been selected) constitute a set of inputs to the Flight Control Computations The vehicle attitude and attitude rate data is another set of inputs The vector $\underline{\theta}$ shown in the figure represents the vehicles Euler angles ψ, θ, ϕ, and the vector $\underline{\dot{\theta}}$ represents the vehicles body axis rates p, q, r These may be obtained from inertial sensors but, for flight control purposes, standard flight control system rate, heading, and vertical gyros are sufficiently accurate

The flight control system takes these inputs plus the inputs from the pilot's controls and depending on the mode selected, computes commands to the basic helicopter controls In the figure, $\Delta\delta_c$ is the vector of incremental commands to the pitch collective, roll cyclic, yaw cyclic and collective controls of the helicopter

In addition, the flight control system sends out a set of command displays, $\Delta\delta_d$, for the pilot's direction. These are appropriate for the flight control mode which has been selected

In the unguided modes, there is no position information but the vehicle is controllable with the same modes as available for guided flights except for AUTO (automatic) A more detailed description of these flight control and guidance laws follows

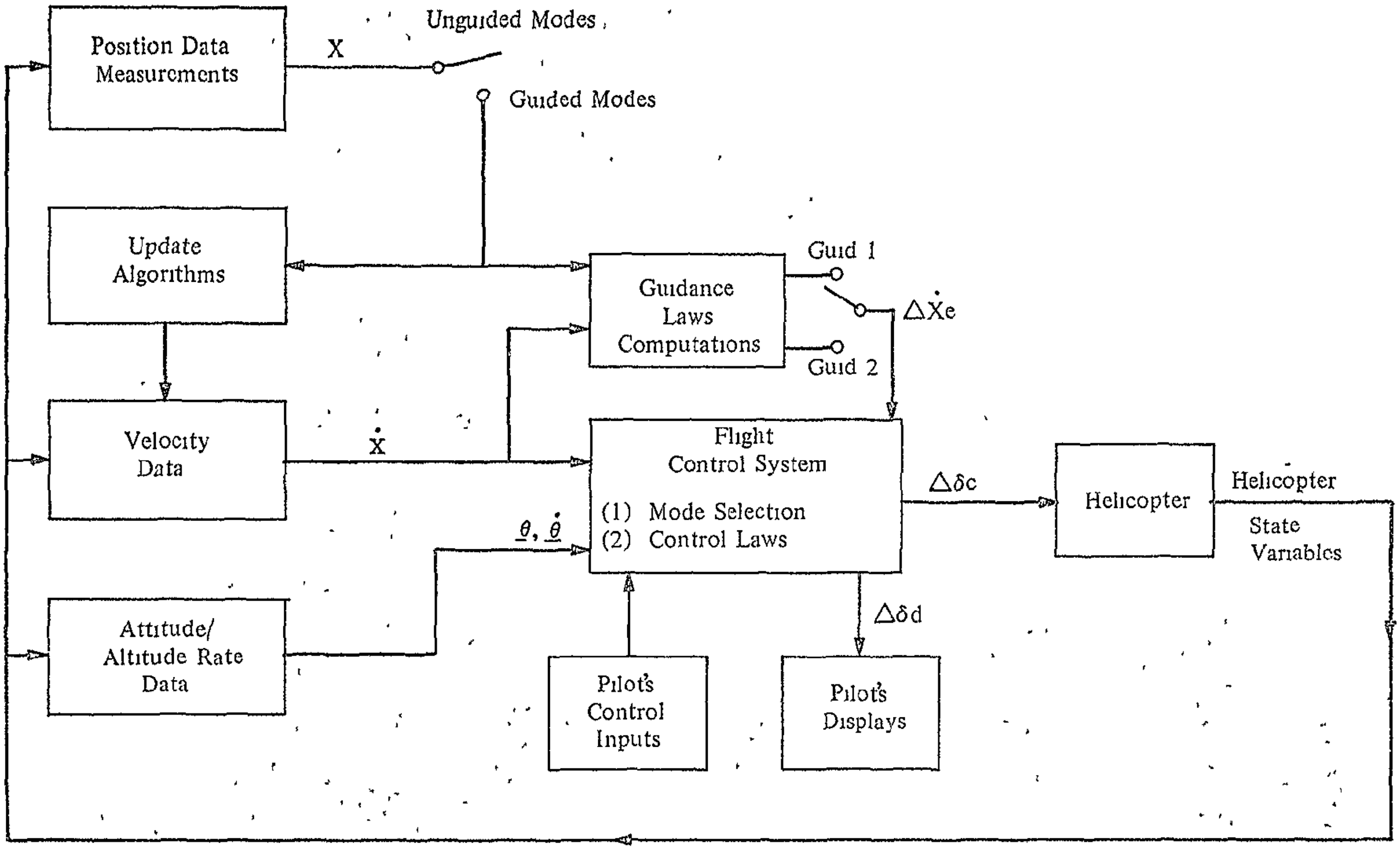

Figure II-1. Conceptual Diagram-Flight Control and Landing System

B FLIGHT CONTROL

1 Modes

There are eight pilot selectable modes of operation of the flight control laws (1) Disengage, (2) SAS, (3) Attitude I, (4) Attitude II, (5) Velocity I, (6) Velocity II, (7) Velocity III, and (8) Automatic In the first of these modes the system is inactive except for mode sampling and initialization activities The next six modes are manual modes of operation where command errors are normally displayed to the pilot on flight director needles and the pilot nulls these errors by inputting commands to the flight control laws through the electric stick or sidearm controller, rudder pedals, and collective stick The last mode of operation is a completely automatic mode where incremental velocity error inputs to the flight control laws are obtained from the guidance laws In this mode, actual velocity errors are displayed on the flight director needles for monitoring purposes The types of control, the form and source of the commands, and the form of the displays for each of these modes, except the Disengage mode, are listed in Table III-4 shown in the next section of this report

All of the manual modes and the automatic modes of operation of the flight control laws are designed to be used in conjunction with either the Guid I or Guid II modes The manual flight control modes can also be used when the guidance is in the Disengage mode although no command errors will be available on the flight director needles in this case The automatic flight control mode cannot be used when the guidance is in the Disengage mode In addition, all of these possible modes of operation apply in both the flight phase to hover and in the landing flight phase

2 Flight Control Laws

The flight control laws for the various modes of operation have been divided into command laws and control laws The command laws convert the pilot control inputs into command inputs to the flight control laws for the selected mode of operation There are separate command laws for the SAS Mode, the Attitude Modes, and each of the Velocity Modes By doing this, it is only necessary to include a single set of velocity control laws for the three Velocity Modes since the control inputs in each mode can be converted into velocity commands that are compatible with these

The control laws generate the incremental output commands to the electric hydraulic control system Also, in conjunction with the command laws, they also generate the display information in each mode, therefore, no separate display laws are required The command laws have been developed in a cascading manner where there are separate laws for the SAS, attitude, and velocity loops Each of these control laws receives its input either from the corresponding command law or next outer loop depending on the mode of operation This was done to eliminate the necessity of duplicating the inner loops in the digital flight control program sections for the higher order modes

This separation of the command and control laws also permits the laws for the outer loops to be updated at a slower rate than is used for those in the inner loops, therefore, the command and control laws have been grouped into fast and slow loop computations for efficiency in the airborne program In general, the fast loop computations contain the (1) SAS loop control laws, (2) SAS command laws, and (3) attitude control laws The slow loop computations contain the (1) attitude command laws, (2) velocity control laws, and (3) velocity command laws In some cases, certain equations in the inner loops can be updated in the slow loop computations These will be described in the report

C GUIDANCE

1 General

The guidance section of the Digital Flight Control and Landing System for the CH-46C helicopter will have three modes of operation (1) Disengage, (2) Guidance I, and (3) Guidance II The guidance laws for the Guidance II mode of operation have been developed by Bell Aerospace Company during this study The Guidance I laws are to be independently developed for comparison purposes The guidance laws have outputs defined as velocity errors in a coordinate system which is the ANF coordinate system rotated through the yaw Euler angle such that the X axis lies in the horizontal plane (heading-vertical system) The flight control system will accept guidance commands in this form from any proposed guidance laws

2 Modes

The Guidance II laws are for the landing mission of the CH-46C helicopter and have been designed to operate in conjunction with a digital flight control system which has several manual modes and an automatic mode of operation as described above There are two modes of operation of these laws (1) an Acquisition to Hover Mode, and (2) a Landing Mode In each mode, they generate velocity error commands for the flight control system In the manual modes of flight control, these errors are used by the flight control system to generate command errors for display and the pilot manually controls the helicopter based on these displays In the automatic mode of flight control, these errors are used by the flight control system to generate automatic commands to control the helicopter

In the Acquisition to Hover Mode, the laws generate velocity error commands to bring the helicopter from Aquisition conditions to a hover condition over the pad In the Land Mode, the laws generate velocity error commands to bring the helicopter from hover to touchdown. In the Land Mode, the laws check to determine if the hover conditions are acceptable before starting to generate commands for landing If the hover conditions are not acceptable for landing, the laws continue to generate hover commands until acceptable conditions are met

3 Guidance II Laws

The Guidance II laws generate velocity errors between a velocity landing profile and the sensed helicopter velocities The profile that is used is a constant speed glide type as shown in Figure II-2 As shown in this figure, the flight along this profile is divided into the following phases (1) acquisition, (2) level flight deceleration, (3) glide acquisition, (4) glide transition, (5) glide, (6) flare, (7) hover, and (8) land In each phase, separate longitudinal guidance laws are used to generate total forward and vertical velocity commands along the profile A single lateral guidance law is used to generate a total lateral velocity command These total velocity commands are then differenced with the sensed helicopter velocities and transformed into velocity errors in the vertical heading frame These errors form the command inputs to the flight control system

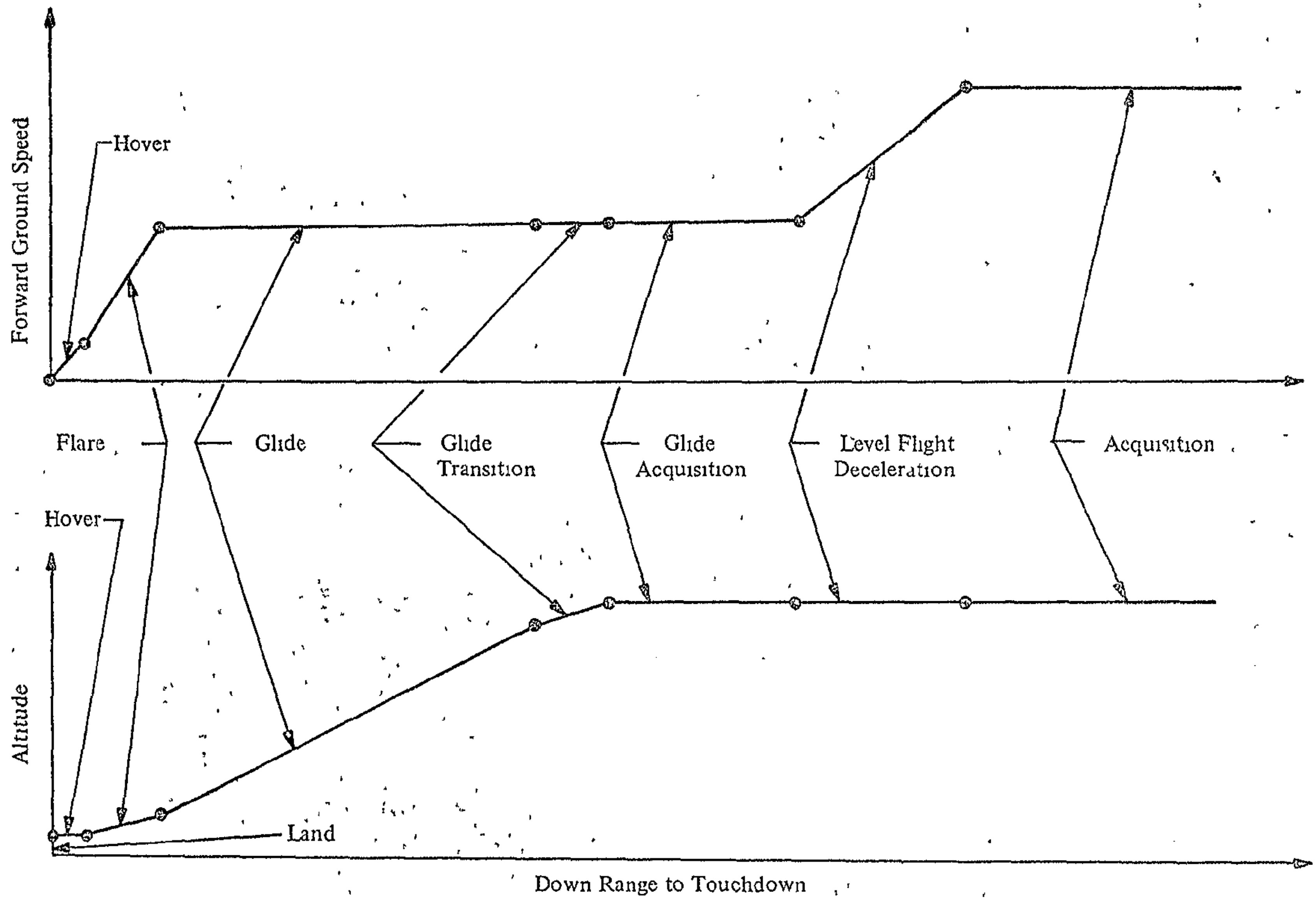

Figure II-2 Landing Mission Phases

D GENERAL CONCLUSIONS

1 Command information using the command bars and glide slope deviation index on a Flight Director Indicator display were developed suitable for each of the manual modes It was found that all modes could be flown to touchdown

2 The simple rate damping mode (SAS) described in this report is unsatisfactory for flight control because of the excessive pilot work load It is also unsatisfactory as a candidate for a backup mode because the change in adaptation from a low work load to the SAS mode, suddenly and in mid-flight, generally resulted in loss of mission The SAS mode could be flown to touchdown if the mission started in this mode and the pilot did not let the system "get away" from him

3 Backup modes in an operational system will require the attitude hold feature

4 In terms of performance measured by in flight errors and vehicle rates and attitude angles at touchdown all manual modes except SAS were equivalent but the equivalence was established at the expense of varying degrees of pilot's work load Except for the sidearm controller the velocity modes were best with the attitude mode with velocity control in the vertical axis (collective) judged next best Attitude control with raw collective followed these modes in terms of pilot's preference

5 Problems were encountered with the type and installation of sidearm controller available The results, however, justify the conclusion that velocity mode control with a proper, human factors design of the sidearm controller would be a very acceptable mode

6 The fully automatic mode (AUTO) had significantly better overall performance in terms of errors from the required flight profile However, the requirement to satisfy certain conditions before the guidance would proceed with the LAND phase, made all systems equivalent in terms of velocities, attitude angles and dispersion errors at hover Only the length of time in hover before satisfying the necessary conditions to proceed with the descent to touchdown were affected

7. The flight control system performance with winds and gusts met the accuracy requirements for landing under minimal visibility conditions The principal dispersion at touchdown was due to the errors in instrumentation assumed for the error models in measurement and not to the flight control system or the pilot's ability to fly the command displays

With ideal measurements of position, the vertical impact velocity at touchdown averaged about 3 8 ft/sec (4 ft/sec being the preprogrammed nominal) and had a standard deviation of 0 78 ft/sec The average error from the touchdown point in the forward direction was 13 8 feet with a standard deviation of 4 ft This indicates some system bias was present due to tolerance on LAND conditions The average error in the Y direction was 1 1 ft with a standard deviation of 6 1 ft These results were obtained in averaging over 180 runs piloted and automatic and including the undesirable SAS mode Each mode represents no more than 1/6 of the cases averaged so that the results stated are not biased in favor of any particular configuration.

The averages stated were obtained under combinations of wind conditions (15 knots steady, 2.5 ft/sec one sigma horizontal gusts, 0 75 ft/sec one sigma vertical gusts, headwind, tailwind, crosswind)

To these errors, whatever position measurement errors are specified must be added statistically This is a function of the measurement system selected In the baseline system, it is a function of the last GSN-5 update If the update is made while the helicopter is in hover phase while awaiting the LAND signal, the additional error can be negligible

8 The Flight Control System design did not require programmed gain changes or gain changes as a function of flight condition except for the lateral guidance law gain

III DETAILED DESCRIPTION OF SYSTEM

A. BASELINE SYSTEM

Figure III-1 depicts the baseline system as originally conceived in Bell's response to NASA/ERC's RFP for this study It outlines the major hardware elements in block diagram form The four helicopter controls,

- δ_r yaw cyclic
- δ_a roll cyclic
- δ_e pitch collective
- δ_c collective

are controlled by electrohydraulic servos, termed the EISS (Electric Input Servo System) The EISS is part of the existing VSS (Variable Stability System) system aboard the NASA/LARC CH-46C helicopter The helicopter's position is measured by the GSN-5, ground based precision radar, and the position coordinates (x, y, z) in the ANF (Approach Navigation Frame) coordinate system are transmitted via the Gemini data link to the helicopter

The ANF frame is defined as follows

Origin	Fixed to touchdown point
X-Axis	Horizontal and parallel to the runway axis in the direction of approach
Z-Axis	Vertical and Directed downward
Y-Axis	Completes orthogonal triad

Aboard the CH-46C helicopter, a strapdown inertial sensing system (ISU) is updated by the GSN-5 measurements The updating and processing of the ISU outputs is accomplished by computations with an airborne digital computer using appropriate algorithms

Using the vehicles attitude angles, angular rates, position and velocity which are available from these computations and the pilot's inputs, the computer generates output commands to the EISS based on flight control and guidance laws which have also been mechanized on the airborne digital computer.

The basic purpose of the study was to provide a design for a flexible, multi-mode digital flight control system for the CH-46C for flight research in V/STOL guidance and control Additionally, the guidance laws were to be formulated which would be suitable for demonstrating the flight control system's performance in landing the helicopter under minimum visibility conditions The study and resulting design was based on analysis and simulation

Both manual and automatic modes of control, with displayed information appropriate for each mode, were required These modes were initially then to be

(1) disengaged
(2) rate damper (pilot input)

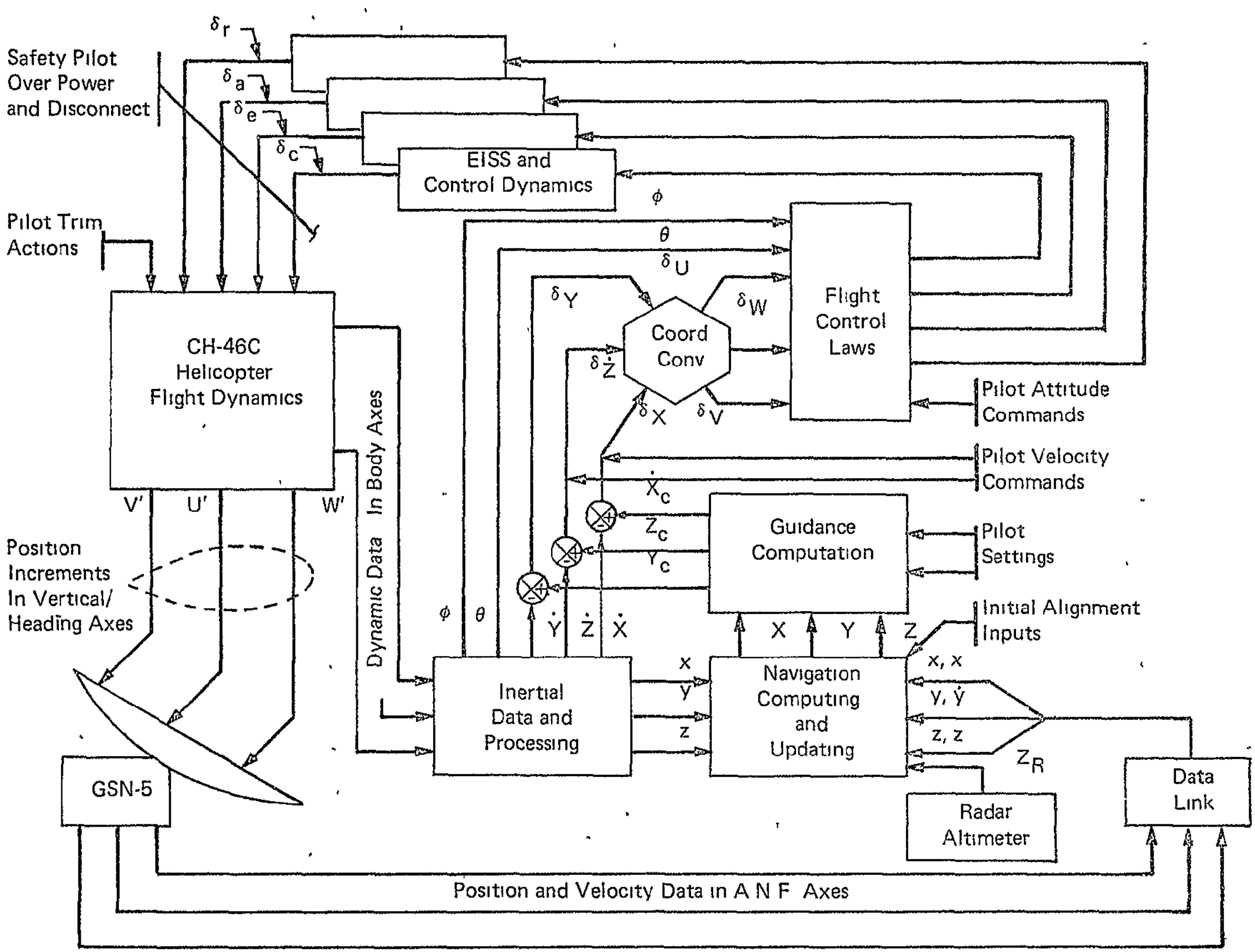

Figure III-1 Simplified Block Diagram

(3) attitude/attitude rate (pilot input)
(4) translational velocity command (pilot input, stick)
(5) translational velocity command (pilot input, side arm controller)
(6) fully automatic

These modes evolved during the course of the study to the modes described in Section III B 3 Since in this report it is convenient to refer to the mode designations ultimately developed, the current designations and their principal features are

SAS - The helicopter is controlled through the pilot's stick, rudder pedals and the collective stick Angular body rates in the three axes are fed back The collective stick control is the same as for the bare helicopter

ATT 1 - The pilot's stick controls the pitch and roll angles of the helicopter The rudder pedals control the side slip angle above 35 knots and the heading angle below 35 knots The collective stick control is the same as for the bare helicopter

ATT 2 - This mode is the same as ATT 1 except that the collective stick control is converted to a vertical velocity control

VEL 1 - The pilot's stick controls the forward acceleration in the Heading Vertical coordinate system and either lateral acceleration in this coordinate system or the course rate depending on speed The collective stick controls the vertical velocity The Heading-Vertical coordinate system is defined by

Origin	At a defined point in the aircraft
X-Axis	The orthogonal projection of the Body X axis onto the local horizontal plane
Z-Axis	Vertical and directed downward
Y-Axis	Completes orthogonal triad

Above 35 knots, the lateral control is accomplished by a course change and below 35 knots, by a side slip The rudder pedals function as they do for ATT 1

VEL.2 - The pilot's stick controls the forward velocity in the Heading Vertical coordinate system and either the lateral velocity in this coordinate system or course depending on speed Above 35 knots, the lateral control is accomplished by a course change and below 35 knots, by a side slip.

The other controls remain as for VEL 1

VEL 3 - This mode is the same as VEL 2 except that a sidearm controller is used for forward and lateral velocity control instead of the pilot's control stick and only velocity is controlled in the lateral axis instead of either velocity or course

AUTO - This is a fully automatic mode where velocity errors in the Heading Vertical frame are generated by guidance functions

The landing mission profile, described in detail in Section III 3, is briefly summarized here to facilitate the following discussion The profile requires that the helicopter

(1) intercept the centerline at any airspeed
(2) decelerate to 42 knots range rate
(3) intercept a 6° glide slope and descend
(4) at approximately 1550 ft ground range and 150 ft altitude, decelerate and flare to 50 ft altitude and 10 knots range rate
(5) at 200 ft ground range and 50 ft altitude, decelerate to hover above the touchdown (T D.) at 50 ft
(6) descend to T D point vertically

B. FLIGHT CONTROL LAWS

1 Design Philosophy and Assumptions

The total problem of designing a flight control system may be subdivided into distinct phases for each of which a definite philosophy must be adopted and assumptions made These phases, in their logical study sequence, are

(1) definition of scope of design and purpose of the flight control system
(2) definition of vehicle and operational requirements
(3) configuration design
(4) detail design approach
(5) system evaluation and design modifications

This section describes the point of view adopted for each of these phases for the purpose of the study

a. Definition of Scope

As stated in Section III A, the flight control system design was based on the requirement for a practical, multimode digital flight control system to control the CH-46C helicopter at NASA/LARC. The purpose of the flight control system was to provide a flexible research tool for flight investigation of control system, guidance and display requirements for V/STOL area navigations and landings under minimal visibility conditions

During the course of the program, it became apparent that a large number of variables could be considered in every aspect of the study For example, in the area of displays alone, a large number of parameters suitable for investigation exist

(1) Conventional aircraft instruments versus nonconventional displays
(2) Situation versus command information
(3) Variation of displayed data with flight control mode
(4) Variation of displayed data with pilot's control element
(5) Scale factor or sensitivity of displayed information
(6) Possible shaping of data to avoid PIO (Pilot Induced Oscillation) or pilot disorientation
(7) Influence of data displayed on pilot's work load
(8) Influence of data displayed on system performance
(9) Backup displays for flight safety or possible mission completion

These areas have been, and continue to be, fruitful subjects for investigation and taken in combinations present a great many possibilities

In addition, the other areas such as sensor blending, complexity of flight control and guidance laws, digital programming considerations, flight control and guidance sensor specifications, sampling rate and quantization studies and alternative mission profiles each involve a number of parameters which could be investigated

The necessary contraints of budget and schedule restricted the scope of the study to a practical bound This implies that many useful ideas could not be explored within the range of this study The system design presented in this report, therefore, represents one method of attaining the objectives described at the beginning of this section

The flight control system was to incorporate the modes listed in Section III A All modes except AUTO are manual modes SAS was a derivative of the original rate damper mode, ATT 1 and ATT 2 were derivatives of the original attitude/attitude rate mode, VEL 1, VEL 2, VEL 3 were derivatives of the original velocity command modes

The SAS mode was to be regarded as the most primitive mode for which the FCS objectives could be met and its inclusion was regarded primarily to investigate the possibility for a backup flight safety mode for a future operational system

It was further decided that the displays would be based on the Flight Director Indicator as defined by MIL-I-27193B(USAF) In the manual modes, longitudinal and lateral command errors would be displayed on the horizontal and vertical command bars and the collective error on the displacement index In these modes, the display would show the difference between where the pilot has positioned his control and collective sticks and where the automatic system would have positioned it In the AUTO mode, these indicators display the velocity error along each of three axes of the Heading Vertical frame

The flight control system design was not required to incorporate redundancy or to provide automatic monitoring and switchover to the Safety Pilot in the event of malfunction System safety was to be insured by monitoring of the conventional helicopter displays and visual cues by the Safety Pilot who has the option of taking control of the vehicle at all times

b Definition of Requirements

(1) General Requirements

The flight control system (FCS) was to have the basic modes listed in the previous paragraph modified as determined by the study to attain the objectives listed in that paragraph These modes were to be pilot selectable by suitable cockpit switch functions with the selection clearly indicated Each mode was to be available by selecting the appropriate switch irrespective of the flight control mode which was operative prior to the selection There was to be no transient introduced by the switching The Control stick position, the pedal position, side arm controller (SAC) position and all instantaneous outputs of the attitude and velocity sensors at the instance of mode switching were to become the reference values for the selected mode

Mode selection was required to be suitably interlocked with the guidance system and with the displays such that illogical combinations were not possible An example of an illogical combination is the selection of an automatic landing mode without the presence of guidance information In fact, it was recognized early that the AUTO mode of the FCS could not be clearly separated from the guidance requirements, and where clarity is served, arbitrary separation into flight control and guidance is not adhered to in this discussion

Initially, the philosophy which was adapted with respect to automatic modes of FCS operation was to permit pilot overrides or assists This policy changed during the course of the study when it became apparent that, in a number of cases, this had the reverse effect and deteriorated the performance The requirement for transient free mode switching, furthermore, made this unnecessary since the pilot was capable of switching to a manual mode if he felt the need for direct control.

The FCS was to be capable of controlling the helicopter over the entire speed range of 0 to 140 knots Performance between 80 and 140 knots was to be considered secondary to performance in the low speed regime Due to the large speed variation, the philosophy was adopted that the helicopter-FCS combination should behave as an airplane at high speeds and as a helicopter at low speeds It was logical to use the airspeed measured by the Pitot tube to separate these flight phases and, further, to use the airspeed below which the Pitot tube measurements becomes unreliable as the dividing line. This was taken to be an airspeed of 35 knots after filtering to remove gust effects

During the course of the study it became apparent that the FCS design was not completely separable from the guidance function in that as touchdown is approached, the speed which is of interest shifts from airspeed to groundspeed To illustrate this point, if a 30 knot headwind exists and the helicopter's ground speed approaches zero under the direction of the guidance laws, the behavior of the helicopter FCS combination would be that of the high speed flight phase down to a ground speed of 5 knots This behavior with respect to such functions as turn coordination is not desirable so close to the touchdown point where sideslip maneuvers are more efficient for small flight path corrections For this reason, the FCS switching functions which are speed dependant were to be based on an effective speed, V'_a, where

$$V'_a = V_{af}, \text{ if } V_{af} < \dot{V}^h_x$$

$$= \dot{V}^h_x, \text{ if } V_{af} > V^h_x$$

$$V_{af} = \text{filtered airspeed} = \frac{V_a}{1 + s\,\tau_{V_a}}$$

V_a = Pitot measured airspeed

τ_{V_a} = airspeed filtering time constant

V^h_x = forward velocity in vertical heading frame

For all modes, except SAS, turn coordination when $V_a' > 35$ knots was to be assisted by feeding a suitably modified function of the roll angle control, $\Delta\Phi_c$, into the yaw cyclic control channel

For all modes, when $V_a' > 35$ knots, side slip was to be reduced by feeding a suitably modified function of β, the measured sideslip angle, into the Yaw Cyclic Control Channel

For the ATT 1, ATT 2, VEL 1, VEL 2 and VEL 3 modes, a heading hold with pilot control was to be incorporated when $V_a' < 35$ knots For the AUTO mode, when $V_a' < 35$ knots and crosswinds were present, a blend of crab angle and roll angle was to be used to maintain the vehicle on the demonstration Landing Profile described in Section III B Guidance Laws The blend required that the helicopter head into the average relative wind such that the average roll angle required for crosswind compensation would not exceed 5° This was based on pilot inputs that indicated 5° of steady roll angle would be unacceptable

Compensation for loss of vertical lift due to helicopter bank was judged to be an operational requirement which was to be satisfied by feeding a suitably modified function of the bank angle into the collective channel

The flight control system was to incorporate control stick, side arm controller and pedal thresholds such that pilot induced oscillations (PIO) were minimized The thresholds were not to exceed 5% of the total travel of the pilot's control

Stick, pedal and sidearm controller commands were to be commands with respect to the heading vertical coordinate system in the Velocity modes and Attitude modes and the vehicle body axis system in the SAS mode

The flight control laws and flight control sensors were to be considered together such that sensor noise did not result in faulty signals or exceed a 1 sigma noise of 0 1 in in the collective, pitch differential collective, roll cyclic or yaw cyclic channels of the EISS or result in saturation of these channels These requirements were based on the Data Base used (see Section IV A) which indicated that the EISS hysteresis in each channel was to be taken as 0 1 in

Further constraints imposed on the FCS design by the EISS and helicopter control boost system were that the pitch collective, roll cyclic, yaw cyclic, and collective were related to the commanded values of these controls by an approximate quadratic transfer function with natural frequancy of 15 hertz and a damping factor of 0 6

To simplify mechanization, it was a goal of the design that within the constraints imposed by performance requirements, the minimum number of control laws should include as much of the flight profile and flight conditions as feasible However, these laws could be linear or nonlinear and could differ for each operational mode if required by performance specification or sensor constraints The balance between simplicity and performance is a judgement factor

The FCS design had to be based on the existing EISS and pilot's controls aboard the CH-46C helicopter The existing trim system would relieve stick and pedal forces but not reset any stored references in the FCS The FCS would be self trimming where necessary to meet the requirements

The characteristics of the existing Feel and Trim System were given as

The scale factors required to convert inches of pilot controls to volts input to the EHS actuators
Pitch Axis, 3 92 in /volt
Collective Axis, 6 41 in /volt
Roll Axis, 2 41 in /volt
Yaw Axis, 1 36 in /volt

CH-46 Electric Stick Characteristics

The stick forces are force/displacement gradients and were given as

Pitch differential collective, 1 0 lb/in
Roll cyclic, 1 0 lb/in
Inches measured at a radius of 25 in

The pedal force is a force/displacement gradient and was given as

Yaw Cyclic, 4 0 lb/in

The collective force is a friction force which may be adjusted by the pilot The force was given as being variable from essentially zero to at least 5 lb measured at a radius of 18 0 in

The electric stick has linear pots which vary on stick position and infinite resolution The output voltages were given as

Pitch Axis, 0.4 volts/in
Collective Axis, 0 33 volts/in
Roll Axis, 0 4 volts/in
Yaw Axis, 0 8 volts/in

CH-46C Trim System Characteristics

The force trim system for pitch differential collective and roll cyclic operate from the "coolie hat" button on the stick Each axis has its own trim The button activates a motor which runs to relieve the force at 1 0 in /sec

The trim on the pedals is similar to that on the stick with the trim button being on the collective stick

There is no trim for the collective stick

The range and sensitivity of the sensors to be used were given as follows

stick, pitch	±5.5 in	0 4 volts dc/in
stick, roll	±3 6 in	0 4 volts dc/in
pedals	±2 3 in	0 8 volts dc/in
collective stick	0 to 12 8 in	0 33 volts dc/in

α, β vanes	±0 35 radians	9 8 volts dc/radian
Pitot tube	35 to 150 knots	0 08 volts dc/knot

An additional ground rule with repect to the interfacing of the EISS and the FCS output is illustrated in Figure III-2 This figure, taken from Bell Report No 6200-933033, depicts the requirements that the EISS in its disengaged mode is configured such that

(1) The hydraulic actuators driving each of the four controls are bypassed
(2) All electrical inputs to the EISS are being cancelled
(3) The drive voltage to each hydraulic control valve is displayed for pilot monitoring

The EISS is not engaged by the pilot unless the NULL METER indicates that all electrical inputs to the EISS have been cancelled This insures against transients on EISS engagement

(2) Dynamic Performance Requirements

In searching for dynamic performance criteria, a number of factors were considered and an approach formulated from which working criteria could be established The approach was based on the following considerations

First, the fundamental performance requirement was considered to be that the FCS controls the helicopter to the profile defined by the mission The tolerance and constraints imposed by this requirement are described in Section III C The implication of this viewpoint was that the ultimate justification of the flight control laws would be a satisfactory evaluation of the full system on the simulator

It was necessary to have requirements for the design of the subsystems before the full simulation could be evaluated These were defined on the basis of transient response because the nonlinearities (hysteresis, quantization, limiting) of the system made frequency response or pole-zero criteria artificial and because transient response is conveniently observed in evaluation by simulation This viewpoint leads naturally towards considering the dynamic response in terms of the residual oscillations after transients have died out, response in the nominally linear range and to response to saturation command signals

Consistant with the philosophy of trading off performance for simplicity, the view was adopted not to require uniform levels of performance or higher performance than necessary in view of the full simulation evaluation which would be the ultimate test Higher performance was desired during transition, hover and touchdown then when the vehicle was flying high and fast

The FCS helicopter combination should also meet the requirements of MIL-H-8501A, "Helicopter Flying and Ground Handling Qualities" where this specification applies

The requirements in light of this approach were specified as in the following paragraphs

The FCS system was permitted residual oscillation due to EISS nonlinearities sensor noise, sensor package hysteresis or quantizing of sensor information or quantizing of commands to the EISS This was not to exceed ±1 0° or $\frac{0.5}{f^2}$ degrees, whichever is smaller, about any axis and

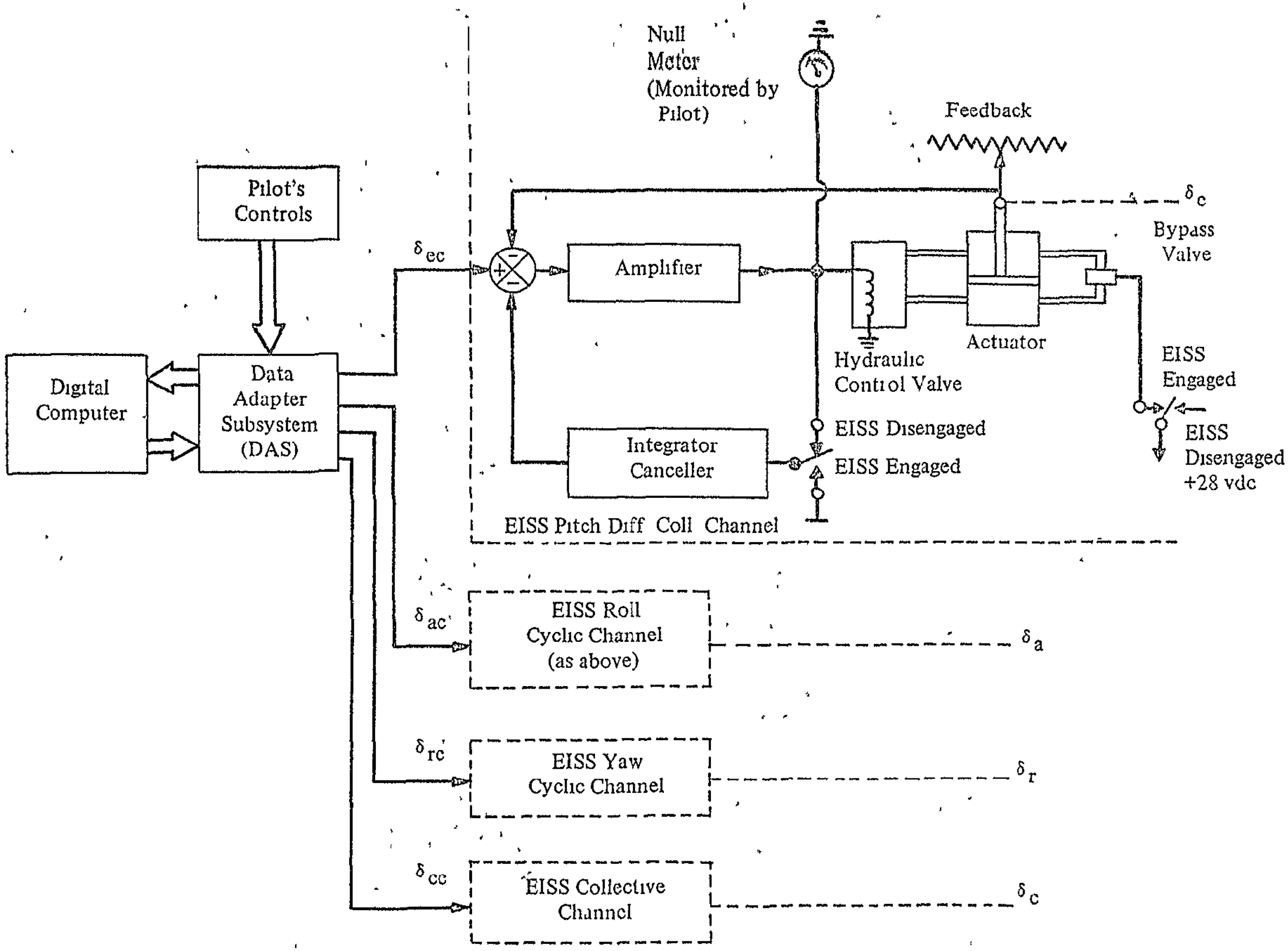

Figure III-2 EISS Initial Condition Switching

± 1 or $\frac{0.5}{f}$ ft/sec along any axis, whichever is smaller where f is the frequency in Hertz

For input signals at least five times the largest threshold, hysteresis, signal quantum or command quantum in a given channel, but not large enough to cause signal, velocity or position saturation of any element in that channel, the FCS requirements for each mode were specified Superposition of the residual oscillations on other response requirements was considered permissable

The SAS mode was simply to meet the requirements of MIL-H-8501A, relating to rate damping Since this was to be evaluated as a possible backup mode, no more than accepted helicopter handling characteristics were to be required

The ATT 1 mode by definition, was to have an unaugmented collective, hence, as for SAS, the vertical control would required to meet specifications of MIL-H-8501A only

In response to a step change in attitude angle command about any axis, the ATT 1 mode would not be permitted to overshoot the final value by more than 15% of the total commanded change, would attain 90% of the total commanded change in less than 1 5 sec after the step command initiation and would remain at the final value within 5% or less of the total commanded change within 5 sec after step command initiation

The ATT 2 mode would satisfy the same requirements as the ATT 1 mode with respect to attitude angle commands since, by definition, the control laws were the same

The vertical control characteristics of the ATT 2 mode would be such that the response to a step velocity command would exhibit a maximum allowable overshoot of the final velocity in accordance with

$$\Delta V_{ZO} = 0.06\, \Delta V_{ZC} \qquad \text{for } 0 < V_a < 10 \text{ knots}$$
$$= (-0.4 + 0.10\, V_a)\, \Delta V_{ZC} \qquad \text{for } 10 < V_a < 40 \text{ knots}$$
$$= (-4.0 + 0.2\, V_a)\, \Delta_{ZC} \qquad \text{for } V_a > 40 \text{ knots}$$

where ΔV_{ZO} is the maximum allowable overshoot, ΔV_{ZC} is the magnitude of the step command and V_a is the forward airspeed in knots

The vertical velocity would attain at least 90% of the total commanded change within one second after the initiation of the step command in vertical velocity command

The VEL 1, VEL 2 and VEL 3 modes would satisfy the same requirements as the ATT 2 mode with respect to vertical control characteristics since, by definition, the vertical control laws in these modes would be the same

The VEL 1, VEL 2 and VEL 3 modes would respond to a step change in forward and lateral commands such that the maximum overshoot in response to a step command would be in accordance with

$$\Delta H_{(X,Y)\,O} = (0\ 05 + 0\ 004\ V_a)\ \Delta H_{(X,Y)\,C} \quad \text{for } 0 < V_a < 40 \text{ knots}$$
$$= 0\ 2\ \Delta H_{(X,Y)\,C} \quad \text{for } V_a > 40 \text{ knots}$$

where $\Delta H_{(X,Y)\,O}$ is the maximum allowable overshoot, $\Delta H_{(X,Y)\,C}$ is the step command size and V_a is the airspeed in knots In VEL 2 and VEL 3, ΔH is an incremental velocity In the VEL 1 mode, ΔH is an incremental acceleration, 80% or more of the total commanded change would be realized within five sec after the initiation of the step command

For saturation command inputs the FCS would constrain the vehicle limits as follows

In all FCS modes

Pitch angle rate $< 25°$/sec
Roll angle rate $< 25°$/sec
Yaw angle rate $< 25°$/sec

In all FCS modes except SAS

|Roll angle| $< 45°$
Yaw angle unlimited
|Pitch angle - nominal pitch angle| $< 10°$

Nominal pitch angle is the pitch angle required to trim the helicopter for the flight condition being experienced

In SAS, ATT 1, ATT 2 modes

Maximum angles would be limited by direct pilot control

c Configuration Design

The flight control laws for the various modes of operation were divided into comman laws and control laws The command laws convert the pilot control inputs into command inputs to the flight control laws for the selected mode of operation There were separate command laws for the SAS Mode, the Attitude Modes, and each of the Velocity Modes By doing this, it was only necessary to include a single set of velocity control laws for the three Velocity Modes since the control inputs in each mode could be converted into velocity commands that are compatible with these

The control laws were to the incremental output commands to the EISS In addition in conjunction with the command laws, they also were to generate the display information in each mode As a result of this, no separate display laws were required The command laws were to be developed in a cascading manner with separate laws for the SAS, attitude, and velocity loops Each of these control laws was to receive its input either from the corresponding command law or next outer loop depending on the mode of operation This was done to eliminate the necessity of duplicating the inner loops in the digital flight control program sections for the higher order modes

This separation of the command and control laws also would permit the laws for the outer loops to be updated at a lower rate than for those in the inner loops As a result of this, the command and control laws were grouped into fast and slow loop computations for efficiency in the airborne program In general, the fast loop computations were to contain these laws (1) SAS loop control, (2) SAS command, (3) attitude control The slow loop computations would contain (1) attitude command, (2) velocity control, (3) velocity command laws

d Design Approach

Assembling valid data on which to base the study and a paper design using the data provided in the RFP, were parallel first items in the design approach In addition to the equilibrium aerodynamic data on the CH-46C which was received as part of the original RFP, further data was requested and received from Boeing Vertol as listed in Section IV B 1

It was judged to be essential that nonequilibrium flight conditions be simulated A number of approaches toward simulating nonequilibrium data from the available equilibrium data were explored These, and the technique selected are described in Section IV C

The second set of items required to complete the Data Base was the development of the subsystem error models These subsystems were the strapdown navigational system, GSN-5 Radar and Gemini Uplink, Radar Altimeter, Pitot Tube, Angle of Attack and Side Slip Vanes These models were first developed in analog form and then recast in a form for optimum digital implementation These are discussed in Section IV

In parallel with the establishment of the Data Base, preliminary design of the flight control system began using the data contained in the RFP Because of the large number of flight conditions and the many loops involved (angular rate, angle, velocity and ultimately position) it was decided to automate the procedure for selection of the gains

The philosophy which was adapted was to use the classic root locus method to determine the coefficients of an assumed form of feedback law Where δ_{NC} is the command to the N control channel of the EISS and θ_N is the principal vehicle parameter to be controlled in the loop under analysis, then if the form

$$\frac{\Delta\delta_{NC}}{\Delta\theta_N} = K_1 + sK_2 + \frac{K_3}{s}$$

is assumed for the feedback law, then the problem was to determine K_1, K_2 and K_3 The criterion for selecting these coefficients was to hold the dominant pole on the 0 7 damping line, and raise its natural frequency until the required compensation became excessive When these had been determined for one loop, they were held constant while the next loop was closed and the process repeated. The concept was to continue in this manner proceeding from the fastest inner loops, successively to the slowest outer loops

This was programmed for digital computation and included the helicopter response to control action, the transfer function of the control actuators, noise filters and simulated sampling rate lags

This procedure worked well for the short period control loops but it was not found possible within schedule constraints to develop a general algorithm to express the selection logic for successive trials in the outer loops and although convergence was obtained over some ranges of flight conditions, others diverged defeating the design objective Since at this point in the study an all digital check simulation of the mission became available which did provide the outer loop gains, the attempt to perfect the root locus program to give valid outer loop results was dropped However, the inner loop coefficients which had been determined were valid starting points for the FCS design The all digital check program was then also used to check the inner loop response to steps in accordance with the requirement discussed previously

The design then proceeded to the hybrid simulation refinement phase where all of the fast moving helicopter dynamics except for the stability derivatives were simulated on two AD4 and one PACE 231R analog computers and the control laws and stability derivatives were simulated on the IBM 7090 digital computer Due to the size of the analog simulation and typical analog hardware problems, the realiability and repeatability of this simulation was poor and did not allow for sufficient up time for evaluations

The availability of the all digital check program made it possible to consider shifting more of the simulation to the digital computer The crucial point was whether the simulation could be run in real time This was unimportant for the AUTO mode but imperative in the manual modes where a pilot would fly the system It was found possible to program the IBM 7090 such that real time performance was attainable in all modes This resulted in shifting all but the cockpit interface equipment and the wind model to the digital computer

The s domain laws were digitized using Tustin's method in converting the laws found by the preliminary analysis and in converting the helicopter simulation to the digital domain

It was felt that strict adherence to flight control laws developed in the s domain would not fully exploit the capability of the digital computer In this respect, it was found that the limit cycling due to hysteresis in each channel of the EISS could be reduced further by a nonlinear law. On the analog computer a conventional lead/lag hysteresis network had been used to reduce the limit cycle amplitude Paper analysis using describing function techniques confirmed the analog results A 20% reduction in the amplitude of the limit cycle was attained By using a digital variable gain compensation technique the limit cycle was reduced 70%

The necessity for varying the coefficients in the flight control laws as a function of airspeed was explored It was found that the requirements previously discussed were attainable with fixed gains, considerably simplifying the FCS mechanization

e. System Evaluation

As previously stated, performance on the full simulation was considered the ultimate justification of the flight control (and guidance) laws At this point, performance measurement criteria were required.

Ideally, performance evaluation should result in a single score Only in this way can different systems be compared and ranked unambiguously However, it is frequently not possible to set up criteria which satisfy this ideal when there are important factors which are entirely dissimilar This was found to be the case in setting up the criteria for the simulator tests

First, it was desired to have a measurement of performance in terms of how well the landing profile was being followed This measurement was termed the PI (Performance Index) and was based on the normalized rms value of the altitude error, altitude rate errors, lateral error, lateral rate error and forward velocity error The relationship is shown in Table III-1 Note that the normalization procedure allowed for different values for the maximum errors as the helicopter was further away from touchdown The lower the PI the better the performance with a PI of unity (1) meaning that all errors held at their maximum allowable throughout the flight

Due to the averaging process taken over the whole flight, it is conceivable that some portion of the flight could have large errors and still the flight have an overall PI which is low provided the time duration of the poor performance was low In general, this is unimportant since it implies large errors for short periods of time, a situation which generally exists only on initiation of control However, if the circumstances were such that the large errors occurred at, or near, touchdown, this could result in a disasterous landing with a low PI Therefore, the conditions at touchdown are special and must be looked at independently of any possible overall PI The radial error from the nominal T D point is a second performance criterion Important and independent, the impact velocity at touchdown was considered to constitute a third measure of performance

Finally, it was recognized that equally good performance could be achieved in terms of PI and touchdown conditions by the different flight control system modes but that in some modes this was attained at the expense of heavy pilot work load Thus, pilot opinion constituted a fourth measurement which was required For this purpose the rating scale of Table III-2 was used (from "The Use of Pilot Rating in the Evaluation of Aircraft Handling Qualities," by G E Cooper and R F Harper, Jr , NASA Technical Note D-5153)

TABLE III-1
PERFORMANCE INDEX

$$PI = \frac{1}{T\,n} \int_0^T \sqrt{\sum_{i=1}^{n} \left(\frac{\Delta x_i}{\Delta x_{i_{max}}}\right)^2}\, dt$$

where $\Delta x_i = \Delta h, \Delta \dot{h}, \Delta X, \Delta \dot{X}, \Delta Y$

$\Delta h = h_c - h$, altitude error

$\Delta \dot{h} = \dot{h}_c - \dot{h}$, altitude rate error

$\Delta \dot{X} = \dot{X}_c - \dot{X}$, forward velocity error

$\Delta Y = Y$, lateral error

$\Delta \dot{Y} = \dot{Y}$, lateral rate error

$\Delta h_{max} = 20 + (\frac{180}{10,000})\ X \leqslant 100$ ft

$\Delta \dot{h}_{max} = 4 + (\frac{36}{10,000})\ X \leqslant 20$ ft/sec

$\Delta \dot{X}_{max} = 0.5\ \dot{X} \leqslant 20$ ft/sec

$\Delta Y_{max} = 100 + (\frac{900}{10,000})\ X$

$\Delta \dot{Y}_{max} = 20 + (\frac{180}{10,000})\ X$

T = Total flight time

n = number of Δx_i considered (five)

TABLE III-2

HANDLING QUALITIES RATING SCALE
(COOPER-HARPER RATINGS)

Adequacy For Selected Task Or Required Operation*		Aircraft Characteristics	Demands On The Pilot In Selected Task Or Required Operation*	Pilot Rating
Yes		Excellent Highly Desirable	Pilot compensation not a factor for desired performance	1
		Good Negligible Deficiencies	Pilot compensation not a factor for desired performance	2
		Fair-Some Midly Unpleasant Deficiencies	Minimal pilot compensation required for desired performance	3
Is it Satisfactory without Improvement? No	Deficiencies Warrant Improvement	Minor But Annoying Deficiencies	Desired performance requires considerable pilot compensation	4
		Moderately Objectionable Deficiencies	Adequate performance requires considerable pilot compensation	5
Yes		Very Objectionable But Tolerable Deficiencies	Adequate performance requires extensive pilot compensation	6
Is Adequate Performance attainable With a Tolerable Pilot Workload? No	Deficiencies Require Improvement	Major Deficiencies	Adequate performance not attainable with maximum tolerable pilot compensation Controllability not in question	7
		Major Deficiencies	Considerable pilot compensation is required for control	8
Yes		Major Deficiencies	Intense pilot compensation is required to retain control	9
Is it Controllable? No	Improvement Mandatory	Major Deficiencies	Control will be lost during some portion of required operation	10
Pilot Decisions				

* Definition of required operation involves designation of flight phase and/or subphases with accompanying conditions

2 Final Flight Control Laws

The final flight control laws resulted in a design which is summarized in two companion documents

1 Systems Performance/Design Requirements Specification Bell Aerospace No 6200-933033

2 Final Flight Control Softwave Package Bell Aerospace No 6200-933011

This portion of the final report necessarily draws heavily on these documents

a Data Requirements

The Flight Control System has as its inputs the body axis angular rates (p, q, r), the Euler Angles (ψ, θ, ϕ), the ANF frame velocities (V_x^{an}, V_y^{an}, V_z^{an}), the Heading Vertical frame velocities (V_x^h, V_y^h, V_z^h), the pilot's control stick and pedal commands (δ_{ep}, δ_{ap}, δ_{rp}, δ_{cp}), the indicated airspeed (V_a), the sideslip angle (β), and the FCS and Guidance Law discretes

The output of the FCS are the commands (δ_{ec}, δ_{ac}, δ_{rc}, δ_{cc}) to the EISS Table III-3 lists the minimum requirements for the measured and output data

System noise in Table III-3 is defined as erroneous signals which may cause control system movements or saturations but which do not result in perceptible helicopter motions For purposes of the study, noise is defined as those components of error signal whose power spectra lie above 20 radians/sec Those components of error signal whose power spectra lie below 20 radians/sec are defined as errors

b Control Modes

Table III-4 summarizes the flight control modes

c Pilot's Interface with FCS

Table III-5 lists the control laws from the pilot's control stick, collective stick, rudder pedals, and side arm controller Table III-6 identifies the commands displayed to the pilot on the Flight Director Indicator with Table III-7 listing the command indicator (horizontal or vertical bar, glide slope index) senativities

d Flight Control Laws

This section is abstracted from Bell Report No 6200-933011, Final Flight Control Software Package Figure III-3 and III-4 are the block diagrams of the longitudinal and lateral flight control laws.

Tables III-8, 9, 10, and III-11 summarize the flight control laws for the pitch, roll, yaw and collective channels respectively in each of the FCS modes The symbols used are defined in the listed tables

TABLE III-3
DATA REQUIREMENTS FOR FCS

Parameter	Minimum Sampling Rate (Samples/Second)	Maximum Quantization	Maximum Allowable Noise (rms)	Maximum Error	Range of Operation
Vertical Heading Velocities	8	0 1 ft/sec	0 2 ft/sec	$\pm (0\ 04\ V_x^h + 0\ 25)$ ft/sec where V_x^h is (ft/sec)	$V_{x,}^h$ -50 to +250 ft/sec $V_{y,}^h$ ±50 ft/sec $V_{z,}^h$ ±30 ft/sec
ANF Velocities	8	0 1 ft/sec	0 2 ft/sec	$\pm (0\ 04\ V_x^h + 0\ 25)$ ft/sec	$V_{x,}^{an}$ $V_{y,}^{an}$ ±250 ft/sec $V_{z,}^{an}$ ±30 ft/sec
Body Axis Angular Rates	32	0 2°/sec	0 5°/sec	$\pm (0\ 06 + 0\ 005\ \dot{p})^\circ$/sec p = p, q, r	± 60°/sec
Euler Angles	32	0 1°	0 2°	± 0 2°	±90° Pitch, Roll ± 180° Yaw
Indicated Airspeed	8	0 5 ft/sec	5 ft/sec	± 3% of actual for airspeeds above 30 knots	+30 to +250 ft/sec
Sideslip Angle	32	0 02°	0 2°	± 0 3°	±0 35 radians
Commands to EISS	32	0 005 in	0 05 in	N A	See Table III-5
Pilots Commands to FCS	32 for SAS 8 for all other modes	See Table III-7 and Convert to 0 01 inch of Command Bar Displacement	N A	N A	See Table III-5

TABLE III-4
CONTROL MODE DEFINITIONS

	Command and Source				Type of Control			
Mode	Diff Coll	Cyclic	Coll.	Diff Cyclic	Diff Coll.	Cyclic	Coll	Diff Cyclic
SAS	ES	ES	CS	RP	Pitch Rate Damping	Roll Rate Damping	Direct	Sideslip hold, $V_a' > 35$ kts Yaw Rate Damping, $V_a' < 35$ kts
ATT I	ES	ES	CS	RP (ψ_c)	Pitch Attitude Hold	Roll Attitude Hold	Direct	Sideslip Hold, $V_a' > 35$ kts Heading Hold, $V_a' < 35$ kts
ATT II	ES	ES	CS	RP (ψ_c)	Pitch Attitude Hold	Roll Attitude Hold	Vertical Velocity Hold	Sideslip Hold, $V_a' > 35$ kts Heading Hold, $V_a' < 35$ kts
VEL I	ES	ES	CS	RP (ψ_c)	Forward Velocity Rate Hold	Lateral Velocity Rate or Course Rate Hold	Vertical Velocity Hold	Sideslip Hold, $V_a' > 35$ kts Heading Hold, $V_a' < 35$ kts
VEL II	ES	ES	CS	RP (ψ_c)	Forward Velocity Hold	Lateral Velocity or Course Hold	Vertical Velocity Hold	Sideslip Hold, $V_a' > 35$ kts Heading Hold, $V_a' < 35$ kts
VEL III	SAC	SAC	CS	RP (ψ_c)	Forward Velocity Hold	Lateral Velocity Hold	Vertical Velocity Hold	Sideslip Hold, $V_a' > 35$ kts Heading Hold, $V_a' < 35$ kts
AUTO	GUID	GUID	GUID	FCL (ψ_c)	Forward Velocity Hold	Lateral Velocity Hold	Vertical Velocity Hold	Sideslip Hold, $V_a' > 35$ kts Heading Hold, $V_a' < 35$ kts to Hover Yaw into Wind, Hover

NOTE

ES	Electric Stick	GUID	Guidance
CS	Collective Stick	FCL	Flight Control Laws
RP	Rudder Pedals	V_a'	Effective Speed
SAC	Side-arm Controller	ψ_c	Yaw Rate Command

TABLE III-5
PILOT'S CONTROLS PARAMETERS

Control	Control Travel	Command Laws	
		SAS (p_c, q_c, r_c deg/sec)	ATT 1 (θ_c, ϕ_c, ψ_c deg)
Longitudinal Stick (δ_{ep}, in)	±5 5	$q_c = 47\left(\frac{\delta_{ep}\ -0\ 1}{5\ 4}\right), \delta_{ep} \geqslant 0\ 1$ $= 0, -0\ 1 < \delta_{ep} < 0\ 1$ $= 47\left(\frac{\delta_{ep} + 0\ 1}{5\ 4}\right), \delta_{ep} \leqslant -0\ 1$	$\theta_c = 45\left(\frac{\delta_{ep}\ -0\ 1}{5\ 4}\right), \delta_{ep} \geqslant 0\ 1$ $= 0, -0\ 1 < \delta_{ep} < 0\ 1$ $= 45\left(\frac{\delta_{ep} + 0\ 1}{5\ 4}\right), \delta_{ep} \leqslant -0\ 1$
Lateral Stick (δ_{ap}, in)	±3 6	$p_c = 47\left(\frac{\delta_{ap}\ -0\ 1}{3\ 5}\right), \delta_{ap} \geqslant 0\ 1$ $= 0, -0\ 1 < \delta_{ap} < 0\ 1$ $= 47\left(\frac{\delta_{ap} + 0\ 1}{3\ 5}\right), \delta_{ap} < -0\ 1$	$\phi_c = 60\left(\frac{\delta_{ap}\ 0\ 1}{3\ 5}\right), \delta_{ap} \geqslant 0\ 1$ $= 0, -0\ 1 < \delta_{ap} < 0\ 1$ $= 60\left(\frac{\delta_{ap} + 0\ 1}{3\ 5}\right), \delta_{ap} < -0\ 1$
Pedals (δ_{rp}, in)	±2 3	$r_c = 8\ 5\left(\frac{\delta_{rp}\ -0\ 1}{2\ 2}\right), \delta_{rp} \geqslant 0\ 1$ $= 0, -0\ 2 < \delta_{rp} < 0\ 2$ $= 8\ 5\left(\frac{\delta_{rp} + 0\ 1}{2\ 2}\right), \delta_{rp} < -0\ 1$	$\psi_c = 17\left(\frac{\delta_{rp}\ -0\ 1}{2\ 2}\right), \delta_{rp} \geqslant 0\ 1$ $= 0, -0\ 1 < \delta_{rp} < 0\ 1$ $= 17\left(\frac{\delta_{rp} + 0\ 1}{2\ 2}\right), \delta_{rp} < -0\ 1$
Collective Lever (δ_{cp}, in)	12 8	Raw Collective as for bare helicopter	Raw Collective as for bare helicopter
Longitudinal Side Arm Controller (δ_{ep}, deg)	± 10	Not Used	Not Used
Lateral Side Arm (δ_{ap}, deg)	± 10	Not Used	Not Used

TABLE III-5 (CONT)

Control	Control Travel	Command Laws: ATT 2 (V^h_{cz} ft/sec)	Command Laws: VEL 1 (V ft/sec/sec)
Longitudinal Stick (δ_{ep}, in)	±5 5	Same as ATT 1	$V^h_{cx} = 9\left(\frac{\delta_{ep}-0\ 1}{5\ 4}\right), \delta_{ep} \geq 0\ 1$ $= 0, -0\ 1 < \delta_{ep} < 0\ 1$ $= 9\left(\frac{\delta_{ep}+0\ 1}{5\ 4}\right), \delta_{ep} \leq -0\ 1$
Lateral Stick (δ_{ap}, in)	±3 6	Same as ATT 1	$\dot{V}^h_{cy} = 6\left(\frac{\delta_{ap}-0\ 1}{3\ 5}\right), \delta_{ap} \geq 0\ 1$ $= 0, -0\ 1 < \delta_{ap} < 0\ 1$ $= 6\left(\frac{\delta_{ap}+0\ 1}{3\ 5}\right), \delta_{ap} \leq -0\ 1$
Pedals (δ_{rp}, in)	±2 3	Same as ATT 1	Same as ATT 1
Collective Lever (δ_{cp}, in)	12 8	$V^h_{cz} = 40 + 80\left(\frac{\delta_{cp}}{12\ 8}\right)$	Same as ATT 2
Longitudinal Side Arm Controller (δ_{ep}, deg)	±10	Not Used	Not Used
Lateral Side Arm (δ_{ap}, deg)	±10	Not Used	Not Used

TABLE III-5 (CONT)

Control	Control Travel	Command Laws: VEL 2 (V ft/sec)	Command Laws: VEL 3 (V ft/sec)
Longitudinal Stick (δ_{ep}, in)	±5 5	$V^h_{c_x} = 36\left(\frac{\delta_{ep} - 0\ 1}{5\ 4}\right),\ \delta_{ep} \geq 0\ 1$ $= 0,\ -0\ 1 < \delta_{ep} < 0\ 1$ $= 36\left(\frac{\delta_{ep} + 0\ 1}{5\ 4}\right),\ \delta_{ep} \leq -1\ 0$	Not Used
Lateral Stick (δ_{ap}, in)	±3 6	$V^h_{cy} = 24\left(\frac{\delta_{ap} - 0\ 1}{3\ 5}\right),\ \delta_{ap} \geq 0\ 1$ $= 0,\ -0\ 1 < \delta_{ap} < 0\ 1$ $= 24\left(\frac{\delta_{ap} + 0\ 1}{3\ 5}\right),\ \delta_{ap} < 0\ 1$	Not Used
Pedals (δ_{rp}, in)	±2 3	Same as ATT 1	Same as ATT 1
Collective Lever (δ_{cp}, in)	±12 8	Same as ATT 2	Same as ATT 2
Longitudinal Side Arm Controller (δ_{ep}, deg)	±10	Not Used	$V^h_{cx} = 20\left(\frac{\delta_{ep} - 2\ 0}{8\ 0}\right) + 4\int\left(\frac{\delta_{ep} - 2\ 0}{8\ 0}\right) dt,$ $\delta_{ep} \geq 2\ 0^\circ$ $= 0,\ -2\ 0^\circ < \delta_{ep} < 2\ 0^\circ$ $= 20\left(\frac{\delta_{ep} + 2\ 0}{8\ 0}\right) + 4\int\left(\frac{\delta_{ep} + 2\ 0}{8\ 0}\right) dt$ $\delta_{ep} \leq 2\ 0^\circ$
Lateral Side Arm (δ_{ap}, deg)	±10	Not Used	$V^h_{cy} = 20\left(\frac{\delta_{ap} - 2\ 0}{8\ 0}\right) + 4\int\left(\frac{\delta_{ap} - 2\ 0}{8\ 0}\right) dt,$ $\delta_{ap} \geq 2\ 0^\circ$ $= 0,\ -2\ 0^\circ < \delta_{ap} < 2\ 0^\circ$ $= 20\left(\frac{\delta_{ap} + 2\ 0}{8\ 0}\right) + 4\int\left(\frac{\delta_{ap} - 2\ 0}{8\ 0}\right) dt$ $\delta_{ap} \leq 2\ 0^\circ$

TABLE III-6
COMMANDS DISPLAYED

Mode	Display ARU-2B/A Flight Director Indicator		
	Horizontal Needle	Vertical Needle	Collective Bug (Glide Slope Index)
SAS	Incremental differential collective pitch rate command	Incremental cyclic roll rate command	Incremental collective command
ATT 1	Incremental differential collective pitch attitude command	Incremental cyclic roll command	Same as SAS
ATT 2	Same as ATT 1	Same as ATT 1	Incremental vertical velocity command
VEL 1	Incremental forward velocity command in Heading Vertical Frame	Incremental lateral velocity command in Heading Vertical Frame	Same as ATT 2
VEL 2	Same as VEL 1	Same as VEL 1	Same as ATT 2
VEL 3	Same as VEL 1	Same as VEL 1	Same as ATT 2
AUTO	Forward velocity error in Heading Vertical Frame	Lateral velocity error in Heading Vertical Frame	Vertical velocity error

TABLE III-7
FDI DISPLAY SENSITIVITIES

Differential Collective Command Error	0 4 in /in
Cyclic Command Error	0 4 in /in
Collective Command Error	0 5 in /in
Pitch Attitude Command Error	2 87 in /rad
Roll Attitude Command Error	1 43 in /rad
Forward Velocity Command Error	-0 05 in /ft/sec
Lateral Velocity Command Error	+0 025 in /ft/sec
Vertical Velocity Command Error	-0 1 in /ft/sec

Note: Units refer to inches of command bar displacement of the ARU-2B/A Flight Director Indicator per unit (as appropriate) of command error 0 01 inches is considered the minimum discernable command bar displacement

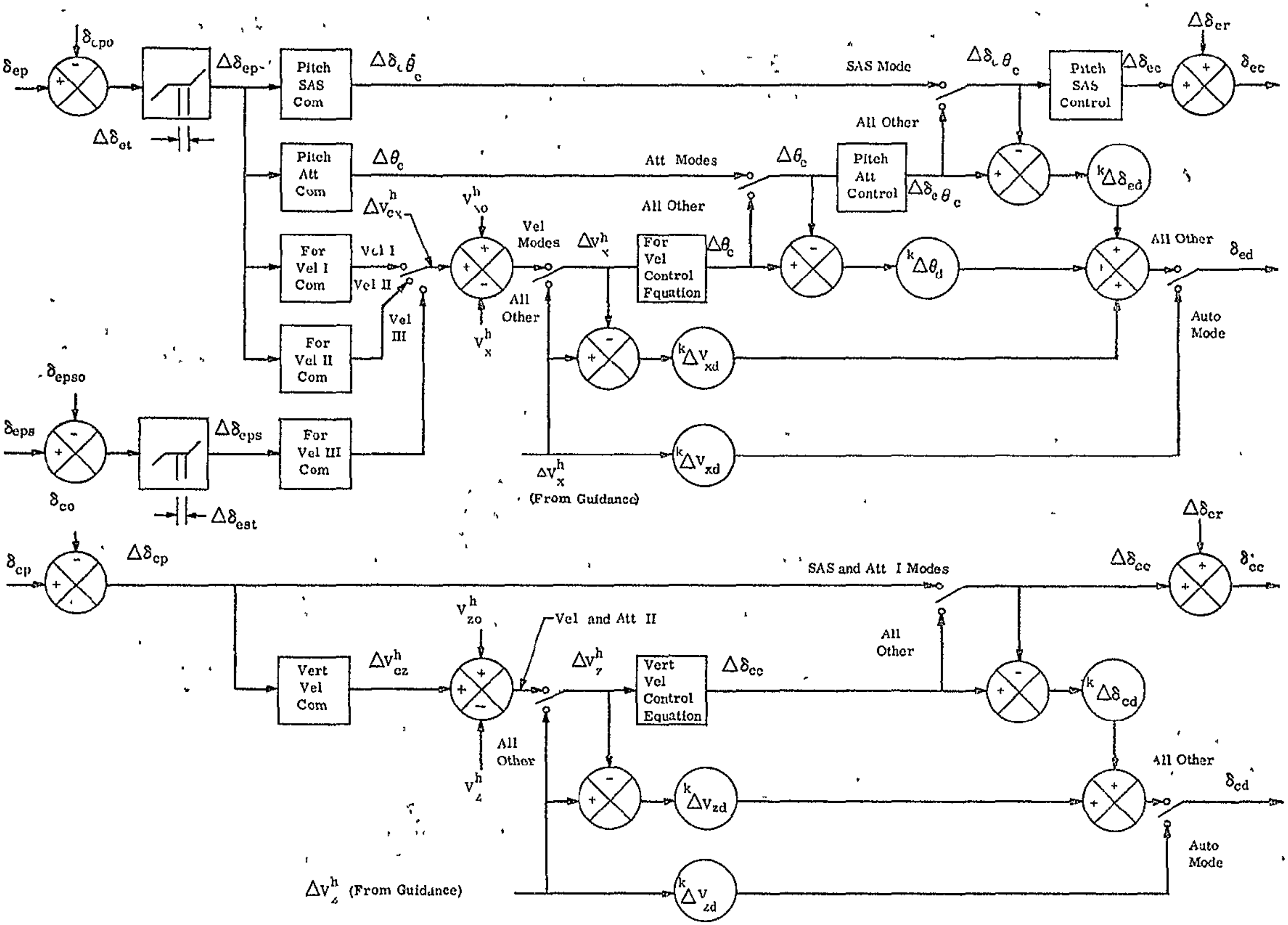

Figure III-3. Longitudinal Flight Control Laws

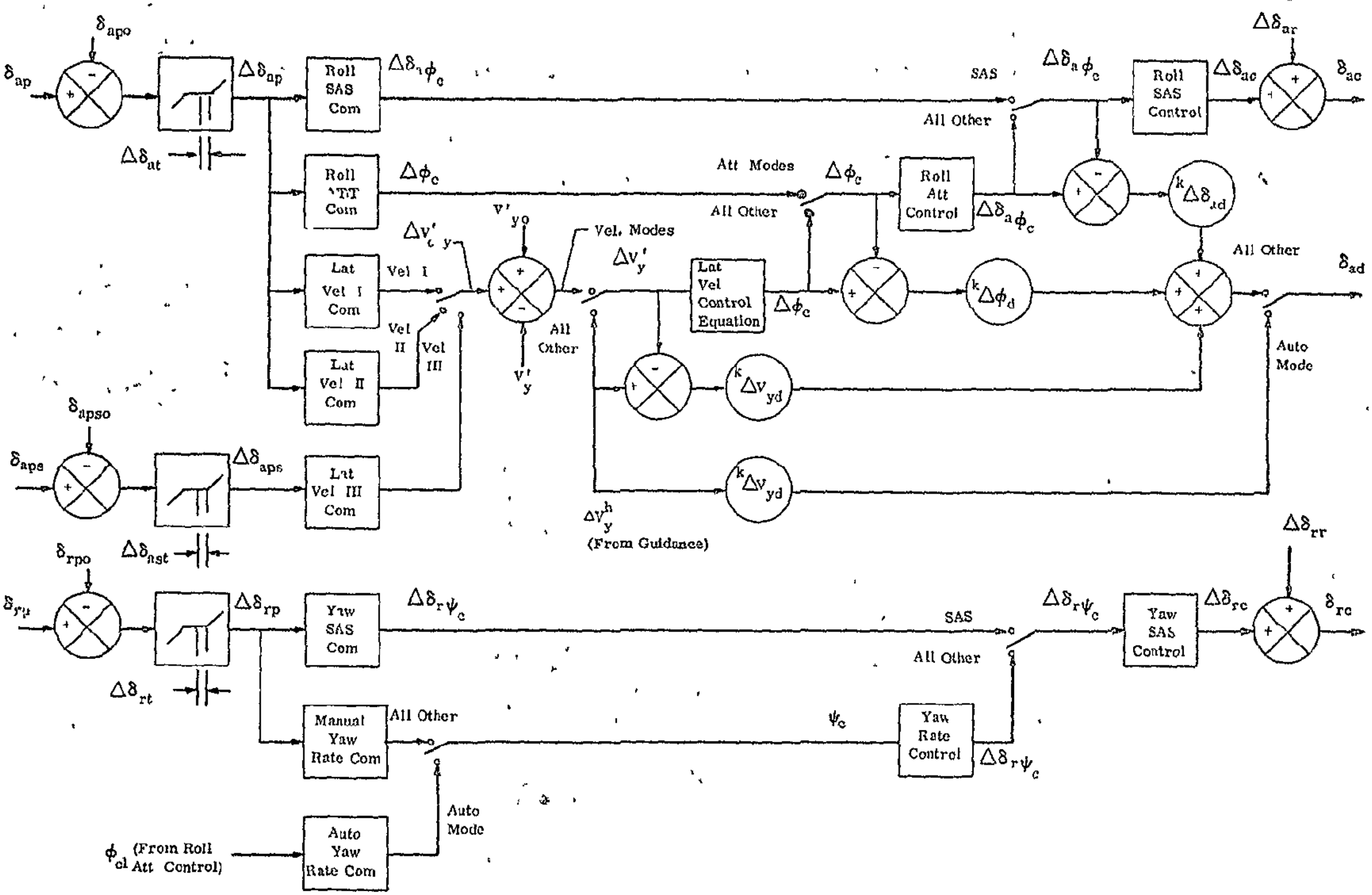

Figure III-4. Lateral Flight Control Laws

TABLE III-8
PITCH DIFFERENTIAL COLLECTIVE FCS LAWS

$\Delta\delta_{ec}$	=	$K_{\theta H}(1+\frac{0\ 2}{s})\,F$	
F	=	$\Delta\delta_{ep} - 6\ 5q$	for SAS
	=	$2\ 0\,\Delta\delta_{ep} - 6\ 5q + 13\ 5\,(\theta_o - \theta)$	for ATT 1 & 2
	=	$(0\ 2 + \frac{0\ 36}{s} + \frac{0\ 034}{s^2})\,\Delta\delta_{ep} - 6\ 5q + 13\ 5\,(\theta_o - \theta) + 0\ 2\,(1 + \frac{0\ 1}{s})\,(V^h_{xo} - V^h_x)$	for VEL 1
	=	$(1\ 35 + \frac{0\ 41}{s} + \frac{0\ 027}{s^2})\,\Delta\delta_{ep} - 6\ 5q + 13\ 5\,(\theta_o - \theta) + 0\ 2\,(1 + \frac{0\ 1}{s})\,(V^h_{xo} - V^h_x)$	for VEL 2
	=	$(16\ 2 + \frac{3\ 24}{s} + \frac{0\ 32}{s^2})\,\Delta\delta_{eps} - 6\ 5q + 13\ 5\,(\theta_o - \theta) + 0\ 2\,(1 + \frac{0\ 1}{s})\,(V^{h'}_{xo} - V^h_x)$	for VEL 3
	=	$(0\ 2 + \frac{0\ 02}{s})\,\Delta V^h_{gx} - 6\ 5q + 13\ 5\,(\theta_o - \theta)$	for AUTO

Symbols (in order of appearence above)

$\Delta\delta_{ec}$,	incremental differential collective command (inches)
$K_{\theta H}$,	hysteresis compensation gain in pitch (see text)
$\Delta\delta_{ep}$,	incremental electric stick pitch input (inches)
q,	angular rate about the Y body axis (rad/sec)
θ_o,	initial value of θ (radians)
θ,	Euler pitch attitude (radians)
V^h_{xo},	initial value of V^h_x (ft/sec)
V^h_x,	forward velocity in vertical heading frame (ft/sec)
$\Delta\delta_{eps}$,	incremental side arm controller pitch input (max ±0 5 inches)
V^h_{gx},	forward velocity error from guidance laws in vertical heading frame (ft/sec)

TABLE III-9
ROLL CYCLIC FCS LAWS

$\Delta\delta_{ac}$	=	$K_{\phi H}\left(1+\frac{0.2}{s}\right)F$	
F	=	$\Delta\delta_{ap} - 7.5p$	for SAS
	=	$4.5\,\Delta\delta_{ap} - 7.5p + 15.0\,(\phi_o - \phi)$	for ATT 1 & 2
	=	$\left(0.23+\frac{0.4}{s}+\frac{0.04}{s^2}\right)\Delta\delta_{ap} - 7.5p + 15.0\,(\phi_o-\phi) + 0.23\left(1+\frac{0.1}{s}\right)(V^h_{yo} - V^h_y)$	for VEL 1, $V'_a < 35$ knots
	=	$\left(0.23+\frac{0.4}{s}+\frac{0.04}{s^2}\right)\frac{V'_a}{60}\,\Delta\delta_{ap} - 7.5p + 15.0\,(\phi_o-\phi) + 0.23\left(1+\frac{0.1}{s}\right)(V^h_{yo} - V'_a\xi)$	for VEL 1, $V'_a > 35$ knots
	=	$\left(1.5+\frac{0.45}{s}+\frac{0.03}{s^2}\right)\Delta\delta_{ap} - 7.5p + 15.0\,(\phi_o-\phi) + 0.23\left(1+\frac{0.1}{s}\right)(V^h_{yo} - V^h_y)$	for VEL 2, $V'_a < 35$ knots
	=	$\left(1.5+\frac{0.45}{s}+\frac{0.03}{s^2}\right)\frac{V'_a}{60}\,\Delta\delta_{ap} - 7.5p + 15.0\,(\phi_o-\phi) + 0.23\left(1+\frac{0.1}{s}\right)(V^h_{yo} - V'_a\,\xi)$	for VEL 2, $V'_a > 35$ knots
	=	$\left(5.4+\frac{1.6}{s}+\frac{0.01}{s^2}\right)\Delta\delta_{aps} - 7.5p + 15.0\,(\phi_o-\phi) + 0.23\left(1+\frac{0.1}{s}\right)(V^h_{yo} - V^h_y)$	for VEL 3
	=	$0.23\left(1+\frac{0.1}{s}\right)V^h_y - 7.5p + 15.0\,(\phi_o-\phi)$	for AUTO

Symbols (in order of appearance above)

$\Delta\delta_{ac}$,	incremental roll cyclic command (inches)
$K_{\phi H}$,	hysteresis compensation gain in roll (see text)
$\Delta\delta_{ap}$,	incremental electric stick roll input (inches)
p,	angular rate about X body axis (radians/sec)
ϕ_o,	initial value of ϕ (radians)
ϕ,	Euler roll attitude (radians)
V^h_{yo},	initial value of V^h_y (ft/sec)
V^h_y,	lateral velocity in vertical heading frame (ft/sec)
V'_a,	effective speed (ft/sec)
ξ	arctan (V^{an}_y/V^{an}_x), course (radians)
V^{an}_y,	lateral velocity in approach navigation frame (ft/sec)
V^{an}_x,	forward velocity in approach navigation frame (ft/sec)
$\Delta\delta_{aps}$,	incremental side arm controller roll input (max ±1.25 inches)

TABLE III-10
YAW CYCLIC FCS LAWS

$\Delta\delta_{rc}$	=	$K_{\psi H}\ (1+\frac{0\ 2}{s})\ (\Delta\delta_{rp} - 15r)$	for SAS, $V'_a < 35$ knots
	=	$K_{\psi H}\ (1+\frac{0\ 2}{s})\ (\Delta\delta_{rp} - 15r - \frac{19\beta}{1+0\ 5s})$	for SAS, $V'_a > 35$ knots
	=	$K_{\psi H}\ (1+\frac{0\ 2}{s})\ [\frac{1\ 8}{s}\Delta\delta_{rp} + 14\ (\psi_o - \psi) + 1\ 9\ \Delta\delta_{rp} - 15r\ ]$	for all ATT and VEL modes and $V'_a < 35$ knots
	=	$K_{\psi H}\ (1+\frac{0\ 2}{s})\ [\ 1\ 9\ \Delta\delta_{rp} - 15r - \frac{19\beta}{1+0\ 5s}]$	for all ATT and VEL modes and $V'_a > 35$ knots
		$+ 2\ 3\ (1+\frac{0\ 2}{s})\ \phi_c$	
	=	$K_{\psi H}\ (1+\frac{0\ 2}{s})\ [\ 14\ (\psi_o - \psi) - 15r\ ]$	for AUTO, $V'_a < 35$ knots
	=	$K_{\psi H}\ (1+\frac{0\ 2}{s})\ [\frac{14}{V_x^h}\ \frac{g}{1+6s}\ \phi_c + 14\ (\psi_o - \psi) - 15r\ ]$	for AUTO in HOVER and LAND
	=	$K_{\psi H}\ (1+\frac{0\ 2}{s})\ (-15r - \frac{19\beta}{1+0\ 5s}) + 2\ 3\ (1+\frac{0\ 2}{s})\ \phi_c$	for AUTO, $V'_a > 35$ knots

Symbols (in order of appearance above)

$\Delta\delta_{rc}$,	incremental differential cyclic command (inches)
$K_{\psi H}$,	hysteresis compensation gain in yaw (see text)
$\Delta\delta_{rp}$,	incremental rudder pedal input (inches)
V'_a	effective speed (ft/sec)
r,	angular rate about Z body axis (radians/sec)
β,	side slip angle (radians)
ψ_o,	initial value of ψ (radians)
ψ,	Euler yaw attitude (radians)
ϕ_c,	roll attitude command (radians)

TABLE III-11
COLLECTIVE FCS LAWS

For SAS

$\Delta\delta_{cc} = \Delta\delta_{cp}$

For ATT 2, VEL 1, VEL 2, VEL 3 Modes,

$$\Delta\delta_{cc} = -0\ 2\ (1+\frac{1}{s})\ (V^h_{zo} - V^h_z + 6\ 25\ \Delta\delta_{cp}) + 3\ (1 - \cos\ \Phi)$$

For AUTO Mode ,

$$\Delta\delta_{cc} = -0\ 2\ (1+\frac{1}{s})\Delta V^h_z + 3\ (1 - \cos\ \phi)$$

Symbols (in order of appearance above)

$\Delta\delta_{cc}$, incremental collective command (inches)

V^h_{zo}, initial value of V^h_z (ft/sec)

V^h_z, vertical velocity in Vertical Heading Frame (ft/sec)

$\Delta\delta_{cp}$, incremental collective stick input (inches)

Φ, Euler roll attitude (radians)

ΔV^h_z, vertical velocity error from guidance (ft/sec)

In these laws, reference is made to $K_{\theta H}$, $K_{\phi H}$, $K_{\psi H}$, hysteresis gain compensations With the level of hysteresis assumed for the EISS and power boost, the limit cycle amplitude (as high as ± 1 5 degrees of pitch in the differential collective channel) was unacceptable Figure III-5 shows the pitch attitude loop without hysteresis compensation being stepped by successive ± 2° steps The 140 knot condition is illustrated to bring out the effect since it is more pronounced at higher air speed

To reduce the amplitude of the limit cycle, a Tustin method difference equation for a conventional lead/lag hysteresis compensator of the form, (0 0625 s + 1) / (0 0125 s + 1), was developed and included in the simulation However, it was found that the difference equation for this compensator had underdamped characteristics at all sampling rates below about 80 updates/sec As a result of this when a run was made at an update rate of 32 times/sec, this compensator actually increased the amplitude of the limit cycle

Since it was not desired to increase the required sampling rate for the airborne system, other forms of difference equations were investigated It was found that by using a first backwards difference method, a difference equation for the lead/lag compensator could be developed that was not underdamped at update rates of 32 times/sec However, when this difference equation was programmed in the simulation and a run was made, it was found that only a 20% reduction in the amplitude of the limit cycle was obtained and this was still unacceptable

At this point, conventional lead/lag compensators were abandoned and a look was taken at variable gain compensation techniques Basically, these techniques are ones where the gain is increased as required to overcome the deadzone that is causing the hysteresis

Theoretically, the gain required to compensate for pure hysteresis is,

$$K_H = \frac{|\Delta\delta_c| + \Delta\delta_H}{|\Delta\delta_c|}$$

where $\Delta\delta_c$ = command input
$\Delta\delta_H$ = half the width of the hysteresis deadzone

However, in order to obtain exact compensation with this technique, there must be no system lags between the compensation and the hysteresis and the hysteresis must be pure hysteresis Since this is never the case in real physical systems, the gain must be limited to prevent stability problems In the simulation, this type of gain was mechanized on the incremental pitch command (proportional part of proportional plus integral term) and was limited to a maximum value of two

$$k_{\delta_e/H} = \frac{|\Delta\delta_e| + \Delta\delta_{e/H}}{|\Delta\delta_e|} \leqslant 2\ 0$$

A run was then made with this variable gain hysteresis compensator and it was found that it significantly reduced the amplitude of the limit cycle as shown in Figure III-6 which repeats the conditions of Figure III-5 with the compensator To insure that an exact knowledge of the actual hysteresis in the vehicle is not required with this technique, additional tests were made, one with the hysteresis in the vehicle set to zero and one with it set to double the expected value No deleterious effects to imperfect compensation resulted and the technique was incorporated into the FCS laws

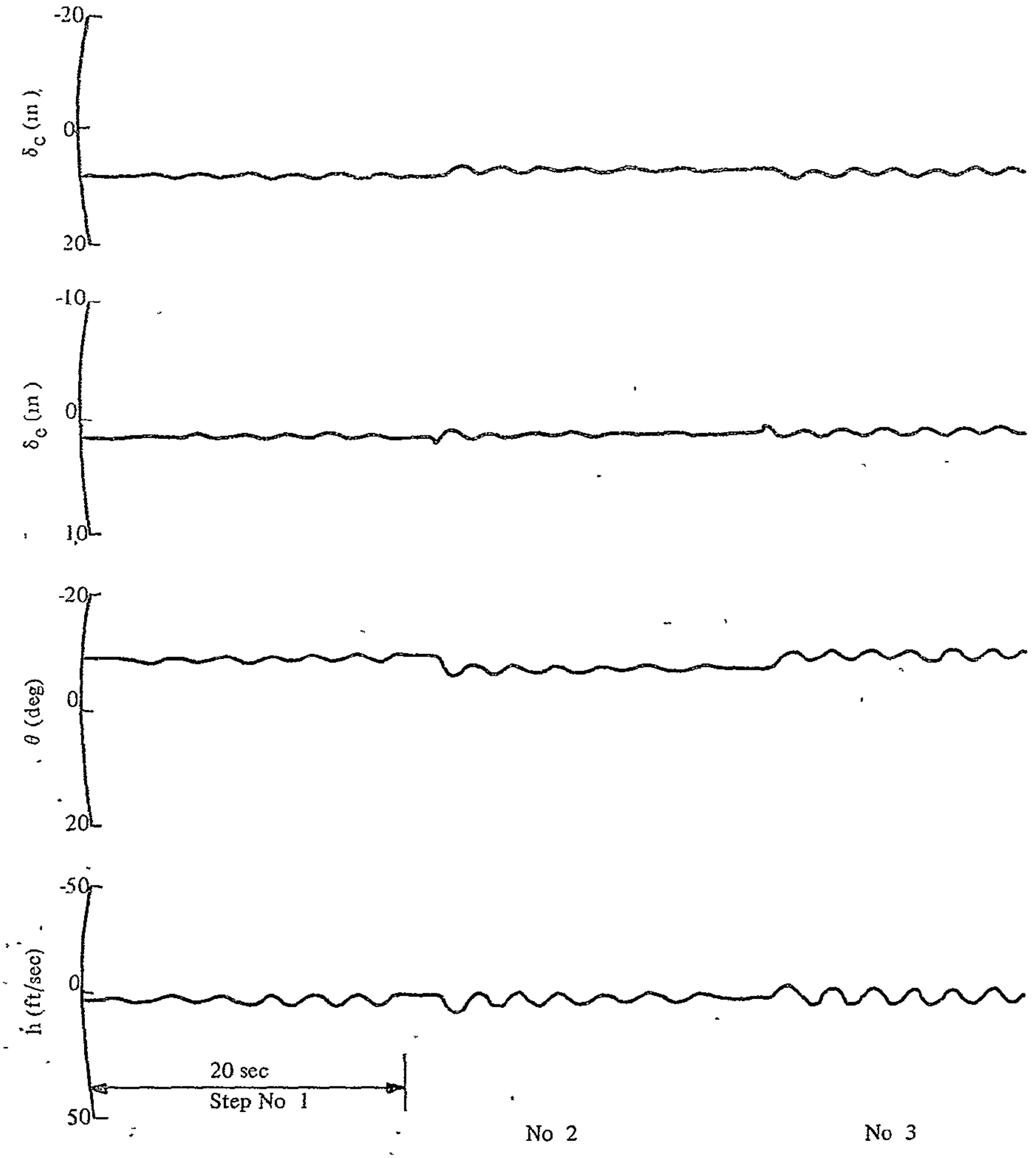

Figure III-5 Pitch Limit Cycle with No Hysteresis Comp

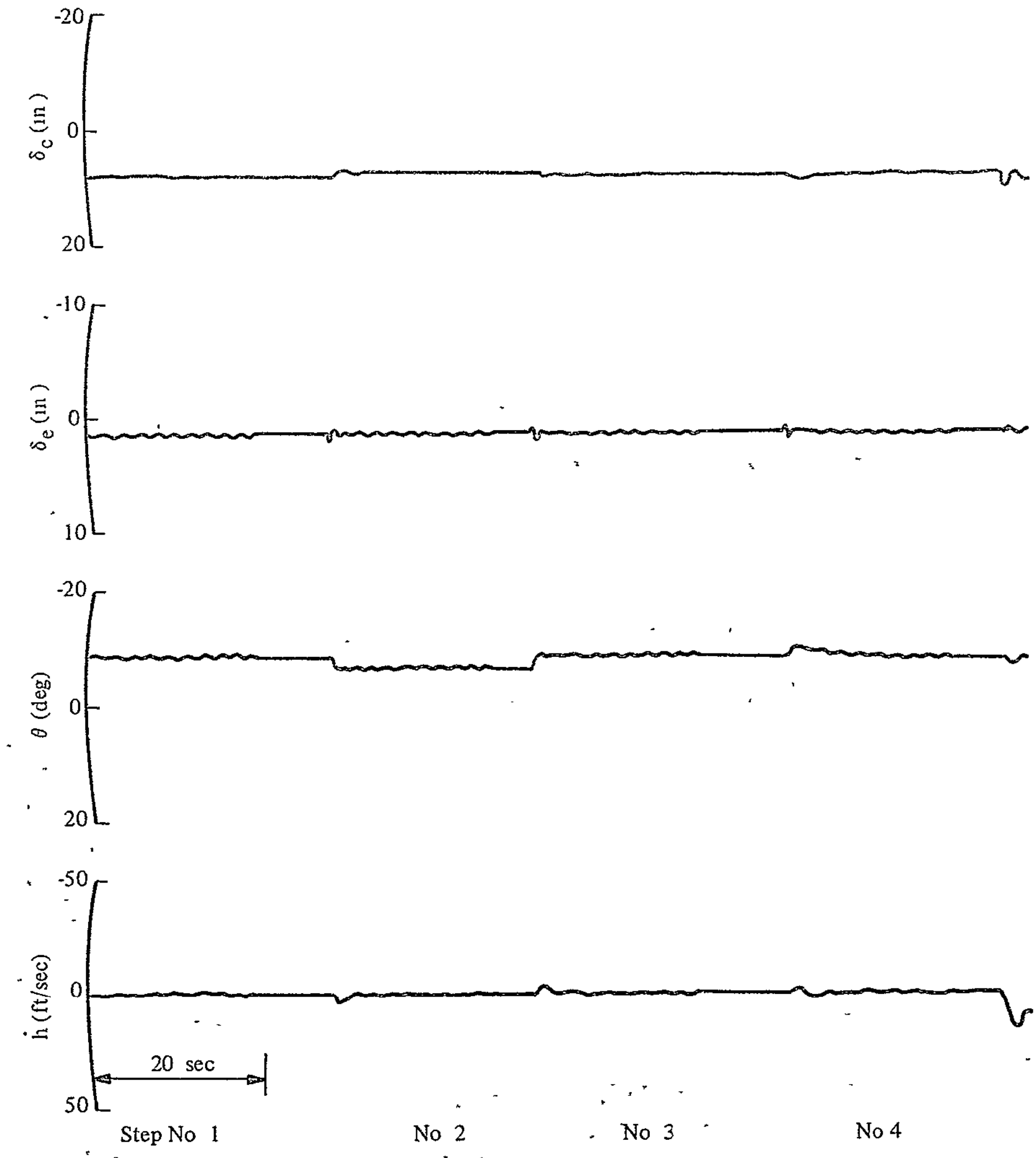

Figure III-6 Pitch Limit Cycle with Variable Gain Comp

In these tables, reference is made to Va', the effective speed Va' is defined as:

$$V_a = V_{af}, \quad \text{if } V_{af} \leq V_x^h$$
$$= V_x^h, \quad \text{if } V_{af} \leq V_x^h$$

where $$V_{af} = \frac{V_a}{1 + 2s}$$

The pitch attitude commands are limited in all modes except SAS This is required, not only by safety considerations, but because step changes in forward velocity resulted in unacceptable pitch transients The pitch angle command was limited to ± 0 174 radians about the trim pitch attitude The pitch trim altitude is approximated by,

$$\theta_{trim} = 0\ 1438, \quad \text{if } V_{af} \leq 35 \text{ knots}$$
$$= 0\ 165 - 0\ 297 \left(\frac{V_{af}}{236}\right)^2, \text{ if } V_{af} > 35 \text{ knots}$$

The FCS laws are expressed in the Tables III-8, 9, 10, and III-11 in terms of Laplacian operator, s Since difference equations are required for digital mechanization, Tustin's method is employed In this method, the Laplacian operator, s, is approximated by a difference equation of the form

$$s = \frac{2}{\Delta t}\left(\frac{1 - \Delta}{1 + \Delta}\right),$$

where Δt is the update interval and Δ is the backwards difference operator This method was selected because its accuracy is more than adequate for that required in the flight control and guidance laws, it is easy to program, it is guaranteed to preserve stability and it has the cascading property This last feature is important in the development of control laws since it permits the difference equation for any function in a loop to be modified independently of the difference equations for any other functions that might exist in the loop

Using this method, difference equations were derived for the integrators, filters, and lead/lag networks in the flight control laws The resulting difference equations are as follows

(1) Integrator

$$y = \left(\frac{1}{s}\right) x$$

$$y_n = y_{n-1} + .5\,\Delta t\,(x_n + x_{n-1})$$

(2) Filter

$$y = \left(\frac{1}{\tau s + 1}\right) x$$

$$y_n = \left[x_n + x_{n-1} + (-1 + b) y_{n-1}\right] / (1 + b)$$

where $b = 2\tau/\Delta t$

(3) Lead/lag

$$y = \left(\frac{\tau_{lead}\ s + 1}{\tau_{lag}\ s + 1}\right)$$

$$y_n = \left[(1 + a)\, x_n + (1 - a)\, x_{n-1} + (-1 + b)\, y_{n-1}\right] / (1 + b)$$

where $a = 2\,\tau_{lead}/\Delta t$

$b = 2\,\tau_{lag}/\Delta t$

C. GUIDANCE LAWS

1 Guidance Requirements and Design Approach

a General

As discussed in Section I, the primary emphasis in this study was on the development of flight control laws for a Digital Flight Control and Landing System (DFCLS) The emphasis on the development of guidance laws was secondary and the primary purpose of it was to obtain laws which would be adequate for evaluating the flight control laws on a typical landing mission in both ground based simulators and airborne flight tests. In the airborne system, the laws developed in this study will be used in the Guidance II Mode of operation of the DFCLS For this purpose, the following general requirements for the guidance laws were established

(1) The guidance laws must be adequate to evaluate the flight control laws on a typical landing mission but need not be optimum However, the guidance profile must be one from which a safe and satisfactory landing of the helicopter can be made

(2) The guidance laws must be compatible with the baseline system They must accept their inputs from the radar updated strapdown system and output velocity error commands to the flight control laws in the heading vertical frame (HVF)

Based on these requirements, the basic design approach was to develop a nominal profile guidance system. This approach was selected over the more complex predictive guidance and terminal guidance approaches for the following reasons

(1) Nominal profiles of the constant speed glide type are the standard type currently flown by helicopters to make safe and satisfactory landings

(2) Nominal profile guidance systems are simple to develop, generally have small computer requirements relative to predictive and terminal guidance systems and are adequate for evaluating flight control laws during landing

For the selected nominal guidance system approach, a nominal guidance profile type was selected and the detailed characteristics of this profile in the ANF were developed A method for generating the velocity error commands between the total ANF profile commands and the actual helicopter flight conditions were developed To obtain compatability with the flight control system transformations were also developed for converting the velocity command errors to the HVF A detailed description of the design approach in each of these areas is discussed in the following sections.

b. Selection of Nominal Profile

A profile of the constant speed glide type was selected for the guidance laws since it is the standard type flown by helicopters during landing and is adequate to evaluate flight control laws For this profile, the following detailed requirements were established

(1) The profile will begin at any acceptable conditions the helicopter is acquired at and end at the touchdown point The helicopter will not be required to fly to a fixed acquisition point

(2) The profile will not require the helicopter to fly up or down to a fixed glide slope interception point
(3) The profile will not require the helicopter to slow down prematurely such that excessive time and fuel is required during the landing
(4) There will be no discontinuities in the commands along the profile

The basic design approach in developing a detailed characteristics of a nominal constant speed glide profile was to develop one that was continuous from acquisition to touchdown and not fixed to any specific acquisition conditions To do this, the profile was divided into the following phases in the ANF longitudinal plane (1) acquisition, (2) level flight deceleration, (3) glide acquisition, (4) glide transition, (5) glide, (6) flare, (7) hover, and (8) land These phases are illustrated in Figure III-7 In this figure, the solid portions of the profile are fixed and the dotted portions float depending on the conditions the helicopter is acquired at The desired profile characteristics for all phases are listed in Table III-12 A description of each phase and its purpose is as follows

(1) Land - The land phase profile is a straight vertical descent from hover to touchdown For a given desired hover attitude and desired sink rate at touchdown, the profile for this phase is fixed The purpose of this phase is to smoothly accelerate the helicopter from the zero hover sink rate to the desired sink rate for touchdown and hold it at this rate until touchdown occurs
(2) Hover - The hover phase profile is a constant altitude forward deceleration flight from the end of flare to stationary hover over the pad For a given hover attitude and forward speed at the end of flare, this phase is fixed The purpose of this phase is to smoothly decelerate the helicopter from the specified range rate at the end of flare to stationary hover over the pad and to provide time to satisfy acceptable conditions for landing in the presence of disturbances
(3) Flare - The flare phase profile is a constant forward and constant vertical deceleration flight from the desired forward speed and sink rate at the end of glide to the desired forward speed and zero sink rate at the end of flare For given desired conditions at the end of glide and end of flare, this phase is fixed The purpose of this phase is to smoothly brake the forward speed and sink rate of the helicopter at deceleration rates that are acceptable to the pilot
(4) Glide - The glide phase profile is a constant speed, constant glide slope glide from the glide slope interception point to the beginning of flare The length of this phase is not fixed since its purpose is to bring the helicopter from the altitude at which it is acquired to the beginning of flare at an acceptable glide slope
(5) Glide Transition - The glide transition phase profile is a constant speed, constant vertical acceleration flight from level flight at the acquisition altitude to the sink rate for the desired glide slope For a given desired vertical acceleration, this phase is fixed relative to the floating glide interception point The purpose of this phase is to provide a smooth transition from level flight to glide
(6) Glide Acquisition - The glide acquisition phase profile is a constant speed, constant altitude flight from the end of the level flight deceleration phase to the glide transition point The length of this phase is fixed relative to the glide transition point. The purpose of this phase is to allow for a reasonable length of constant speed flight prior to glide transition

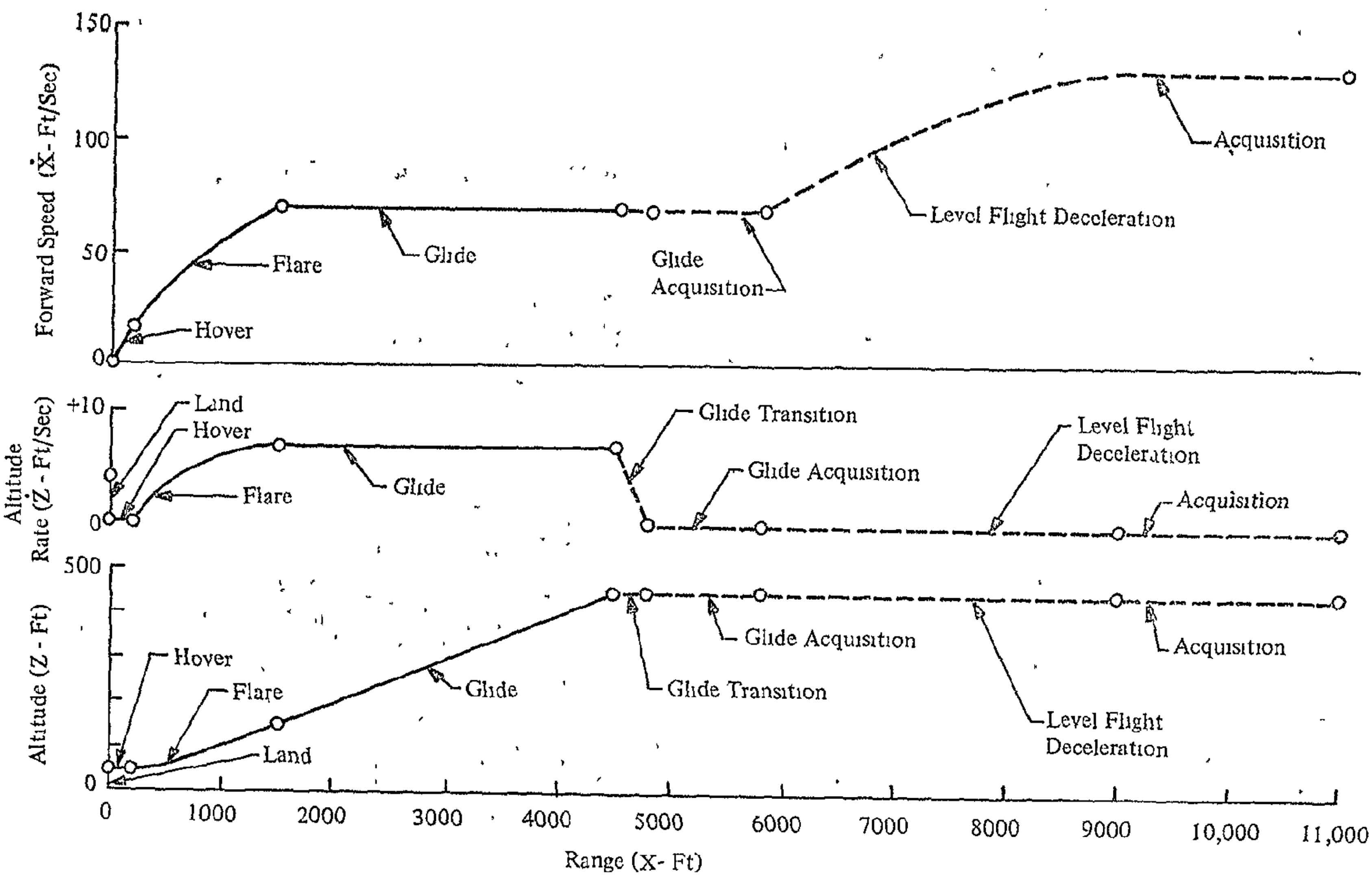

Figure III-7 Normal Profile Phases

TABLE III-12

DESIRED NOMINAL PROFILE CHARACTERISTICS

Characteristic	Description	Nominal Value
X_{sh}	Desired range at start of hover	200 ft
X_g	Desired forward glide speed	71 ft/sec
X_{sh}	Desired forward speed at start of hover	71 ft/sec
$\ddot{X}_d$	Desired forward deceleration rate during level flight deceleration and flare	2 ft/sec^2
ΔX_{ga}	Desired range increment for glide acquisition at glide speed	1000 ft
Z_h	Desired hover altitude	-50 ft
Z_l	Desired sink rate at touchdown	4 ft/sec
$\ddot{Z}_l$	Desired vertical acceleration during landing	2 ft/sec^2
Z_d	Desired vertical acceleration during glide transition	2 ft/sec^2
γ_g	Desired glide slope angle during glide	6 deg

(7) Level Flight Deceleration - The level flight deceleration phase profile is a constant altitude, constant forward deceleration flight from the velocity at acquisition to the speed desired for glide Since the velocity the helicopter can be acquired at, is not fixed, the lengths of this phase is not fixed

(8) Acquisition - The acquisition phase flight profile is a constant altitude, constant speed flight from the conditions at acquisition to the beginning of the level flight deceleration phase Since the range at acquisition is not fixed, the length of this phase is not fixed The purpose of this phase together with the level flight deceleration and glide transition phases is to prevent the helicopter from being slowed down prematurely at long distances prior to the glide transition point

The desired profile in the ANF lateral plane was defined as simply a straight centerline projected outward from the centerline of the runway

c Development Nominal Command Generation Method

In developing a method for generating the total ANF commands along the nominal profile as a function of ANF range, the basic design approach was to develop equations which could be used to generate the commands along the nominal profile in flight from the desired profile characteristics, instead of developing stored fixed profile commands This approach was selected for several reasons

(1) The in flight computed profile approach enables the helicopter to be acquired at any acceptable altitude and held at this altitude until the glide slope is intercepted It does not require the helicopter to fly up or down from the acquisition altitude to a fixed glide slope interception point

(2) This approach also enables the helicopter to be acquired at any acceptable forward speed and range and to be decelerated at a desired rate to a desired glide speed at a fixed distance and time prior to glide slope interception This insures that the helicopter will not be decelerated prematurily to a slow speed which would result in excessive time and fuel consumption during the landing

(3) This approach allows the desired nominal profile characteristics to be updated in flight through the Manual Communication Unit This eliminates the need for reading new profile programs into the airborne computer when it is desired to change the nominal profile characteristics as would be required with a stored fixed profile approach

Although not an objective during this study, the in-flight computed profile approach is also readily adaptable to predictive guidance systems In such systems, the equations for computing the nominal profile commands from the desired profile characteristics could be readily adapted to predict best new profiles from the current helicopter flight conditions

The equations necessary to compute the nominal profile commands from the desired profile characteristics were developed by first deriving the equations for computing the required range and altitude at the start of each phase from the desired profile characteristics This was done by obtaining the closed form solutions to the integrals of the desired accelerations and/or velocities during each phase These closed form solutions were then algebraically manipulated to obtain new equations for computing commands along the profile as a function of the current ANF range

For example, for a constant forward deceleration flare along the ANF x axis, the range along the flare is,

$$X = \int_0^{\Delta t_f} \int_0^{\Delta t_f} X_d \; dt\, dt$$

$$= 0.5\, \dot{X}_d \;\Delta t_f^2 + \dot{X}_{sh}\, \Delta t_f + X_{sh}$$

The time required for flare is,

$$\Delta t_f = (\dot{X}_g - \dot{X}_{sh}) / \dot{X}_d$$

Substituting this into the range equation gives the following equation for computing the range at the start of the flare as a function of the desired profile characteristics

$$X_{sf} = 0.5\, \frac{(\dot{X}_g - \dot{X}_{sh})^2}{X_d} + \dot{X}_{sh}\, \frac{(\dot{X}_g - \dot{X}_{sh})}{X_d} + X_{sh}$$

Algebraic manipulation of this equation gives the following equation for computing the forward velocity command during the flare as a function of the current range

$$(X_c - X_{sh}) = \frac{\dfrac{-X_{sh}}{X_d} + \sqrt{\left(\dfrac{\dot{X}_{sh}}{\dot{X}_d}\right)^2 + \dfrac{2\,(X - X_{sh})}{X_d}}}{1/\ddot{X}_d}$$

$$= -\dot{X}_{sh} + \sqrt{\dot{X}_{sh}^2 + 2\ddot{X}_d\,(X - X_{sh})}$$

$$\dot{X}_c = \sqrt{\dot{X}_{sh}^2 + 2X_d\,(X - X_{sh})}$$

The equations for the remaining phases of the nominal profile were derived in a similar manner

d. Development of Guidance Laws

Guidance laws were developed using a simple control law of the following form

$$\Delta\dot{x} = k_x\,(x_c - x) + (\dot{x}_c - \dot{x})$$

where

x_C is a commanded ANF flight variable

x is a current ANF flight variable

For the forward ANF velocity law the first term was not necessary since the forward ANF range is used as the independent variable in generating the total ANF commands along the nominal profile

Nominal gains for these guidance laws were selected based on Bell's experience with automatic landing systems and the response characteristics of the flight control laws These gains were updated by simulator evaluation runs On these runs it was found that the lateral gain required to meet acceptable conditions for landing at hover resulted in unnecessarily large and rapid roll maneuvers for correcting lateral errors at longer ranges As a result of this, this gain was made a function of range All other gains remained constant

Since the commands along the nominal profile in the ANF longitudinal plane are continuous from the point of acquisition, no limits were required on the forward and vertical velocity guidance laws since large errors will not develop under normal operating conditions However, in the lateral ANF plane, the lateral position command is simple projection of the runway centerline and will not intercept the helicopter when it is laterally offset at acquisition As a result of this, this command is not continuous from acquisition and large errors can result To prevent large errors from resulting in an orbiting situation, it was necessary to develop limits for limiting the magnitude of the lateral ANF velocity error that can be commanded by the lateral position error term in the lateral guidance law This was done by limiting the lateral ANF velocity command to a value equivalent to that for a 30° heading at high speeds

To obtain compatability with the flight control system, transformations were developed to transform the ANF velocity errors to HVF velocity errors Although this could always be done simply by resolving the ANF velocity errors through the heading angle, it was not deemed desirable to do this at high speed since it would make the commanded forward speed of the helicopter in the HVF a function of the heading required to correct for lateral errors and disturbances To prevent this, it was decided to command the ANF velocity errors directly in the HVF coordinate system at high speeds This causes the actual ANF velocities of the helicopter to be lower than the commanded velocities any time that it is a heading relative to the runway centerline However, this does not affect the ability of the helicopter to fly the range and altitude profile for each phase since it only increases the flight time for each phase. An added advantage of this feature is that it lowers the forward deceleration rates required when the helicopter as at a heading relative to the centerline for correcting lateral errors

2 Detailed Description of Guidance

a. Nominal Profile

When the helicopter is first acquired, the acquisition speed and altitude are saved

$$\dot{X}_O = \sqrt{\dot{X}^2 + \dot{Y}^2}$$

$$Z_O = Z$$

The initial acquisition and desired profile characteristics are then used to compute the required range and altitude at the start of each phase in the longitudinal plane of the profile that is not defined by either the desired characteristics or the acquisition conditions The range and altitude at the start of the flare are computed as

$$X_{sf} = -0.5 \frac{(\dot{X}_g - \dot{X}_{sh})^2}{\ddot{X}_d} + \frac{\dot{X}_g \ (\dot{X}_g - \dot{X}_{sh})}{\ddot{X}_d} + X_{sh}$$

$$Z_{sf} = Z_h - 0.5 \frac{\dot{X}_g \tan \gamma_g \ (\dot{X}_g - \dot{X}_{sh})}{\ddot{X}_d}$$

The range at the start of glide is computed as

$$X_{sg} = X_{sh} - (Z_o - Z_{sf}) / \tan \gamma_g$$

The range at the start of the glide transition is computed as

$$X_{st} = X_{sg} + \frac{\dot{X}_g^2 \tan \gamma_g}{\ddot{Z}_t}$$

The range at the start of glide acquisition is computed as

$$X_{sga} = X_{st} + \Delta X_{ga}$$

The range at the start of the level flight deceleration phase is computed as

$$X_{sd} = -0.5 \frac{(\dot{X}_o - \dot{X}_g)^2}{\ddot{X}_d} + \frac{\dot{X}_o \ (\dot{X}_o - \dot{X}_g)}{\ddot{X}_d} + X_{sga}$$

The total forward velocity, altitude, and altitude rate commands for the appropriate flight phase in the longitudinal plane of the profile are then computed If the helicopter is in the initial acquisition phase ($|X| > X_{sd}$), the commands are,

$$\dot{X}_c = \dot{X}_o$$

$$Z_c = Z_o$$

$$\dot{Z}_c = 0$$

If the helicopter is in the level flight deceleration phase ($X_{sga} < |X| \leq X_{sd}$), the total commands are computed as

$$\dot{X}_c = \sqrt{\dot{X}_g^2 + 2\ddot{X}_d\,(|X| - X_{sga})}$$

$$Z_c = Z_o$$

$$\dot{Z}_c = 0$$

If the helicopter is in the glide acquisition phase ($X_{st} < |X| \leqslant X_{sga}$), the total commands are

$$\dot{X}_c = \dot{X}_g$$

$$Z_c = Z_o$$

$$\dot{Z}_c = 0$$

If the helicopter is in the glide phase ($X_{sf} < |X| \leqslant X_{sg}$) The total commands are computed as·

$$\dot{X}_c = \dot{X}_g$$

$$Z_c = Z_{sf} + (|X| - X_{sf}) \tan \delta_g$$

$$\dot{Z}_c = -\dot{X}_g \tan \delta_g$$

If the helicopter is in the glide transition phase ($X_{sg} < |X| \leqslant X_{st}$), the total commands are computed as

$$\dot{X}_c = \dot{X}_g$$

$$Z_c = Z_o$$

$$\dot{Z}_c = -\left[\frac{|X| - X_{sg}}{X_{st} - X_{sg}}\right] \dot{X}_g \tan \gamma_g$$

To be totally correct, the altitude command in this phase should be a parabolic function of time However, since the purpose of this phase, which is to proved a smooth transition to the glide without discontinuities, can be accomplished with just a linear altitude rate term, the altitude command is left constant

If the helicopter is in the flare phase ($X_{sh} < |X| \leqslant X_{sf}$), the total commands are computed as·

$$\dot{X}_c = \sqrt{\dot{X}_{sh}^2 + 2\ddot{X}_d\,(|X| - X_{sh})}$$

$$Z_c = Z_{sh} - 0\,5\,\frac{\dot{X}_g \tan \gamma_g\,(\dot{X}_c - \dot{X}_{sh})^2}{\ddot{X}_d\,(\dot{X}_g - \dot{X}_{sh})}$$

$$\dot{Z}_c = \frac{\dot{X}_g \tan \gamma_g\,(\dot{X}_c - \dot{X}_{sh})}{\ddot{X}_d\,(\dot{X}_g - \dot{X}_{sh})}$$

If the helicopter is in the hover phase ($|X| < X_{sh}$), the total commands are computes as

$$\dot{X}_c = -\left(\frac{X}{X_{sh}}\right)\dot{X}_{sh}$$

$$Z_c = Z_h$$

$$\dot{Z}_c = 0$$

If the pilot selects the Land Mode and conditions are acceptable for landing, the total commands are generated as follows

$$\dot{X}_c = -\left(\frac{X}{X_{sh}}\right)\dot{X}_{sh}$$

$$\dot{Z}_c = \int_{t_o}^{t} \ddot{Z}_1 \, dt \leqslant \dot{Z}_1$$

$$Z_c = \int_{t_o}^{t} Z_c \, dt + Z_h$$

where t_o = time at point that land phase is started

The total lateral commands in all phases are of course zero in the ANF system

$$Y_c = 0$$

$$\dot{Y}_c = 0$$

b Guidance Laws

The forward velocity guidance law is

$$\Delta\dot{X} = \dot{X}_c - X^1$$

where

$$\dot{X}^1 = \dot{X}^h \text{ in HVF at high speed}$$

$$= \dot{X} \text{ at low speed}$$

The lateral velocity guidance law is,

$$\Delta\dot{Y} = k_y (Y_c - Y) + (\dot{Y}_c - \dot{Y}^1)$$

where

$$k_y = 0\,3 - 0\,00002\,|X|$$

$$0\,1 \leqslant k_y \leqslant 0\,2$$

$$\dot{Y}^1 = \dot{X} \sin \psi \text{ at high speed}$$

$$= \dot{Y} \text{ at low speed}$$

To prevent orbiting, the first term in the lateral law is limited

$$-\dot{X}_l \sin \psi_{max} \leq k_y (Y_c - Y) \leq \dot{X}_l \sin \psi_{max}$$

where

$$\dot{X}_l = |\dot{X}_c|, \text{ if } \dot{X}_c > \dot{X}_{sh}$$

$$= \dot{X}_{sh}, \text{ if } \dot{X}_c \leq \dot{X}_{sh}$$

ψ_{max} = maximum desired heading for correcting lateral errors prior to hover (30° nominally)

This limit limits the ANF lateral velocity command due to the first term to that corresponding to a nominal heading of 30° prior to hover and to a fixed value of about 8 5 ft/sec during the hover and land phases

The vertical velocity law is,

$$\Delta \dot{Z} = 0\ 2 (Z_c - Z) + (\dot{Z}_c - \dot{Z})$$

As mentioned previously, these velocity errors are commanded directly in the HVF at high speed

$$\Delta \dot{X}^h = \Delta \dot{X}$$

$$\Delta \dot{Y}^h = \Delta \dot{Y}$$

$$\Delta \dot{Z}^h = \Delta \dot{Z}$$

At low speeds, these errors are transformed into the HVF through the heading angle, ψ

$$\Delta \dot{X}^h = \Delta \dot{X} \cos \psi + \Delta \dot{Y} \sin \psi$$

$$\Delta \dot{Y}^h = -\Delta \dot{X} \sin \psi + \Delta \dot{Y} \cos \psi$$

$$\Delta \dot{Z}^h = \Delta \dot{Z}$$

The speed used to make this switch is total ground speed $(\sqrt{\dot{X}^2 + \dot{Y}^2})$ unless the filtered airspeed is less than this, in which case the filtered airspeed is used The speed at which the switch is made is 35 knots This speed was selected since it is the same speed at which the flight control laws in the Automatic Mode can start yawing the helicopter into the wind. In this case, large heading angles can develop and the ANF velocity errors must be transformed through the heading angles to insure that the HVF velocity errors will correspond exactly to the ANF errors relative to the ANF profile

To prevent discontinuities from occuring in the HVF velocity errors when a switch occurs, the differences between the direct and transformed HVF velocity errors at the time of switch are washed out This is done by computing these differences at the point of switch and linearly washing these out to zero over a 10 second period after the switch

3. Guidance Implementation

The guidance equations for Guidance II Mode of the Digital Flight Control and Landing System have been designed to be implemented in a direct manner on the airborne digital computer A general flow diagram of the implementation required is shown in Figure III-8 A description of the implementation shown in this figure and its operation is as follows The required guidance inputs are obtained from the radar updated strapdown navigational system A logical test on the guidance mode is then required to determine if the helicopter is first being acquired If it is, the acquisition conditions are stored and the ranges at the start of each profile phase are computed from these and the desired profile characteristics A test on the helicopter range is then required to determine the phase that the helicopter is currently in If it is in any phase prior to hover, the total commands along the profile are then generated as a function of current range for the appropriate phase If the helicopter range is less than the required value at the start of hover, further tests are required to determine if the flight conditions are acceptable for going into the land phase, if the helicopter is not already in the land phase The conditions that must be met for landing are as follows

$$\sqrt{X^2 + Y^2} \leqslant 50 \text{ ft}$$

$$|Z - Z_h| \leqslant 5 \text{ ft}$$

$$\sqrt{\dot{X}^2 + \dot{Y}^2} \leqslant 4 \text{ ft/sec}$$

$$|\dot{Z}| \leqslant 2 \text{ ft/sec}$$

$$|\phi| \leqslant 2\ 5 \text{ deg}$$

$$|\dot{\psi}| \leqslant 2 \text{ deg/sec}$$

If these conditions are not met, a "Ready to Land" discrete which activates the "Ready to Land" light in the cockpit is left off and the total hover commands are computed If the conditions for landing are satisfied, this discrete is turned on to indicate to the pilot that the Land Mode can now be selected A further test on the Land Mode discrete input is then required to determine if the pilot wants to land If the Land Mode is not selected, the system continues to use the total hover commands If the Land Mode is selected, the system computes the total commands for landing

If the helicopter is already in the land phase when the range is less than the required value at the start of hover, the system continues to compute the total commands for landing unless the pilot disengages the Land Mode This prevents flight conditions which are temporarily outside of the acceptable values during the landing from causing the system to "chatter" between the land and hover commands

In all phases, the guidance laws are then used to generate velocity errors from the total commands and the current helicopter flight conditions These errors are then converted into velocity errors in the HVF which are the required system outputs

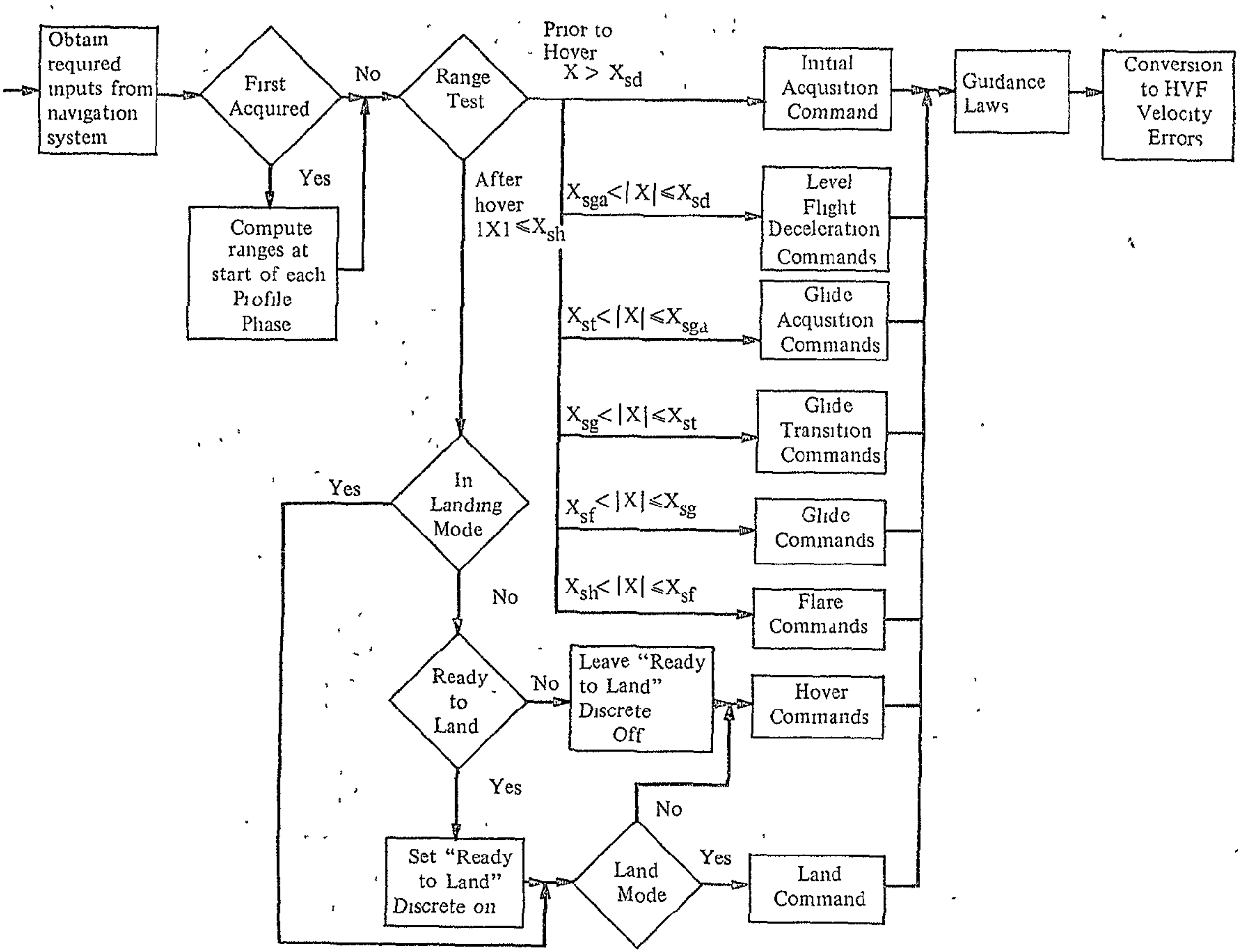

Figure III-8 Flow Diagram of Guidance II Laws

IV SIMULATION

A GENERAL

To evaluate the performance of the Digital Flight Control and Landing System a comprehensive piloted hybrid simulation was developed The simulation contains a model of the CH-46C helicopter, the digital flight control and guidance laws, error models for the flight data systems, and a cockpit simulator To develop this simulation, a data base was first established from data provided by NASA-ERC and from data obtained and/or developed under this contract A detailed description of this data is contained in the following section of this report

Based on this data and the simulation requirements, a hybrid simulation design was developed and mechanized on hybrid computing equipment early in the study In this design, all of the equations of motion for the helicopter were mechanized on analog computers since they are fast moving and it appeared that they could not be simulated in real time on a digital computer The stability derivatives, which are slow moving but complicated functions of flight conditions, were mechanized on the digital computer The digital flight control and guidance laws were mechanized on the digital computer since they were designed for mechanization on an airborne digital computer The flight data systems error models were also mechanized on the digital computer

During the study, an all digital simulation of the helicopter was also developed It was originally intended that this simulation would only be used to check the hybrid simulation and to make some preliminary non-piloted evaluation studies on the digitized control laws However, in checking the hybrid simulation it was rapidly found that the reliability and repeatability of the digital simulation was so much better than that for the hybrid version that it became desirable to use the digital version for all evaluation studies To determine if this could be done in real time, the Bell Aerospace Company Simulation Analyzer Program was used to determine the largest integration intervals that could be used with several numerical integration techniques while maintaining fined bounds on roundoff, truncation, and propagated errors

From this it was found that the allowable integration intervals with a second order Adams integration method were large enough to permit the helicopter equations to be digitally solved in real time As a result of this, the hybrid mechanization of the helicopter equations in the hybrid simulation was replaced by an all digital mechanization This form of hybrid simulation was then used for all final evaluation studies A detailed description of the final mechanization of this simulation is contained in Section IV C of this report

B DATA USED IN SIMULATION

1 Bare Helicopter

a. Equations of Motion

The equations of motions used to represent the bare helicopter were obtained by modifying a set of linearized 6 DOF body axis equations provided by NASA-ERC A description of the modified equations is contained in the following paragraphs

The equations are linearized about nominals for the vehicle body axis velocites, angular rates, attitudes, and control deflections at the rotor Of these, the vehicle longitudinal and vertical body axis velocities (U and W), pitch attitude (θ) and control deflections at the rotor (δ_{er}, δ_{cr}, δ_{ar}, and δ_{rr}) vary over large ranges where their effects are nonlinear Since these nonlinearities would result in sizeable errors if the perturbations in these variables became excessively large, the nominals for these variables must be updated with changing flight conditions to prevent this To allow for this, these nominals are made variables in the equations of motion All other nominals are constants

Winds are included in the equations of motion They are introduced in the ANF coordinate system and transformed to body axis winds through the Euler angles The body axis winds are then added to the perturbational body axis velocities to obtain perturbational body axis airspeeds These perturbational airspeeds are used to compute all aerodyanmic and rotor forces and moments

Provisions are included for handling large Euler attitude angles in the following transformations (1) gravity to components along body axis, (2) body angular rates to Euler attitude rates, (3) body axis velocities to ANF velocities, and (4) ANF winds to body axis winds This is necessary since the pitch trim attitude has a large range and since large roll and yaw attitudes are required for correcting typical lateral errors

In the equations of motion, the following assumptions are made:

(1) All second order terms are zero except where large angles are involved.

(2) $V_o \doteq 0 \quad \therefore \quad \Delta V = V$ | $R_o = 0 \quad \therefore \quad \Delta R \doteq R$

$P_o = 0 \quad \therefore \quad \Delta P = P$ | $\psi_o = 0 \quad \therefore \quad \Delta\psi = \psi$

$Q_o = 0 \quad \therefore \quad \Delta Q = Q$ | $\phi_o = 0 \quad \therefore \quad \Delta\phi = \phi$

With these assumptions, the body axis equations are,

$$\Delta\dot{U} = -W_o Q - g\,(\sin\ \theta\ - \sin\ \theta_o) + X_A/m$$

$$\dot{V} = W_o P - U_o R + g \sin\ \phi\ \cos\ \theta\ + Y_A/m$$

$$\Delta\dot{W} = U_o Q + g\,(\cos\ \phi\ \cos\ \theta\ - \cos\ \theta_o) + Z_A/m$$

$$\dot{P} = (-J_{XZ}\,\dot{R} + \Delta L_A)/I_{XX}$$

$$\dot{Q} = \Delta M_A/I_{YY}$$

$$\dot{R} = (-J_{XZ}\,\dot{P} + \Delta N_A)/I_{ZZ}$$

The aerodynamic and rotor forces and moments are,

$$\Delta X_A = X_U\ \Delta U_A + X_W\ \Delta W_A + X_Q Q + X_{\delta_e}\ \Delta\delta_{er} + X_{\delta_c}\ \Delta\delta_{cr}$$

$$\Delta Y_A = Y_V\, V_A + Y_P P + Y_R R + Y_{\delta_a}\ \Delta\delta_{ar} + Y_{\delta_r}\ \Delta\delta_{rr}$$

$$\Delta Z_A = Z_U\ \Delta U_A + Z_W\ \Delta W_A + Z_Q Q + Z_{\delta_e}\ \Delta\delta_{er} + Z_{\delta_c}\ \Delta\delta_{cr}$$

$$\Delta L_A = L_V V_A + L_P P + L_R R + L_{\delta_a} \Delta\delta_{ar} + L_{\delta_r} \Delta\delta_{rr}$$

$$\Delta M_A = M_U \Delta U_A + M_W \Delta W_A + M_Q Q + M_{\delta_e} \Delta\delta_{er} + M_{\delta_c} \Delta\delta_{cr}$$

$$\Delta N_A = N_V V_A + N_P P + N_R R + N_{\delta_a} \Delta\delta_{ar} + N_{\delta_r} \Delta\delta_{rr}$$

where,

$$\Delta U_A = \Delta U - U_W$$

$$\Delta V_A = V - V_W$$

$$\Delta W_A = \Delta W - W_W$$

The Euler angle rates equations are,

$$\dot{\psi} = \frac{1}{\cos\theta} (R \cos\phi + Q \sin\phi)$$

$$\Delta\dot{\theta} = Q \cos\phi - R \sin\phi$$

$$\dot{\phi} = P + \dot{\psi} \sin\theta$$

These Euler angles are used in two transformations The ANF axis winds to body axis winds transformation is,

$$\begin{bmatrix} U_W \\ V_W \\ W_W \end{bmatrix} = \begin{bmatrix} C\theta C\psi & C\theta S\psi & -S\theta \\ C\psi S\theta S\phi - S\psi C\phi & S\psi S\theta S\phi + C\psi C\phi & C\theta S\phi \\ C\psi S\theta C\phi + S\psi S\phi & S\psi S\theta C\phi - C\psi S\phi & C\theta C\phi \end{bmatrix} \begin{bmatrix} \dot{X}_W \\ \dot{Y}_W \\ \dot{Z}_W \end{bmatrix}$$

The body axis velocities to ANF velocities transformation is,

$$\begin{bmatrix} \dot{X} \\ \dot{Y} \\ \dot{Z} \end{bmatrix} = \begin{bmatrix} C\psi C\theta & C\psi S\theta S\phi - S\psi C\phi & C\psi S\theta C\phi + S\psi S\phi \\ S\psi C\theta & S\psi S\theta S\phi + C\psi C\phi & S\psi S\theta C\phi - C\psi S\phi \\ -S\theta & C\theta S\phi & C\theta C\phi \end{bmatrix} \begin{bmatrix} U \\ V \\ W \end{bmatrix}$$

In the above equations, the perturbations for those flight variables whose nominals change with flight conditions are defined as follows

$$U = \int \Delta \dot{U}\, dt + U_I$$

$$W = \int \Delta \dot{W}\, dt + W_I$$

$$\theta = \int \Delta\dot{\theta}\, dt + \theta_I$$

$$\Delta U = U - U_o$$

$$\Delta W = W - W_o$$

$$\Delta\theta = \theta - \theta_o$$

The control perturbations are defined as,

$$\Delta\,\delta_{er} = \delta_{ei} - \delta_{ero}$$

$$\Delta\,\delta_{cr} = \delta_{cr} - \delta_{cro}$$

$$\Delta\,\delta_{ar} = \delta_{ar} - \delta_{aro}$$

$$\Delta\,\delta_{rr} = \delta_{rr} - \delta_{rro}$$

The nominal values for the vehicle pitch attitude and the control trim positions are determined as functions of the flight conditions from the tables of stability derivatives and nominals.

$$\begin{vmatrix} \theta_o \\ \delta_{ero} \\ \delta_{cro} \\ \delta_{aro} \\ \delta_{rro} \end{vmatrix} = f\,(V_{H/A}, \dot{h}_{eq}, h, cg, m)$$

The nominal values for the vehicle longitudinal and vertical body axis velocities are then defined as,

$$U_o = V_{H/A} \cos\theta_o - \dot{h}_{eq} \sin\theta_o$$

$$W_o = V_{H/A} \sin\theta_o + \dot{h}_{eq} \cos\theta_o$$

b Stability Derivatives

The linearized stability derivatives for the CH-46C helicopter were partly provided by NASA-ERC and partly obtained from Boeing Vertot under this contract These are presented in Tables IV-1 through IV-14 The flight conditions for and the source of the data in each table are as follows

TABLE IV-1 DATA BASE

WEIGHT	13400 LB.
C.G. POSITION	NORMAL
RATE OF DESCENT	0 FPM
ALTITUDE	0 FT.

*Extrapolated Data

VELOCITY	0	20	40	60	80	80*	100	120	140
XU/M	-0.02540	-0.00181	-0.02156	-0.03604	-0.04642	-0.04622	-0.05579	-0.06456	-0.07206
XW/M	0.05449	0.06818	0.08255	0.08944	0.08548	0.11451	0.10343	0.08523	0.05666
XQ/M	0.60185	0.74915	0.87508	0.84957	0.73079	1.53696	1.24372	0.77601	0.25183
XDE/M	0.17696	0.13988	0.12312	0.14237	0.16406	-0.06944	-0.05165	-0.03776	-0.01954
XDC/M	1.20482	0.97467	0.87948	0.80253	0.68335	1.02239	0.88200	0.72040	0.48341
ZU/M	0.06009	-0.12594	-0.08296	-0.02192	0.01396	0.04049	0.06077	0.06546	0.04980
ZW/M	-0.36933	-0.48399	-0.63639	-0.80152	-0.92055	-0.91867	-1.00063	-1.04552	-1.10516
ZQ/M	-0.71511	-1.16872	-1.77844	-1.81400	-1.81986	-2.19788	-2.22039	-2.25955	-2.47935
ZDE/M	-0.00407	0.21183	0.51943	0.56820	0.52527	0.50918	0.46341	0.41480	0.36743
ZDC/M	-7.43006	-7.23138	-7.65410	-8.52446	-9.49005	-9.37251	-10.26600	-11.08740	-11.71110
MU/IYY	0.00656	0.00645	-0.00587	-0.00670	-0.00582	-0.00261	-0.00185	-0.00120	-0.00089
MW/IYY	-0.00285	0.00978	0.01630	0.01363	0.01154	0.01151	0.00956	0.00774	0.00691
MQ/IYY	-0.73173	-0.96002	-1.31158	-1.45996	-1.52219	-1.60359	-1.62003	-1.59067	-1.51570
MDE/IYY	0.35447	0.35364	0.40144	0.45022	0.48135	0.49134	0.51572	0.53335	0.54565
MDC/IYY	-0.04765	-0.04252	0.04556	0.06776	0.06725	0.05112	0.04707	0.03948	0.03505
THETA 0	9.30627	8.19834	6.62235	4.75227	2.32294	4.49882	1.43387	-2.26671	-6.63310
DELTAE 0	0.66523	-0.06503	-0.23516	0.28888	0.77817	-0.41839	-0.06119	0.16392	0.34298
DELTAC 0	5.01959	4.47346	3.73135	3.51111	3.84917	3.82271	4.67777	6.04983	8.02025
YV/M	-0.02664	-0.05408	-0.07986	-0.11823	-0.15121	-0.15528	-0.18040	-0.19766	-0.23442
YP/M	-0.76514	-0.95618	-1.15981	-1.24824	-1.23341	-1.15874	-1.02295	-0.76619	-0.29372
YR/M	-0.12517	-0.18179	-0.20082	-0.12813	-0.05819	0.10316	0.13380	0.12514	0.22125
YDA/M	0.99794	0.99700	0.97673	0.96426	0.96955	0.94614	0.97123	1.01613	1.10225
YDR/M	0.14652	0.13634	0.11652	0.10583	0.09849	0.10887	0.11641	0.13883	0.15262
LV/IXX	-0.00778	-0.01305	-0.01338	-0.01720	-0.02442	-0.02059	-0.03188	-0.04724	-0.05080
LP/IXX	-0.50730	-0.57483	-0.64045	-0.65271	-0.62549	-0.59158	-0.52243	-0.41134	-0.23476
LR/IXX	-0.02297	-0.04571	-0.05943	-0.02270	0.01172	0.06746	0.09531	0.11659	0.19955
LDA/IXX	0.46536	0.46558	0.45954	0.45575	0.45805	0.44938	0.45820	0.47354	0.50528
LDR/IXX	-0.12638	-0.13036	-0.13422	-0.13544	-0.13910	-0.13077	-0.13256	-0.13248	-0.14433
NV/IZZ	0.00013	0.00037	-0.00123	-0.00290	-0.00415	-0.00553	-0.00536	-0.00377	-0.00060
NP/IZZ	-0.01831	-0.02076	-0.02598	-0.03947	-0.05344	-0.05699	-0.06864	-0.07797	-0.07471
NR/IZZ	-0.05847	-0.05450	-0.04597	-0.05020	-0.05438	-0.04087	-0.05078	-0.06642	-0.12617
NDA/IZZ	0.03001	0.02923	0.02764	0.02663	0.02633	0.02630	0.02696	0.02857	0.02970
NDR/IZZ	0.17534	0.17578	0.17261	0.17032	0.17141	0.16698	0.17146	0.17933	0.19536
DELTAA 0	0.12983	0.08462	0.09191	0.13466	0.17931	0.20322	0.29754	0.44154	0.49785
DELTAR 0	-0.17764	-0.04701	-0.08508	-0.33705	-0.61293	-0.46945	-0.75397	-1.04713	-1.14123

TABLE IV-2 DATA BASE

WEIGHT	13400 LB.
C.G. POSITION	NORMAL
RATE OF DESCENT	1500 FPM
ALTITUDE	0 FT.

*Extrapolated Data

VELOCITY	0	20	40	60	80	80*	100*	120*	140*
XU/M	0.01143	0.02237	-0.01281	-0.03179	-0.04306	-0.04600	-0.05400	-0.06100	-0.07300
XW/M	0.04368	0.05111	0.10637	0.10919	0.10653	0.12600	0.11500	0.10900	0.08100
XQ/M	1.02536	0.93903	1.55534	1.45965	1.37043	2.12500	1.89700	1.60800	0.78100
XDE/M	0.16625	0.12347	0.08223	0.12593	0.14599	-0.09250	-0.07000	-0.06100	-0.04200
XDC/M	1.13928	0.94352	0.82126	0.88028	0.82702	1.16550	1.08800	0.91800	0.62900
ZU/M	-0.13435	-0.23640	-0.12619	-0.02151	0.01777	0.03650	0.06100	0.07000	0.06500
ZW/M	-0.28748	-0.26321	-0.82254	-0.90575	-0.98052	-0.93400	-0.97200	-1.07500	-1.12100
ZQ/M	-0.79039	0.30060	-2.45731	-2.40596	-2.42975	-3.25950	-2.67400	-2.50400	-2.44600
ZDE/M	0.00615	0.19996	0.94841	0.77315	0.71536	0.79550	0.58500	0.50300	0.42000
ZDC/M	-7.45257	-7.38250	-6.35173	-8.00904	-9.05358	-8.78200	-10.14700	-11.11500	-11.87700
MU/IYY	0.01308	0.01863	-0.00906	-0.00696	-0.00635	-0.00150	-0.00200	-0.00300	-0.00100
MW/IYY	0.00368	0.03420	0.00228	0.00469	0.00683	0.00600	0.01000	0.00900	0.00900
MQ/IYY	-0.58241	-0.81810	-1.48310	-1.56553	-1.62304	-1.75200	-1.72500	-1.71600	-1.63000
MDE/IYY	0.34363	0.30612	0.43861	0.47166	0.50338	0.52550	0.53800	0.55700	0.56800
MDC/IYY	-0.05591	-0.16472	0.15368	0.11620	0.10884	0.11650	0.07500	0.05600	0.04600
THETA O	8.98810	8.13867	6.99471	5.34340	3.21352	5.11780	2.35420	-1.06300	-5.78600
DELTAE O	0.03060	-1.69234	-0.56816	0.11550	0.60565	-0.76200	-0.28500	-0.05000	0.11600
DELTAC O	3.89872	3.25038	1.25071	0.90347	1.15881	1.24850	1.94800	3.18800	5.42200
YV/M	-0.08635	-0.04068	-0.11126	-0.15170	-0.18262	-0.18950	-0.21700	-0.23900	-0.22900
YP/M	-1.10440	-1.30270	-1.78540	-1.86230	-1.73270	-1.64750	-1.51600	-1.30400	-1.23200
YR/M	-0.18435	-0.10798	-0.30137	-0.22815	-0.19244	0.19300	0.14800	-0.00900	0.38300
YDA/M	0.98054	0.97047	0.92561	0.89687	0.87675	0.85300	0.84800	0.85900	0.98700
YDR/M	0.14250	0.11217	0.09751	0.07301	0.07008	0.07400	0.07900	0.09100	0.09700
LV/IXX	-0.00996	-0.00799	-0.00448	-0.00371	-0.00284	0.00450	-0.00700	-0.01600	-0.05800
LP/IXX	-0.63036	-0.71659	-0.86876	-0.87455	-0.79734	-0.78450	-0.70200	-0.58400	-0.54600
LR/IXX	-0.05234	-0.02797	-0.10977	-0.07677	-0.05688	0.06650	0.06600	0.03100	0.24500
LDA/IXX	0.45903	0.45705	0.44170	0.43230	0.42630	0.41950	0.41700	0.42000	0.46600
LDR/IXX	-0.12454	-0.13516	-0.13185	-0.13554	-0.13256	-0.12700	-0.12400	-0.12000	-0.14300
NV/IZZ	0.00122	-0.00016	-0.00236	-0.00456	-0.00706	-0.00700	-0.00900	-0.01000	-0.00700
NP/IZZ	-0.02085	-0.01101	-0.02424	-0.04001	-0.05921	-0.04500	-0.06800	-0.09400	-0.10600
NR/IZZ	-0.04986	-0.02575	-0.03287	-0.03310	-0.03704	0.02200	-0.00400	-0.05200	-0.11000
NDA/IZZ	0.02925	0.02744	0.02580	0.02385	0.02313	0.02100	0.02200	0.02300	0.02600
NDR/IZZ	0.17285	0.17149	0.16373	0.15906	0.15540	0.15050	0.15000	0.15200	0.17400
DELTAA O	0.09255	0.04445	0.01404	0.05177	0.09882	0.10550	0.18300	0.26000	0.63400
DELTAR O	-0.07915	0.32928	0.06118	-0.19696	-0.43185	-0.10900	-0.49200	-0.94300	-1.61300

TABLE IV-3 DATA BASE

WEIGHT	13400 LB.
C.G. POSITION	NORMAL
RATE OF DESCENT	1000 FPM
ALTITUDE	0 FT.

VELOCITY	0	20	40	60	80	80*	100	120	140
XU/M	-0.02000	0.01200	-0.01200	-0.03300	-0.04300	-0.04650	-0.05500	-0.06200	-0.07200
XW/M	0.04300	0.05700	0.09400	0.09900	0.09000	0.12150	0.11200	0.10200	0.07400
XQ/M	0.85400	0.94300	1.37200	1.31000	1.16500	1.89700	1.65700	1.32200	0.66700
XDE/M	0.17400	0.12700	0.08200	0.12600	0.15500	-0.08900	-0.06700	-0.05200	-0.03200
XDC/M	1.21400	0.94500	0.79500	0.82100	0.78000	1.12650	1.01600	0.83600	0.57200
ZU/M	0.04300	-0.19700	-0.16200	-0.03600	0.00600	0.03650	0.06100	0.06800	0.06100
ZW/M	-0.29000	-0.35400	-0.72300	-0.84800	-0.89800	-0.91450	-0.98400	-1.07300	-1.10400
ZQ/M	-0.48300	-0.42300	-3.39800	-2.73100	-2.18200	-2.77750	-2.48400	-2.44600	-2.39500
ZDE/M	-0.00800	0.22600	1.02000	0.83300	0.63100	0.68750	0.54700	0.46800	0.39600
ZDC/M	-7.53000	-7.19800	-6.36000	-7.88800	-9.28600	-9.05100	-10.19600	-11.08800	-11.84300
MU/IYY	0.01000	0.01300	-0.01200	-0.00800	-0.00700	-0.00250	-0.00200	-0.00200	-0.00100
MW/IYY	-0.00200	0.02400	0.01100	0.01000	0.01300	0.00900	0.01000	0.00900	0.00800
MQ/IYY	-0.60600	-0.89000	-1.51800	-1.58100	-1.58600	-1.69100	-1.68600	-1.67100	-1.60200
MDE/IYY	0.34800	0.32700	0.44400	0.47600	0.49400	0.51300	0.53100	0.54900	0.56000
MDC/IYY	-0.04800	-0.09800	0.15300	0.12600	0.09100	0.09100	0.06600	0.05100	0.04400
THETA 0	9.27300	8.11000	6.83400	5.10800	2.88700	4.92440	2.03860	-1.51200	-6.11700
DELTAE 0	0.69500	-0.98600	-0.88100	-0.02700	0.62100	-0.61750	-0.19400	0.00500	0.19800
DELTAC 0	4.31600	3.52300	2.28800	1.87500	2.08700	2.10500	2.86400	4.17000	6.29400
YV/M	0.13200	-0.04700	-0.08800	-0.13000	-0.16500	-0.17750	-0.20400	-0.22200	-0.22900
YP/M	-0.99900	-1.22400	-1.51400	-1.62800	-1.58600	-1.47050	-1.35200	-1.15700	-0.82900
YR/M	-0.14500	-0.10100	-0.27100	-0.22200	-0.15100	0.00600	0.04100	0.04000	0.23400
YDA/M	0.99400	0.95800	0.94200	0.92000	0.90600	0.88300	0.88900	0.91500	1.02000
YDR/M	0.14900	0.12000	0.10100	0.08200	0.07800	0.09500	0.09600	0.10200	0.12100
LV/IXX	-0.00900	-0.01000	-0.00600	-0.00500	-0.00700	-0.00100	-0.01100	-0.02900	-0.05600
LP/IXX	-0.58800	-0.68100	-0.77000	-0.79300	-0.75100	-0.71450	-0.64100	-0.53600	-0.40000
LR/IXX	-0.04000	-0.02300	-0.09500	-0.07200	-0.03700	0.00500	0.03500	0.06000	0.17700
LDA/IXX	0.46300	0.44200	0.44800	0.44100	0.43600	0.42800	0.43000	0.43900	0.47600
LDR/IXX	-0.12400	-0.13300	-0.13400	-0.13600	-0.13500	-0.12450	-0.12500	-0.12700	-0.14000
NV/IZZ	0.0	0.0	-0.00300	-0.00500	-0.00700	-0.00700	-0.00800	-0.00800	-0.00500
NP/IZZ	-0.02300	-0.01500	-0.02400	-0.03700	-0.05500	-0.05000	-0.06900	-0.08900	-0.10100
NR/IZZ	-0.04800	-0.03000	-0.03600	-0.03700	-0.04100	-0.00850	-0.02800	-0.06300	-0.10000
NDA/IZZ	0.03000	0.03000	0.02600	0.02400	0.02400	0.02350	0.02400	0.02500	0.02800
NDR/IZZ	0.17400	0.17200	0.16700	0.16300	0.16100	0.15550	0.15700	0.16200	0.18000
DELTAA 0	0.10200	0.03000	0.03500	0.07500	0.12900	0.11100	0.20500	0.33900	0.58400
DELTAR 0	-0.16000	0.16800	0.10700	-0.17700	-0.47600	-0.22050	-0.58400	-1.01200	-1.43800

TABLE IV-4 DATA BASE

WEIGHT	13400 LB.
C.G. POSITION	NORMAL
RATE OF DESCENT	500 FPM
ALTITUDE	0 FT.

*Extrapolated Data

VELOCITY	0	20	40	60	80	80*	100	120	140
XU/M	-0.02200	0.00400	-0.01700	-0.03400	-0.04500	-0.04700	-0.05600	-0.06300	-0.07100
XW/M	0.04800	0.06200	0.08200	0.08900	0.08700	0.11700	0.10900	0.09500	0.06700
XQ/M	0.73400	0.87900	1.07000	1.06700	0.94400	1.66900	1.41700	1.03600	0.55300
XDE/M	0.17600	0.13300	0.11700	0.13900	0.16100	-0.08550	-0.06400	-0.04300	-0.02200
XDC/M	1.20300	0.96900	0.86600	0.82800	0.73100	1.08750	0.94400	0.75400	0.51500
ZU/M	0.05000	-0.16200	-0.11900	-0.03500	0.00900	0.03650	0.06100	0.06600	0.05700
ZW/M	-0.32700	-0.43200	-0.60800	-0.78200	-0.90900	-0.89500	-0.99600	-1.07100	-1.08700
ZQ/M	-0.60100	-0.93000	-1.87300	-2.03000	-1.93300	-2.29550	-2.29400	-2.38800	-2.34400
ZDE/M	-0.01200	0.22200	0.60500	0.63900	0.57400	0.57950	0.50900	0.43300	0.37200
ZDC/M	-7.45300	-7.15300	-7.35900	-8.36600	-9.40000	-9.32000	-10.24500	-11.06100	-11.80900
MU/IYY	0.00800	0.00900	-0.00800	-0.00800	-0.00600	-0.00350	-0.00200	-0.00100	-0.00100
MW/IYY	-0.00300	0.01500	0.02000	0.01500	0.01200	0.01200	0.01000	0.00900	0.00700
MQ/IYY	-0.67000	-0.92600	-1.34400	-1.50000	-1.55500	-1.63000	-1.64700	-1.62600	-1.57400
MDE/IYY	0.35000	0.34200	0.40600	0.45700	0.48700	0.50050	0.52400	0.54100	0.55700
MDC/IYY	-0.04700	-0.06200	0.06400	0.08500	0.07900	0.06550	0.05700	0.04600	0.04200
THETA O	9.33500	8.18800	6.71900	4.93400	2.60200	4.73100	1.72300	-1.96100	-6.44800
DELTAE O	0.73000	-0.41900	-0.57600	0.10800	0.68500	-0.47300	-0.10300	0.06000	0.28000
DELTAC O	4.63300	3.96000	3.02200	2.70000	2.96500	2.96150	3.78000	5.15200	7.16600
YV/M	0.18900	-0.04900	-0.08200	-0.12000	-0.15700	-0.16550	-0.19100	-0.20500	-0.22900
YP/M	-0.91200	-1.08100	-1.33300	-1.44000	-1.40700	-1.29350	-1.18800	-1.01000	-0.42600
YR/M	-0.11700	-0.06130	-0.22300	-0.18000	-0.10500	-0.18100	-0.06600	0.08900	0.08500
YDA/M	0.99400	0.98600	0.95400	0.94200	0.93500	0.91300	0.93000	0.97100	1.05300
YDR/M	0.15900	0.13200	0.10400	0.09000	0.08400	0.11600	0.11300	0.11300	0.14500
LV/IXX	-0.00800	-0.01100	-0.01000	-0.01000	-0.01500	-0.00650	-0.02000	-0.04200	-0.05400
LP/IXX	-0.55800	-0.61900	-0.70300	-0.72400	-0.68700	-0.64450	-0.58000	-0.48800	-0.25400
LR/IXX	-0.02500	-0.00300	-0.07000	-0.05000	-0.01400	-0.05650	0.00400	0.08900	0.10900
LDA/IXX	0.46300	0.46200	0.45400	0.44800	0.44600	0.43650	0.44300	0.45800	0.48600
LDR/IXX	-0.12100	-0.13100	-0.13600	-0.13800	-0.13800	-0.12200	-0.12600	-0.13400	-0.13700
NV/IZZ	0.0	0.0	-0.00200	-0.00400	-0.00500	-0.00700	-0.00700	-0.00600	-0.00300
NP/IZZ	-0.02500	-0.02100	-0.02500	-0.03800	-0.05400	-0.05500	-0.07000	-0.08400	-0.09600
NR/IZZ	-0.05200	-0.03300	-0.04200	-0.04200	-0.04600	-0.03900	-0.05200	-0.07400	-0.09000
NDA/IZZ	0.03000	0.02900	0.02700	0.02600	0.02500	0.02600	0.02600	0.02700	0.03000
NDR/IZZ	0.17500	0.17400	0.17000	0.16700	0.16600	0.16050	0.16400	0.17200	0.18600
DELTAA O	0.12000	0.06500	0.05600	0.09100	0.12100	0.11650	0.22700	0.41800	0.53400
DELTAR O	-0.18800	0.04000	0.00600	-0.25400	-0.53700	-0.33200	-0.67600	-1.08100	-1.26300

TABLE IV-5 DATA BASE

WEIGHT	13400 LB.
C.G. POSITION	NORMAL
RATE OF DESCENT	-500 FPM
ALTITUDE	0 FT.

VELOCITY	0	20	40	60	80	80*	100	120	140
XU/M	-0.02800	-0.00800	-0.02700	-0.03900	-0.04900	-0.05050	-0.05900	-0.06600	-0.07400
XW/M	0.06200	0.07300	0.08000	0.08400	0.07800	0.10450	0.09400	0.07900	0.05200
XQ/M	0.46600	0.59300	0.66900	0.65200	0.48800	1.29750	0.98400	0.52100	-0.11700
XDE/M	0.18000	0.14700	0.12900	0.14800	0.16900	-0.06500	-0.04700	-0.03200	-0.00700
XDC/M	1.20800	0.99200	0.89700	0.79300	0.65400	0.99900	0.85100	0.69400	0.46700
ZU/M	0.06800	-0.09200	-0.05700	-0.00700	0.02100	0.05000	0.06400	0.06400	0.04700
ZW/M	-0.41500	-0.53000	-0.67400	-0.80500	-0.91100	-0.89800	-0.98100	-1.04100	-1.11000
ZQ/M	-0.74200	-1.23600	-1.51200	-1.64200	-1.62200	-2.13200	-2.14800	-2.20000	-2.35500
ZDE/M	0.0	0.20000	0.45300	0.50400	0.48200	0.47150	0.43700	0.39000	0.33400
ZDC/M	-7.44800	-7.34900	-7.86500	-8.74100	-9.63200	-9.51050	-10.33400	-11.09000	-11.63600
MU/IYY	0.00500	0.00400	-0.00400	-0.00600	-0.00500	-0.00150	-0.00100	-0.00100	0.0
MW/IYY	-0.00200	0.00700	0.01200	0.01100	0.01000	0.00900	0.00800	0.00700	0.00600
MQ/IYY	-0.79500	-0.98900	-1.27900	-1.42700	-1.48700	-1.56150	-1.58000	-1.55700	-1.49300
MDE/IYY	0.36000	0.36400	0.39900	0.44500	0.47600	0.48400	0.50900	0.52800	0.53900
MDC/IYY	-0.04800	-0.03400	0.03400	0.05600	0.05900	0.03950	0.03900	0.03500	0.03500
THETA 0	9.34300	8.19300	6.54000	4.53500	2.02700	4.14900	1.09500	-2.50500	-6.64400
DELTAE 0	0.68600	0.15400	0.04500	0.44200	0.83500	-0.24100	0.04100	0.21200	0.37100
DELTAC 0	5.47900	5.03100	4.46200	4.34300	4.71700	4.74650	5.59000	6.90300	8.79600
YV/M	-0.30700	-0.06100	-0.08500	-0.11600	-0.14800	-0.14550	-0.17500	-0.20200	-0.23700
YP/M	-0.69300	-0.81200	-0.98800	-1.06500	-1.04200	-0.97500	-0.83300	-0.57200	-0.03400
YR/M	0.03000	-0.13500	-0.16400	-0.11200	0.11100	-0.12700	0.03000	0.12100	0.22700
YDA/M	1.01200	1.00700	0.99700	0.99100	0.99900	0.98950	1.01400	1.05500	1.15400
YDR/M	0.15700	0.13800	0.12700	0.11600	0.10000	0.13700	0.13600	0.15000	0.16300
LV/IXX	-0.00600	-0.01500	-0.01600	-0.02100	-0.03000	-0.03050	-0.03800	-0.04400	-0.00500
LP/IXX	-0.48000	-0.52300	-0.58000	-0.59300	-0.56400	-0.52800	-0.46100	-0.35600	-0.15200
LR/IXX	0.04600	-0.02200	-0.03400	-0.01000	0.09100	-0.01750	0.06500	0.12900	0.21000
LDA/IXX	0.47000	0.47000	0.46700	0.46500	0.46900	0.46350	0.47300	0.48800	0.52500
LDR/IXX	-0.12500	-0.13100	-0.13400	-0.13700	-0.14400	-0.12850	-0.13300	-0.13500	-0.15000
NV/IZZ	0.0	0.0	0.0	-0.00100	-0.00200	-0.00300	-0.00300	-0.00200	-0.00100
NP/IZZ	-0.02400	-0.02100	-0.02500	-0.03500	-0.04700	-0.05500	-0.06300	-0.06700	-0.06800
NR/IZZ	-0.04900	-0.05900	-0.05600	-0.05700	-0.05100	-0.06550	-0.07500	-0.10000	-0.13300
NDA/IZZ	0.03000	0.02900	0.02800	0.02800	0.02700	0.02950	0.02900	0.02900	0.03000
NDR/IZZ	0.17800	0.17800	0.17600	0.17500	0.17700	0.17450	0.17900	0.18600	0.20400
DELTAA 0	0.14000	0.10400	0.10800	0.14600	0.21000	0.25750	0.33000	0.41100	0.47900
DELTAR 0	-0.20600	-0.11200	-0.14200	-0.35100	-0.64500	-0.52600	-0.77100	-0.96700	-1.09900

TABLE IV-6. DATA BASE

WEIGHT	13400 LB.
C.G. POSITION	NORMAL
RATE OF DESCENT	-1500 FPM
ALTITUDE	0 FT.

*Extrapolated Data

VELOCITY	0	20	40	60	80	80*	100*	120*	140*
XU/M	-0.02649	-0.01935	-0.03260	-0.04491	-0.05277	-0.05907	-0.06542	-0.06888	-0.07788
XW/M	0.07505	0.08122	0.08209	0.07521	0.06568	0.08448	0.07514	0.06654	0.04268
XQ/M	0.15633	0.20875	0.26690	0.17058	0.09717	0.81857	0.46456	0.01098	-0.85466
XDE/M	0.17842	0.16228	0.14484	0.16227	0.18105	-0.05612	-0.03770	-0.02048	0.01808
XDC/M	1.16992	1.04008	0.90570	0.78861	0.62563	0.95222	0.78900	0.64120	0.43418
ZU/M	0.04316	-0.02959	-0.00971	0.00737	0.02520	0.06903	0.07046	0.06108	0.04140
ZW/M	-0.52217	-0.60121	-0.72925	-0.85332	-0.94171	-0.85666	-0.94174	-1.03196	-1.11968
ZQ/M	-1.07268	-1.20010	-1.25010	-1.38662	-1.47426	-2.00024	-2.00322	-2.08090	-2.10630
ZDE/M	0.05444	0.16010	0.36218	0.41296	0.41472	0.39614	0.38418	0.34040	0.26714
ZDC/M	-7.58650	-7.64041	-8.24770	-8.95410	-9.70900	-9.78649	-10.47000	-11.09520	-11.48580
MU/IYY	0.00251	0.00163	0.00321	-0.00458	-0.00467	0.00073	0.00070	-0.00060	0.00178
MW/IYY	-0.00148	0.00327	0.00726	0.00765	0.00730	0.00397	0.00488	0.00552	0.00418
MQ/IYY	-0.93433	-1.03020	-1.24040	-1.37428	-1.42430	-1.47731	-1.49994	-1.48966	-1.44760
MDE/IYY	0.37472	0.37930	0.40095	0.43815	0.46558	0.46932	0.49556	0.51730	0.52570
MDC/IYY	-0.04570	-0.03118	0.01909	0.03637	0.04212	0.01626	0.02286	0.02604	0.03490
THETA 0	9.09615	8.24561	6.51804	4.34680	1.74707	3.44935	0.41726	-2.98158	-6.66580
DELTAE 0	0.56611	0.45249	0.38166	0.63183	1.02115	0.11378	0.24538	0.30816	0.42704
DELTAC 0	6.51301	6.30131	5.94168	5.94845	6.38886	6.59408	7.41446	8.60934	10.34750
YV/M	-0.02060	-0.08482	-0.10455	-0.12256	-0.14842	-0.12594	-0.16420	-0.21068	-0.24216
YP/M	-0.40249	-0.48197	-0.63817	-0.68143	-0.63180	-0.60751	-0.45310	-0.18362	0.48544
YR/M	-0.04204	0.04052	-0.06921	-0.04086	0.01514	-0.58732	-0.17760	0.11272	0.23850
YDA/M	1.03950	1.04228	1.04066	1.04266	1.06287	1.07623	1.09954	1.13274	1.25750
YDR/M	0.14982	0.14802	0.12894	0.11875	0.12938	0.19326	0.17518	0.17234	0.18376
LV/IXX	-0.02127	-0.01846	-0.01978	-0.02294	-0.02866	-0.05032	-0.05024	-0.03752	0.08660
LP/IXX	-0.37496	-0.40345	-0.45470	-0.46318	-0.42905	-0.40083	-0.33814	-0.24532	0.01352
LR/IXX	0.02907	0.06798	0.02113	0.03740	0.07088	-0.18742	0.00438	0.15382	0.23090
LDA/IXX	0.48113	0.48228	0.48271	0.48417	0.49124	0.49174	0.50260	0.51692	0.56444
LDR/IXX	-0.13312	-0.13406	-0.14131	-0.14556	-0.14455	-0.12396	-0.13388	-0.14004	-0.16134
NV/IZZ	0.00108	0.00098	0.00044	0.00052	0.00041	0.00206	0.00172	0.00154	-0.00180
NP/IZZ	-0.02133	-0.02122	-0.02478	-0.02754	-0.03693	-0.05102	-0.05172	-0.04506	-0.05458
NR/IZZ	-0.07653	-0.06348	-0.07218	-0.07450	-0.08262	-0.11476	-0.12344	-0.16716	-0.14666
NDA/IZZ	0.03076	0.03053	0.02924	0.02856	0.02918	0.03589	0.03308	0.02986	0.03060
NDR/IZZ	0.18338	0.18355	0.18366	0.18425	0.18730	0.18954	0.19408	0.19934	0.22128
DELTAA 0	0.16567	0.15081	0.14181	0.15535	0.20065	0.36607	0.39492	0.34992	0.44130
DELTAR 0	-0.23383	-0.21772	-0.28008	-0.42585	-0.61869	-0.63910	-0.80506	-0.80674	-1.01154

TABLE IV-7 DATA BASE

WEIGHT 13400 LB.

C.G. POSITION NORMAL

RATE OF DESCENT 0 FPM

ALTITUDE 2000 FT.

*Extrapolated Data

VELOCITY	0	20	40	60	80	80*	100	120	140
XU/M	-0.02600	-0.00300	-0.02100	-0.03400	-0.04400	-0.04400	-0.05300	-0.06100	-0.06700
XW/M	0.05100	0.06300	0.07500	0.08000	0.07600	0.10300	0.09300	0.07700	0.05400
XQ/M	0.69800	0.85400	0.96900	0.97200	0.84900	1.71700	1.39300	0.86800	0.19400
XDE/M	0.16700	0.13400	0.11800	0.13600	0.15800	-0.06350	-0.04400	-0.02700	0.01700
XDC/M	1.13900	0.91100	0.80300	0.71500	0.59200	0.91400	0.77800	0.62900	0.41900
ZU/M	0.05700	-0.12100	-0.08300	-0.02700	0.00800	0.03100	0.05100	0.05600	0.04200
ZW/M	-0.34900	-0.45500	-0.59100	-0.74500	-0.85800	-0.85500	-0.93200	-0.97300	-1.02200
ZQ/M	-0.57500	-1.00900	-1.41500	-1.63000	-1.64800	-2.13550	-2.18900	-2.27800	-2.34200
ZDE/M	-0.00700	0.18500	0.46700	0.51900	0.48300	0.48250	0.43800	0.38500	0.29000
ZDC/M	-7.01900	-6.83700	-7.21000	-7.98100	-8.85000	-8.76100	-9.56700	-10.31000	-10.90200
MU/IYY	0.00600	0.00600	-0.00500	-0.00600	-0.00500	-0.00300	-0.00200	-0.00100	0.0
MW/IYY	-0.00300	0.00900	0.01500	0.01300	0.01000	0.01100	0.00900	0.00800	0.00700
MQ/IYY	-0.69700	-0.90400	-1.22200	-1.36800	-1.42700	-1.49300	-1.51100	-1.48800	-1.43800
MDE/IYY	0.33400	0.33200	0.37300	0.41900	0.44700	0.45800	0.48000	0.49600	0.50200
MDC/IYY	-0.04500	-0.04100	0.03900	0.06200	0.06400	0.04750	0.04600	0.04100	0.03700
THETA O	9.30600	8.16800	6.60700	4.77300	2.43800	4.59700	1.66800	-1.85500	-6.03300
DELTAE O	0.70400	-0.03300	-0.25900	0.24400	0.69400	-0.29900	-0.08200	-0.09800	0.31300
DELTAC O	5.31900	4.78800	4.03600	3.77100	4.05600	4.04600	4.83500	6.12800	7.98800
YV/M	-0.26600	-0.05300	-0.07700	-0.11100	-0.14200	-0.14650	-0.17000	-0.18600	-0.21900
YP/M	-0.85600	-1.05100	-1.25700	-1.34600	-1.34000	-1.25850	-1.13600	-0.89700	-0.45000
YR/M	-0.16200	-0.02700	-0.19400	-0.15200	-0.07400	-0.13800	-0.03800	0.08400	0.07400
YDA/M	0.99900	1.00000	0.97900	0.96600	0.96700	0.95150	0.97100	1.00900	1.09100
YDR/M	0.14800	0.13400	0.11500	0.10000	0.10500	0.11000	0.11500	0.12000	0.15700
LV/IXX	-0.00800	-0.01300	-0.01400	-0.01700	-0.02400	-0.01950	-0.03000	-0.04400	-0.04800
LP/IXX	-0.55800	-0.62700	-0.69300	-0.70600	-0.69000	-0.64100	-0.58000	-0.47400	0.32800
LR/IXX	-0.04200	0.01700	-0.05300	-0.03400	0.00500	-0.09900	-0.02000	0.09900	0.12200
LDA/IXX	0.46600	0.46600	0.46000	0.45700	0.45800	0.45050	0.45800	0.47200	0.50200
LDR/IXX	-0.12600	-0.13200	-0.13500	-0.13900	-0.12900	-0.13500	-0.13300	-0.13900	-0.13800
NV/IZZ	0.0	0.0	-0.00100	-0.00300	-0.00400	-0.00500	-0.00500	-0.00400	0.0
NP/IZZ	-0.01900	-0.02200	-0.02700	-0.04000	-0.05100	-0.06000	-0.07100	-0.08200	-0.06500
NR/IZZ	-0.05800	-0.03900	-0.04900	-0.05000	-0.05400	-0.04650	-0.06100	-0.08600	-0.11000
NDA/IZZ	0.03000	0.02900	0.02800	0.02700	0.02600	0.02700	0.02700	0.02800	0.02900
NDR/IZZ	0.17600	0.17600	0.17300	0.17100	0.16900	0.16800	0.17100	0.17900	0.19100
DELTAA O	0.13100	0.08700	0.08600	0.13400	0.17100	0.19200	0.28100	0.42200	0.47900
DELTAR O	-0.18200	-0.05200	-0.07100	-0.31800	-0.58000	-0.42350	-0.70200	-0.99700	-1.06700

Bell Aerospace Company

TABLE IV-8 DATA BASE

WEIGHT	13400 LB.
C.G. POSITION	NORMAL
RATE OF DESCENT	0 FPM
ALTITUDE	10000 FT.

VELOCITY	0	20	40	60	80	80*	100	120	140
XU/M		-0.00676	-0.02061	-0.03070	-0.03842		-0.04362		
XW/M		0.04884	0.05402	0.05667	0.05294		0.06963		
XQ/M		1.18274	1.27562	1.32450	1.14199		1.34635		
XDE/M		0.11734	0.10497	0.11848	0.14261		-0.01534		
XDC/M		0.73082	0.60937	0.49189	0.38684		0.55796		
ZU/M		-0.10428	-0.08311	-0.04109	-0.01031		0.02650		
ZW/M		-0.37109	-0.46709	-0.57995	-0.66699		-0.72884		
ZQ/M		-0.78808	-0.96859	-1.36562	-1.54862		-2.08103		
ZDE/M		0.11878	0.32587	0.38735	0.36668		0.33936		
ZDC/M		-5.67725	-5.89510	-6.38311	-6.97350		-7.51348		
MU/IYY		0.00596	-0.00287	-0.00468	-0.00422		-0.00138		
MW/IYY		0.00590	0.01208	0.01080	0.00926		0.00793		
MQ/IYY		-0.74532	-0.98093	-1.10175	-1.13867		-1.20757		
MDE/IYY		0.27308	0.29324	0.32647	0.34753		0.37460		
MDC/IYY		-0.03340	0.02056	0.04493	0.05195		0.03905		
THETA 0		8.00202	6.46507	4.68920	2.57070		2.26076		
DELTAE 0		0.05410	-0.34992	0.06020	0.53133		-0.18811		
DELTAC 0		5.95060	5.14708	4.79474	4.94500		5.50703		
YV/M		-0.05154	-0.06699	-0.09351	-0.11708		-0.13950		
YP/M		-1.33193	-1.55740	-1.66600	-1.64439		-1.38640		
YR/M		-0.22077	-0.24355	-0.19212	-0.10401		-0.09258		
YDA/M		1.00068	0.98003	0.97069	0.96968		0.96484		
YDR/M		0.14586	0.10337	0.08838	0.06990		0.10034		
LV/IXX		-0.01407	-0.01428	-0.01753	-0.02225		-0.02571		
LP/IXX		-0.79973	-0.87323	-0.89489	-0.86718		-0.74691		
LR/IXX		-0.05877	-0.06995	-0.04734	-0.00437		0.00036		
LDA/IXX		0.46831	0.46156	0.45907	0.45956		0.45648		
LDR/IXX		-0.11646	-0.14031	-0.14398	-0.15117		-0.13794		
NV/IZZ		0.00038	-0.00027	-0.00206	-0.00295		-0.00412		
NP/IZZ		-0.02177	-0.02632	-0.03826	-0.05089		-0.06622		
NR/IZZ		-0.06558	-0.05846	-0.05641	-0.06007		-0.06532		
NDA/IZZ		0.02844	0.02707	0.02597	0.02512		0.02637		
NDR/IZZ		0.17277	0.17349	0.17206	0.17250		0.17075		
DELTAA 0		0.08287	0.08326	0.10213	0.16207		0.25359		
DELTAR 0		-0.07643	-0.03872	-0.22665	-0.48305		-0.54755		

TABLE IV-9. DATA BASE

WEIGHT 13400 LB.

C.G. POSITION FORE

RATE OF DESCENT 0 FPM

ALTITUDE 0 FT.

VELOCITY	0	20	40	60	80	80*	100	120	140
XU/M	-0.02612	-0.00238	-0.02127	-0.03559	-0.04563	-0.04613	-0.05574	-0.06492	-0.07218
XW/M	0.05434	0.06828	0.08185	0.08878	0.08500	0.11342	0.10302	0.08599	0.06243
XQ/M	0.68123	0.84128	0.98879	0.99607	0.88251	1.94145	1.57142	0.94491	0.36629
XDE/M	0.18175	0.13644	0.11150	0.12523	0.13583	-0.09885	-0.08439	-0.06606	-0.03277
XDC/M	1.20560	0.98307	0.88235	0.79909	0.68085	1.02612	0.88900	0.73300	0.52023
ZU/M	0.06322	-0.12192	-0.08184	-0.02401	0.01008	0.03930	0.05916	0.06479	0.04906
ZW/M	-0.36895	-0.48482	-0.63339	-0.79968	-0.91843	-0.91459	-0.99750	-1.04458	-1.10393
ZQ/M	-1.13736	-1.73629	-2.40197	-2.67851	-2.79395	-3.00238	-3.14971	-3.32893	-3.55192
ZDE/M	-0.03599	0.18967	0.50720	0.57104	0.54374	0.53420	0.49763	0.45179	0.39978
ZDC/M	-7.42201	-7.25489	-7.69425	-8.54711	-9.48941	-9.37040	-10.25870	-11.09300	-11.72320
MU/IYY	0.00690	0.00609	-0.00546	-0.00648	-0.00499	-0.00222	-0.00115	-0.00050	-0.00023
MW/IYY	-0.00513	0.00653	0.01248	0.00884	0.00580	0.00573	0.00309	0.00085	-0.00057
MQ/IYY	-0.73807	-0.97108	-1.31682	-1.47048	-1.53122	-1.63341	-1.64405	-1.60459	-1.53348
MDE/IYY	0.35342	0.35404	0.40329	0.45335	0.48472	0.49429	0.51899	0.53702	0.54734
MDC/IYY	-0.08891	-0.08332	-0.00503	0.01134	0.00485	-0.01372	-0.02333	-0.03606	-0.04637
THETA 0	9.47577	8.36019	6.79977	4.86323	2.47042	4.41293	1.37417	-2.31055	-6.65376
DELTAE 0	1.19853	0.46617	0.21725	0.65370	1.16758	-0.02036	0.32771	0.50998	0.70454
DELTAC 0	5.02881	4.48307	3.74980	3.54032	3.83774	3.90555	4.72892	6.07823	8.02943
YV/M	-0.02669	-0.05404	-0.08029	-0.11861	-0.15184	-0.15526	-0.18081	-0.19867	-0.23471
YP/M	-0.76215	-0.97080	-1.15800	-1.26960	-1.24640	-1.16699	-1.05610	-0.85751	-0.21591
YR/M	-0.13820	-0.16429	-0.16955	-0.12970	-0.04881	-0.20836	-0.00243	0.34313	0.45010
YDA/M	1.01380	1.01080	0.99098	0.98180	0.98230	0.97032	0.99101	1.03190	1.11760
YDR/M	0.26744	0.25302	0.23252	0.20964	0.21374	0.22768	0.23588	0.24818	0.26719
LV/IXX	-0.00775	-0.01288	-0.01389	-0.01713	-0.02409	-0.02112	-0.03223	-0.04749	-0.05093
LP/IXX	-0.48155	-0.56159	-0.61826	-0.64573	-0.61171	-0.57490	-0.51494	-0.42903	-0.21500
LR/IXX	-0.01718	-0.03337	-0.03813	-0.02025	0.01948	-0.05763	0.04699	0.21651	0.28767
LDA/IXX	0.46452	0.46415	0.45837	0.45628	0.45631	0.45131	0.45866	0.47333	0.50444
LDR/IXX	-0.08132	-0.08649	-0.09048	-0.09745	-0.09563	-0.08424	-0.08616	-0.09182	-0.10153
NV/IZZ	0.00165	0.00058	-0.00091	-0.00229	-0.00339	-0.00459	-0.00429	-0.00259	0.00096
NP/IZZ	-0.00348	-0.00324	-0.03752	-0.04536	-0.06214	-0.06773	-0.07983	-0.08725	-0.06175
NR/IZZ	-0.06500	-0.05691	-0.05050	-0.05120	-0.05602	-0.05764	-0.06814	-0.08431	-0.12644
NDA/IZZ	0.02979	0.02885	0.02727	0.02595	0.02602	0.02665	0.02697	0.02755	0.02843
NDR/IZZ	0.17455	0.17407	0.17093	0.16971	0.16970	0.16894	0.17194	0.17795	0.19374
DELTAA 0	0.18106	0.10490	0.11642	0.13118	0.20698	0.21011	0.33670	0.51408	0.59327
DELTAR 0	-0.31640	-0.16163	-0.18246	-0.39680	-0.69216	-0.54707	-0.86310	-1.19980	-1.33290

TABLE IV-10 DATA BASE

WEIGHT 13400 LB.

C.G. POSITION AFT

RATE OF DESCENT 0 FPM

ALTITUDE 0 FT.

VELOCITY	0	20	40	60	80	80*	100	120	140
XU/M	-0.02493	-0.00110	-0.02275	-0.03752	-0.04765	-0.04771	-0.05661	-0.06428	-0.07333
XW/M	0.05444	0.06882	0.08376	0.09073	0.08680	0.11660	0.10490	0.08542	0.05598
XQ/M	0.47278	0.55272	0.60550	0.56542	0.41751	1.13276	0.86280	0.47079	-0.01182
XDE/M	0.16867	0.14466	0.14875	0.18508	0.21903	-0.01350	0.00654	0.01268	0.00927
XDC/M	1.19776	0.96257	0.87920	0.80702	0.69438	1.03548	0.89060	0.71347	0.47301
ZU/M	0.05728	-0.13227	-0.08444	-0.01892	0.01727	0.04298	0.06281	0.06627	0.05181
ZW/M	-0.36903	-0.48373	-0.64000	-0.80500	-0.92252	-0.92290	-1.00337	-1.04679	-1.10586
ZQ/M	0.01643	-0.01657	-0.16377	-0.18063	0.07086	-0.33864	-0.20274	-0.18242	-0.23794
ZDE/M	0.05155	0.25933	0.52725	0.54601	0.48526	0.48132	0.41256	0.33578	0.27515
ZDC/M	-7.42881	-7.16977	-7.58999	-8.48846	-9.46673	-9.35842	-10.25280	-11.06330	-11.69450
MU/IYY	0.00589	0.00715	-0.00660	-0.00731	-0.00664	-0.00360	-0.00308	-0.00270	-0.00214
MW/IYY	0.00159	0.01613	0.02374	0.02296	0.02246	0.02273	0.02199	0.02101	0.02094
MQ/IYY	-0.73522	-0.96234	-1.31160	-1.47449	-1.53709	-1.61597	-1.63302	-1.60451	-1.55425
MDE/IYY	0.35489	0.35223	0.39700	0.44308	0.47379	0.48682	0.51070	0.52775	0.54186
MDC/IYY	0.03084	0.03478	0.14221	0.17395	0.18611	0.17165	0.18021	0.18517	0.19008
THETA 0	8.98247	7.85991	6.30389	4.39564	1.99886	4.44258	1.39503	-2.30329	-6.65586
DELTAE 0	-0.36082	-1.09382	-1.11713	-0.54350	-0.00194	-1.09732	-0.73354	-0.54753	-0.33376
DELTAC 0	5.02277	4.44246	3.71503	3.53057	3.86946	3.79599	4.65598	6.03707	8.01568
YV/M	-0.02666	-0.05394	-0.08087	-0.11800	-0.15031	-0.15491	-0.17946	-0.19624	-0.23226
YP/M	-0.76750	-0.95746	-1.17144	-1.24159	-1.18989	-1.17602	-1.00044	-0.70098	-0.11992
YR/M	-0.17598	-0.21630	-0.09120	-0.14219	-0.06046	-0.13231	-0.04396	0.05101	0.10331
YDA/M	0.97274	0.96771	0.95283	0.94157	0.94110	0.92364	0.94483	0.98767	1.07454
YDR/M	-0.07735	-0.09021	-0.10613	-0.12550	-0.13279	-0.09158	-0.09264	-0.08746	-0.05750
LV/IXX	-0.00804	-0.01329	-0.01462	-0.01789	-0.02527	-0.02076	-0.03194	-0.04693	-0.05016
LP/IXX	-0.55296	-0.61900	-0.68329	-0.68850	-0.64693	-0.64014	-0.55556	-0.42797	-0.21699
LR/IXX	-0.05590	-0.06586	-0.01732	-0.03768	0.00165	-0.03870	0.01286	0.07665	0.13713
LDA/IXX	0.46883	0.46762	0.46306	0.46017	0.46062	0.45209	0.46011	0.47570	0.50657
LDR/IXX	-0.21032	-0.21491	-0.21801	-0.22321	-0.22555	-0.20645	-0.21088	-0.21739	-0.22255
NV/IZZ	-0.00289	0.00000	-0.00200	-0.00405	-0.00566	-0.00721	-0.00735	-0.00601	-0.00337
NP/IZZ	0.01290	0.00620	-0.00675	-0.02075	-0.03427	-0.03456	-0.04439	-0.05053	-0.03555
NR/IZZ	-0.05254	-0.05195	-0.03292	-0.04546	-0.04884	-0.04448	-0.05704	-0.07878	-0.11367
NDA/IZZ	0.03011	0.02915	0.02773	0.02634	0.02584	0.02727	0.02769	0.02902	0.03251
NDR/IZZ	0.17524	0.17461	0.17191	0.17010	0.16995	0.16675	0.17069	0.17872	0.19453
DELTAA 0	0.09501	0.10597	0.12051	0.12314	0.16061	0.24992	0.30244	0.37302	0.38378
DELTAR 0	0.07237	0.16972	0.05877	-0.20105	-0.47659	-0.32097	-0.57233	-0.74952	-0.75504

TABLE IV-11 DATA BASE

WEIGHT	13400 LB.
C.G. POSITION	AFT
RATE OF DESCENT	0 FPM
ALTITUDE	10000 FT.

*Extrapolated Data

VELOCITY	0	20	40	60	80	80*	100	120	140
XU/M		-0.00610	-0.02109	-0.03204	-0.03844		-0.04409		
XW/M		0.04913	0.05523	0.05732	0.05458		0.06887		
XQ/M		1.04284	1.11325	1.14785	0.97057		1.17891		
XDE/M		0.11609	0.10943	0.13364	0.14429		-0.00663		
XDC/M		0.72526	0.61388	0.50280	0.40639		0.55074		
ZU/M		-0.10802	-0.08336	-0.03657	-0.00687		0.02810		
ZW/M		-0.37024	-0.47079	-0.58311	-0.66901		-0.73036		
ZQ/M		-0.00903	-0.01312	0.02822	-0.12241		-0.61277		
ZDE/M		0.15405	0.32489	0.34552	0.31281		0.28235		
ZDC/M		-5.64627	-5.83849	-6.35464	-6.95898		-7.49086		
MU/IYY		0.00682	-0.00330	-0.00500	-0.00469		-0.00230		
MW/IYY		0.01080	0.01775	0.01802	0.01751		0.01715		
MQ/IYY		-0.74592	-0.99950	-1.12270	-1.15832		-1.21018		
MDE/IYY		0.27217	0.29113	0.32282	0.34476		0.37154		
MDC/IYY		0.02632	0.09502	0.13050	0.14306		0.13884		
THETA 0		7.65085	6.13028	4.31979	2.24015		2.21889		
DELTAE 0		-1.30471	-1.55155	-1.05896	-0.49757		-1.16982		
DELTAC 0		5.94562	5.12954	4.81974	4.96928		5.48120		
YV/M		-0.05183	-0.06713	-0.09342	-0.11642		-0.13886		
YP/M		-1.34060	-1.54850	-1.65520	-1.58310		-1.33490		
YR/M		-0.26074	-0.26982	-0.20445	-0.12337		-0.14663		
YDA/M		0.97591	0.95652	0.95048	0.94507		0.93916		
YDR/M		-0.11110	-0.12006	-0.09533	-0.14780		-0.11746		
LV/IXX		-0.01457	-0.01469	-0.01815	-0.02304		-0.02593		
LP/IXX		-0.85066	-0.91129	-0.93257	-0.88172		-0.76654		
LR/IXX		-0.08507	-0.08967	-0.05864	-0.01904		-0.02907		
LDA/IXX		0.47209	0.46529	0.46415	0.46281		0.45936		
LDR/IXX		-0.22497	-0.22495	-0.20130	-0.23222		-0.21972		
NV/IZZ		0.00012	-0.00073	-0.00282	-0.00399		-0.00555		
NP/IZZ		0.00456	-0.00987	-0.02303	-0.03759		-0.04829		
NR/IZZ		-0.06240	-0.05661	-0.05572	-0.05834		-0.06328		
NDA/IZZ		0.02838	0.02732	0.02602	0.02537		0.02649		
NDR/IZZ		0.17624	0.17272	0.16628	0.17064		0.16989		
DELTAA 0		0.10679	0.11760	0.14024	0.15073		0.23158		
DELTAR 0		0.19807	0.17090	-0.06965	-0.29560		-0.27287		

TABLE IV-12 DATA BASE

WEIGHT 15500 LB.

C.G. POSITION NORMAL

RATE OF DESCENT 0 FPM

ALTITUDE 0 FT.

*Extrapolated Data

VELOCITY	0	20	40	60	80	80*	100	120	140
XU/M	-0.02606	-0.00453	-0.02093	-0.03291	-0.04200	-0.04183	-0.04984	-0.05678	-0.06212
XW/M	0.04740	0.05765	0.06616	0.07052	0.06535	0.09089	0.08148	0.06782	0.05216
XQ/M	0.73514	0.85115	0.92052	0.93829	0.85920	1.46557	1.20014	0.74836	-0.01630
XDE/M	0.15403	0.12503	0.11066	0.12831	0.14787	-0.04724	-0.03261	-0.02290	0.01325
XDC/M	1.06019	0.83650	0.71598	0.61425	0.48606	0.76986	0.65938	0.52661	0.39715
ZU/M	0.05355	-0.11291	-0.08226	-0.03288	0.00092	0.02335	0.04264	0.04743	0.03835
ZW/M	-0.32575	-0.42254	-0.54306	-0.68247	-0.78390	-0.78166	-0.85240	-0.89244	-0.92855
ZQ/M	-0.59946	-0.91194	-1.20630	-1.48572	-1.51634	-1.96210	-1.97566	-1.97216	-2.13191
ZDE/M	-0.00163	0.16095	0.41157	0.46557	0.43829	0.43090	0.39375	0.34673	0.30778
ZDC/M	-6.54750	-6.37990	-6.70150	-7.35390	-8.11797	-8.00617	-8.73415	-9.42604	-9.98020
MU/IYY	0.00679	0.00716	-0.00496	-0.00649	-0.00580	-0.00248	-0.00186	-0.00132	-0.00117
MW/IYY	-0.00291	0.00880	0.01621	0.01402	0.01178	0.01179	0.00988	0.00829	0.00718
MQ/IYY	-0.75590	-0.95462	-1.27610	-1.44447	-1.50013	-1.56926	-1.58520	-1.56141	-1.50602
MDE/IYY	0.35863	0.35707	0.39455	0.44216	0.47122	0.48050	0.50439	0.52310	0.52557
MDC/IYY	-0.04965	-0.04451	0.03618	0.06291	0.06596	0.04879	0.04817	0.04388	0.03912
THETA 0	9.30250	8.12154	6.55685	4.74234	2.49743	4.67390	1.89087	-1.43028	-5.38938
DELTAE 0	0.74095	0.02785	-0.26519	0.21841	0.65591	-0.47903	-0.14579	0.08319	0.28100
DELTAC 0	5.69163	5.16045	4.39169	4.11274	4.33541	4.32822	5.03437	6.22400	7.97623
YV/M	-0.02655	-0.05222	-0.07345	-0.10503	-0.13333	-0.13796	-0.15939	-0.17394	-0.20344
YP/M	-0.88730	-1.02770	-1.21130	-1.29830	-1.29350	-1.25531	-1.13350	-0.89468	-0.31798
YR/M	-0.13899	-0.04739	-0.18509	-0.16205	0.07461	-0.25629	-0.07225	0.05917	0.00712
YDA/M	1.00031	0.99710	0.97654	0.96870	0.96646	0.94911	0.96343	0.99430	1.05555
YDR/M	0.14443	0.13450	0.11584	0.10177	0.10188	0.10575	0.10894	0.11521	0.13537
LV/IXX	-0.00960	-0.01522	-0.01622	-0.01959	-0.02632	-0.02109	-0.03242	-0.04836	-0.05233
LP/IXX	-0.60598	-0.66759	-0.73596	-0.75278	-0.72957	-0.70695	-0.63596	-0.51719	-0.25436
LR/IXX	-0.02248	0.01450	-0.04562	-0.03628	0.07722	-0.08592	0.01507	0.10356	0.09688
LDA/IXX	0.52066	0.52017	0.51266	0.51017	0.51087	0.50227	0.50879	0.52112	0.54599
LDR/IXX	-0.14890	-0.15302	-0.15714	-0.16177	-0.15372	-0.15232	-0.15260	-0.16121	-0.16567
NV/IZZ	0.00012	0.00045	-0.00091	-0.00285	-0.00413	-0.00551	-0.00555	-0.00435	-0.00150
NP/IZZ	-0.02138	-0.01935	-0.02612	-0.03938	-0.05223	-0.05827	-0.06879	-0.07697	-0.08705
NR/IZZ	-0.07150	-0.04773	-0.06054	-0.05867	-0.04619	-0.06299	-0.06901	-0.09353	-0.10462
NDA/IZZ	0.03429	0.03313	0.03138	0.03044	0.02892	0.02990	0.02973	0.03091	0.03302
NDR/IZZ	0.20337	0.20300	0.19946	0.19814	0.19499	0.19455	0.19652	0.20360	0.21616
DELTAA 0	0.14008	0.09373	0.08581	0.12261	0.16838	0.17296	0.26989	0.41799	0.45688
DELTAR 0	-0.18958	-0.06631	-0.06037	-0.28616	-0.56343	-0.39368	-0.67419	-0.95795	-1.03890

TABLE IV-13 DATA BASE

WEIGHT	15500 LB.
C.G. POSITION	AFT
RATE OF DESCENT	0 FPM
ALTITUDE	0 FT.

*Extrapolated Data

VELOCITY	0	20	40	60	80	80*	100	120	140
[illegible]	[illegible]	[illegible]	[illegible]	[illegible]	[illegible]	[illegible]	[illegible]	[illegible]	[illegible]
[illegible]	[illegible]	[illegible]	[illegible]	[illegible]	[illegible]	[illegible]	[illegible]	[illegible]	[illegible]
[illegible]	[illegible]	[illegible]	[illegible]	[illegible]	[illegible]	[illegible]	[illegible]	[illegible]	[illegible]
[illegible]	[illegible]	[illegible]	[illegible]	[illegible]	[illegible]	[illegible]	[illegible]	[illegible]	[illegible]
[illegible]	[illegible]	[illegible]	[illegible]	[illegible]	[illegible]	[illegible]	[illegible]	[illegible]	[illegible]
[illegible]	[illegible]	[illegible]	[illegible]	[illegible]	[illegible]	[illegible]	[illegible]	[illegible]	[illegible]
[illegible]	[illegible]	[illegible]	[illegible]	[illegible]	[illegible]	[illegible]	[illegible]	[illegible]	[illegible]
ZW/M	-0.32585	-0.42223	-0.54786	-0.68611	-0.78492	-0.78329	-0.85288	-0.87325	-0.92929
ZQ/M	0.12677	-0.05132	0.03559	-0.02299	0.13032	-0.26841	-0.19933	-0.21448	-0.39822
ZDE/M	0.04201	0.19703	0.41244	0.42949	0.37432	-0.05066	0.03874	0.27272	0.21815
ZDC/M	-6.55027	-6.33758	-6.63904	-7.30928	-8.08660	-7.96648	-8.70262	-9.39757	-9.92681
MU/IYY	0.00614	0.00815	-0.00560	-0.00710	-0.00644	-0.00374	-0.00315	-0.00263	-0.00229
MW/IYY	0.00171	0.01533	0.02366	0.02349	0.02328	0.02319	0.02258	0.02157	0.02109
MQ/IYY	-0.75031	-0.95580	-1.29310	-1.46145	-1.52768	-1.57150	-1.59824	-1.58550	-1.51087
MDE/IYY	0.35904	0.35551	0.39110	0.43617	0.46456	0.47487	0.49842	0.51712	0.53171
MDC/IYY	0.03115	0.03512	0.13519	0.17373	0.19120	0.17344	0.18455	0.18930	0.19198
THETA 0	9.00799	7.76850	6.22388	4.40978	2.15831	4.60549	1.83185	-1.46397	-5.45226
DELTAE 0	-0.41030	-1.18490	-1.31662	-0.78754	-0.22026	-1.36225	-0.96325	-0.73252	-0.51740
DELTAC 0	5.68575	5.14427	4.36250	4.10901	4.35952	4.32010	5.03387	6.21091	7.99168
YV/M	-0.02651	-0.05233	-0.07348	-0.10462	-0.13268	-0.13760	-0.15866	-0.17272	-0.20268
YP/M	-0.86509	-1.02720	-1.21260	-1.29060	-1.25260	-1.22084	-1.06980	-0.80571	-0.36599
YR/M	-0.18178	-0.22615	-0.20130	-0.15699	-0.08640	-0.17919	-0.09768	-0.00525	0.03705
YDA/M	0.97234	0.96963	0.95188	0.94199	0.94038	0.92918	0.94186	0.96882	1.02314
YDR/M	-0.07733	-0.09725	-0.10843	-0.13169	-0.13814	-0.11050	-0.10985	-0.10209	-0.08288
LV/IXX	-0.00993	-0.01567	-0.01660	-0.02020	-0.02736	-0.02152	-0.03279	-0.04817	-0.05221
LP/IXX	-0.64712	-0.71217	-0.77872	-0.79201	-0.74964	-0.72823	-0.64377	-0.51722	-0.34287
LR/IXX	-0.05326	-0.06908	-0.06305	-0.04144	-0.00306	-0.06172	-0.00718	0.06353	0.12367
LDA/IXX	0.52316	0.52322	0.51670	0.51396	0.51396	0.50706	0.51301	0.52491	0.54577
LDR/IXX	-0.24485	-0.25386	-0.25470	-0.26285	-0.26499	-0.25039	-0.25272	-0.25523	-0.26023
NV/IZZ	-0.00331	0.00009	-0.00151	-0.00391	-0.00558	-0.00708	-0.00746	-0.00654	-0.00412
NP/IZZ	0.01247	0.00606	-0.00536	-0.01946	-0.03654	-0.04354	-0.05332	-0.05580	-0.03048
NR/IZZ	-0.06677	-0.06509	-0.05712	-0.05511	-0.05837	-0.04935	-0.06303	-0.08712	-0.12266
NDA/IZZ	0.03452	0.03305	0.03147	0.02969	0.02915	0.03061	0.03067	0.03133	0.03506
NDR/IZZ	0.20236	0.20220	0.19860	0.19681	0.19643	0.19405	0.19673	0.20247	0.21526
DELTAA 0	0.10521	0.10938	0.12754	0.14089	0.15969	0.22022	0.26998	0.35070	0.38744
DELTAR 0	0.08426	0.17930	0.10222	-0.15547	-0.42583	-0.25776	-0.48124	-0.65784	-0.67194

TABLE IV-14 DATA BASE

WEIGHT	15500 LB.
C.G. POSITION	AFT
RATE OF DESCENT	500 FPM
ALTITUDE	0 FT.

VELOCITY	0	20	40	60	80	80*	100	120	140
XU/M	-0.02300	0.00100	-0.01800	-0.03200	-0.04200	-0.04200	-0.05000	-0.05600	-0.06200
XW/M	0.04200	0.05400	0.06900	0.07200	0.06900	0.09100	0.08500	0.07600	0.05800
XQ/M	0.74800	0.81500	0.88300	0.88200	0.76600	1.35250	1.13200	0.80700	0.26500
XDE/M	0.14500	0.12500	0.12900	0.16300	0.19400	-0.00800	0.01100	0.01800	0.0
XDC/M	1.05500	0.81600	0.70200	0.64100	0.52900	0.82800	0.69900	0.55300	0.41200
ZU/M	0.04300	-0.14800	-0.11400	-0.04100	0.0	0.02100	0.04400	0.04900	0.04200
ZW/M	-0.29100	-0.37800	-0.52900	-0.67300	-0.77900	-0.76200	-0.84900	-0.91700	-0.93200
ZQ/M	0.07800	0.23800	-0.12800	-0.19800	-0.04400	-0.39600	-0.30600	-0.28000	-0.27900
ZDE/M	0.04400	0.21000	0.48400	0.49400	0.42500	0.42500	0.35600	0.28700	0.23300
ZDC/M	-6.56900	-6.25600	-6.39100	-7.18000	-8.01400	-7.94100	-8.69800	-9.37800	-10.00900
MU/IYY	0.00800	0.01200	-0.00800	-0.00800	-0.00700	-0.00350	-0.00300	-0.00300	-0.00200
MW/IYY	0.00100	0.01900	0.02800	0.02500	0.02400	0.02350	0.02300	0.02300	0.02200
MQ/IYY	-0.69700	-0.92400	-1.33400	-1.49900	-1.55900	-1.64500	-1.65600	-1.61800	-1.56300
MDE/IYY	0.35500	0.34500	0.39500	0.44100	0.47100	0.48200	0.50600	0.52400	0.54000
MDC/IYY	0.03100	0.01500	0.14900	0.18800	0.20200	0.18450	0.19300	0.19600	0.19800
THETA 0	8.94100	7.74900	6.30700	4.59300	2.46700	4.89250	2.17100	-1.14600	-5.15100
DELTAE 0	-0.42300	-1.54500	-1.65900	-0.94300	-0.26500	-1.45450	-1.02100	-0.83700	-0.57400
DELTAC 0	5.31800	4.64700	3.65100	3.28900	3.48100	3.38400	4.09200	5.31600	7.09440
YV/M	0.18900	-0.04700	-0.07400	-0.10600	-0.13800	-0.14650	-0.16900	-0.18200	-0.19800
YP/M	-0.96600	-1.17600	-1.36600	-1.45900	-1.43900	-1.35550	-1.24400	-1.04100	-0.57600
YR/M	-0.18700	-0.12200	-0.11700	-0.18300	-0.12000	-0.08400	0.00700	0.12600	0.06800
YDA/M	0.97000	0.96200	0.93700	0.92100	0.91400	0.88900	0.90100	0.93200	0.98800
YDR/M	-0.07900	-0.10200	-0.11600	-0.13800	-0.13700	-0.11850	-0.12000	-0.12400	-0.09700
LV/IXX	-0.01000	-0.01400	-0.01400	-0.01400	-0.01800	-0.01100	-0.02200	-0.04000	-0.05700
LP/IXX	-0.68400	-0.78200	-0.83900	-0.85800	-0.82300	-0.78850	-0.71800	-0.61200	-0.40500
LR/IXX	-0.05800	-0.02900	-0.03400	-0.05000	-0.02500	-0.02200	0.03200	0.11500	0.11000
LDA/IXX	0.52200	0.52000	0.51100	0.50600	0.50200	0.49100	0.49600	0.51000	0.53200
LDR/IXX	-0.24500	-0.25500	-0.25500	-0.26100	-0.25900	-0.24450	-0.24800	-0.25700	-0.25800
NV/IZZ	0.00200	0.0	-0.00200	-0.00500	-0.00700	-0.00800	-0.00900	-0.00900	-0.00600
NP/IZZ	0.00600	0.00700	-0.01000	-0.02500	-0.04200	-0.04050	-0.05300	-0.06100	-0.05400
NR/IZZ	-0.06300	-0.04300	-0.03400	-0.04800	-0.05200	-0.02600	-0.03900	-0.06100	-0.09600
NDA/IZZ	0.03400	0.03300	0.03100	0.02900	0.02800	0.02950	0.02900	0.02900	0.03200
NDR/IZZ	0.20200	0.20000	0.19600	0.19300	0.19100	0.18550	0.18800	0.19500	0.20700
DELTAA 0	0.11600	0.09700	0.11400	0.11000	0.14200	0.14600	0.21400	0.31800	0.40900
DELTAR 0	0.05900	0.24000	0.14300	-0.13100	-0.41800	-0.17500	-0.44800	-0.70700	-0.81900

Table	Weight lb	cg	Attitude	Rate of Descent fpm	Source
IV-1	13,400	Normal	Sea Level	0	NASA
IV-2	13,400	Normal	Sea Level	+1500	NASA
IV-3	13,400	Normal	Sea Level	+1000	Boeing
IV-4	13,400	Normal	Sea Level	+500	Boeing
IV-5	13,400	Normal	Sea Level	-500	Boeing
IV-6	13,400	Normal	Sea Level	-1500	NASA
IV-7	13,400	Normal	2,000 ft	0	Boeing
IV-8	13,400	Normal	10,000 ft	0	NASA
IV-9	13,400	Fore	Sea Level	0	NASA
IV-10	13,400	Aft	Sea Level	0	NASA
IV-11	13,400	Aft	10,000 ft	0	NASA
IV-12	15,500	Normal	Sea Level	0	NASA
IV-13	15,500	Aft	Sea Level	0	NASA
IV-14	15,500	Aft	Sea Level	+500	Boeing

The tables for the fore and aft cg locations are for a cg that is 13 inches ahead and 25 inches behind the nominal cg location respectively For all of these tables, the vehicle inertias, are as follows

$I_{XX} = 9203$ slug ft^2	$I_{ZZ} = 71,786$ slug ft^2
$I_{YY} = 75,914$ slug ft^2	$J_{XZ} = 7114$ slug ft^2

The nomenclature and units for all of these tables is as follows.

XU/M	X_U/m	ft/sec^2/ft/sec	YV/M	Y_V/m	ft/sec^2/ft/sec
XW/M	X_W/m	ft/sec^2/ft/sec	YP/M	Y_P/m	ft/sec^2/rad/sec
XQ/M	X_Q/m	ft/sec^2/rad/sec	YR/M	Y_R/m	ft/sec^2/rad/sec
XDE/M	X_{δ_e}/m	ft/sec^2/in	YDA/M	Y_{δ_a}/m	ft/sec^2/in
XDC/M	X_{δ_c}/m	ft/sec^2/in.	YDR/M	Y_{δ_r}/m	ft/sec^2/in.
ZU/M	Z_U/m	ft/sec^2/ft/sec	LV/IXX	L_V/I_{XX}	rad/sec^2/ft/sec
ZW/M	Z_W/m	ft/sec^2/ft/sec	LP/IXX	L_P/I_{XX}	rad/sec^2/rad/sec
ZQ/M	Z_Q/m	ft/sec^2/rad/sec	LR/IXX	L_R/I_{XX}	rad/sec^2/rad/sec
ZDE/M	Z_{δ_e}/m	ft/sec^2/in.	LDA/IXX	L_{δ_a}/I_{XX}	rad/sec^2/in.
ZDC/M	Z_{δ_c}/m	ft/sec^2/in	LDR/IXX	L_{δ_r}/I_{XX}	rad/sec^2/in.
MU/IYY	M_U/I_{YY}	rad/sec^2/ft/sec	NV/IZZ	N_V/I_{ZZ}	rad/sec^2/ft/sec
MW/IYY	M_W/I_{YY}	rad/sec^2/ft/sec	NP/IZZ	N_P/I_{ZZ}	rad/sec^2/rad/sec
MQ/IYY	M_Q/I_{YY}	rad/sec^2/rad/sec	NR/IZZ	N_R/I_{ZZ}	rad/sec^2/rad/sec
MDE/IYY	M_{δ_e}/I_{YY}	rad/sec^2/in.	NDA/IZZ	N_{δ_a}/I_{ZZ}	rad/sec^2/in.
MDC/IYY	M_{δ_c}/I_{YY}	rad/sec^2/in.	NDR/IZZ	N_{δ_r}/I_{ZZ}	rad/sec^2/in.
THETA O	θ_o	degrees	DELTAA O	$\delta_{a/o}$	in.
DELTAE O	$\delta_{e/o}$	in	DELTAR O	$\delta_{r/o}$	in.
DELTAC O	$\delta_{c/o}$	in.			

The data at the velocity points marked with an asterisk in these tables is data that was established from the basic data by curve fitting techniques The data at the 80* velocity point was extrapolated from the data at speeds greater than 80 knots, which reflects a rear rotor axis trim change, to determine the effect of this trim change alone at 80 knots This was done by averaging the slope of the data between the 60 and 80 knot points and the slope between the 100 and 120 knot points and using this average slope to extrapolate from the 100 knot point, which reflects the rotor axis trim change, back to the 80 knot point

The data at the 100*, 120*, and 140* velocity points for the ±1500 ft/min rate of descent conditions was established by extrapolating data for other rates of descent of these velocity points

2 Actuator and Rotor Dynamics

The functions used to represent the actuator and rotor dynamics in each channel of control are shown in Figure IV-1 As shown in this figure, each channel is represented by a position limit on the input command, a second order EISS response, a rate limit on the EISS response, hysteresis in the mechanical linkage to the rotor, and a record order rotor response

3. Wind Model

The wind model was developed by Bell Aerospace Company under this contract from data obtained from AN/SPN-42 landing dispersions at Patuxent River, Maryland and from gust data taken from towers and low flying aircraft, Reference IV-1 Based on this data, the horizontal wind spectrum is assumed to be of the form,

$$\Phi = N^2 \left[\frac{1}{\left(\frac{100}{V_X^W + 10}\right)^2 \omega^2 + 1} \right],$$

where $N = \frac{\sigma^2}{\pi}\left(\frac{100}{V_X^W + 10}\right)$

σ = rms value of horizontal gusts

V_X^W = horizontal velocity of helicopter along direction of average wind

It is assumed that the gusts are made up of a primary component in the direction of the average wind and a secondary component normal to the direction of the average wind The component in the direction of the average wind is assumed to have an rms value that is a function of the average wind velocity

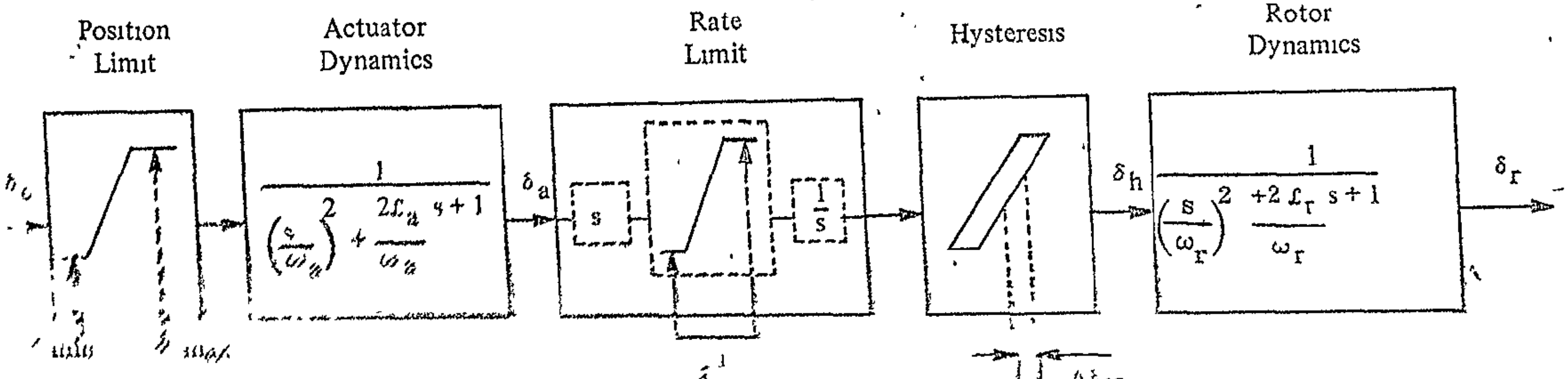

Note: Nominal values used are as follows

Channel	δ_{min}	δ_{max}	ω_a	$\mathcal{L}_a$	$\dot{\delta}_{max}$	$\Delta\delta_H$	ω_r	$\mathcal{L}_r$
Differential Collective	-5.5 in.	+ 5.5 in	15 rad/sec	0 6	10 in /sec	0 1 in	27 rad/sec	0 62
Collective	0 in.	+12.8 in	15 rad/sec	0 6	10 in /sec	0 1 in	27 rad/sec	0 62
Cyclic	-3 6 in	+3 6 in	15 rad/sec	0 6	10 in/sec	0 1 in	27 rad/sec	0 62
Differential Cyclic	-2 3 in	+2.3 in	15 rad/sec	0 6	5 in/sec	0 1 in	27 rad/sec	0 62

Figure IV-1. Actuator and Rotor Dynamics Model

$\sigma_X = 0.1\ V_W \geqslant 2$ ft/sec

where V_W = average horizontal wind velocity

The component normal to the average wind is assumed to have an rms value of 10% of the primary component

The horizontal velocity of the helicopter in the direction of the average wind is,

$$V_X^W = V_h \cos \Delta \xi$$

where V_h = total horizontal ground speed of helicopter ($\sqrt{\dot{X}^2 + \dot{Y}^2}$)

$\Delta\xi$ = angle between course of helicopter ground speed velocity vector and direction of wind

By using these definitions and resolving the wind spectrum through the angle $\Delta\xi$, the wind spectrum along the aircraft x and y body axes are,

$$\Phi_X = \frac{(\sigma_X \cos \Delta\xi + \sigma_y \sin \Delta\xi)^2}{\pi} \frac{100}{(V_h \cos \Delta\xi + 10)} \left[\frac{1}{\left(\frac{100}{V_h \cos \Delta\xi + 10}\right)^2 \omega^2 + 1}\right]$$

$$\Phi_y = \frac{(-\sigma_X \sin \Delta\xi + \sigma_y \cos \Delta\xi)^2}{\pi} \frac{100}{(V_h \cos \Delta\xi + 10)} \left[\frac{1}{\left(\frac{100}{V_h \cos \Delta\xi + 10}\right)^2 \omega^2 + 1}\right]$$

The wind spectrum for vertical turbulence along the z body axis is assumed to be of the form

$$\Phi_z = \frac{\sigma_z^2}{\pi} \frac{Z}{V_h} \left[\frac{1}{\left(\frac{Z}{V_h}\right)^2 \omega^2 + 1}\right]$$

where σ_z = rms value of vertical turbulence (nominally 1.5 ft/sec)

4 Strapdown Navigational System

The attitude and velocity sensor error models were supplied by NASA/ERC Both a general definition of the gyro model and attitude equations and simplified definitions of the attitude and velocity sensor errors for the purposes of simulation were provided The simulation model for the velocity errors was developed from the simplified definition However, since the general definition of the gyro model and attitude equations contained more information on form of the errors that are expected in the attitude data, it was used to develop the simulation model for the attitude errors Therefore, for completeness, both the definitions supplied by NASA-ERC will be included here

a. General Definition of Gyro Model and Attitude Equations

(1) Mathematical Model

The mathematical model for the simulation gyro is given by

$$(Is^2 + Cs)\ A = H\ (W_{IA} - W_{tg}) + N$$

where
- I = gyro float Output Axis (OA) moment of inertia
- C = gyro damping constant
- s = Laplace Transform operator
- A = gyro float angle about OA
- H = gyro spin angular momentum
- W_{IA} = Input Axis (IA) component of angular velocity vector $\underline{W}$
- HW_{tg} = electrically generated torque about OA
- N = an error torque embodying all gyro nonideal performance ($N = 0$ for this study)

(2). Functional Model

The functional model for the simulation gyro is shown in Figure IV-2 where the following identifications are made in terms of the gyro mathematical model

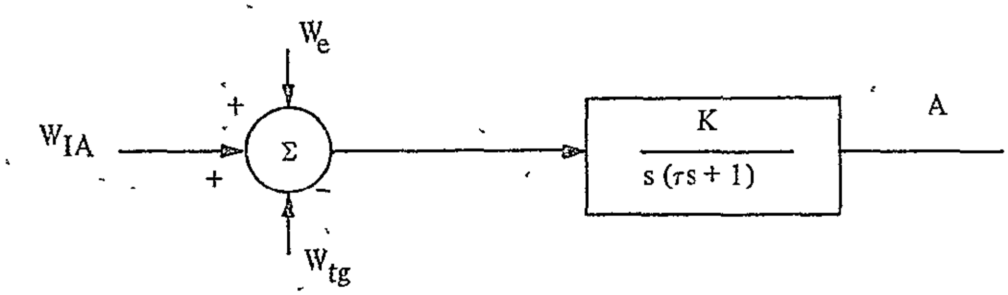

Figure IV-2 Functional Model for the Simulation Gyro

$$K = H/C$$
$$\tau = I/C$$
$$W_e = N/H$$

The functional model for the currently used GG334A rebalance loop is shown in Figure IV-3

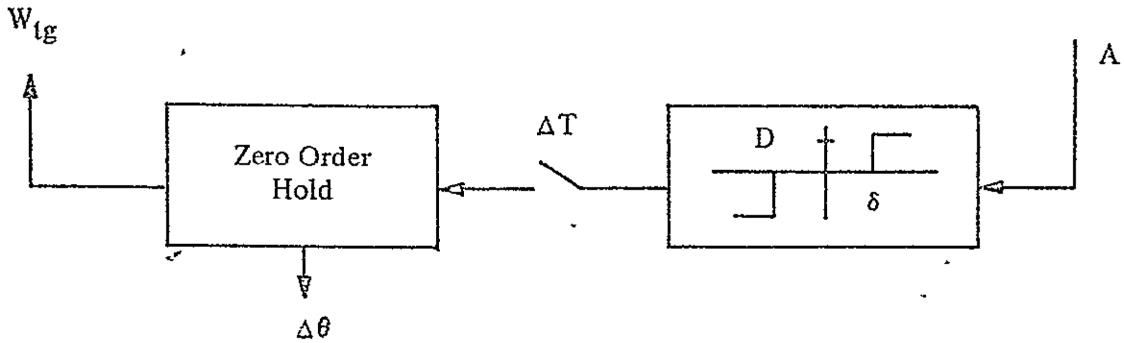

Figure IV-3 Functional Model for GG334A Rebalance Loop

ΔT = sampling interval

D = rebalance signal level

δ = float angle threshold

$\Delta\theta$ = output pulse weight (rad/pulse)

The voltage level W_{tg} of the zero order hold is observed once between sampling instants A + $\Delta\theta$, O, or a $-\Delta\theta$ data pulse is transmitted to the digital computer if W_{tg} = +D, O, -D, respectively

(3) Performance Model

The simulation gyro is intended to model the performance of the Honeywell GG334A used in the V/STOL Phase II Inertial Sensity Unit (ISU) In order to duplicate the GG334A's dynamic performance, the following relationships must be observed

Decide upon $W_{IA, MAX}$ (Maximum permissible W_{IA})

Set $D = W_{IA, MAX}$

Decide upon $\Delta\theta$ = (desired resolution)

Solve for $\Delta T = \Delta\theta / W_{IA, MAX}$

Solve for $\tau = 1\ 8\ \Delta T$

Solve for K such that if a unity feedback loop were closed in Figure IV-2, the resulting system would have a damping ratio of 0 2 Thus

$$K = \frac{1}{0\ 16}$$

Set $\delta = K\Delta\theta$

Then when $\int W_{IA}dt = \Delta\theta$, A has made an excursion equal to δ (neglecting float dynamics)

(4) Direction Cosine Update Equations

In order to compute both angular velocity and attitude, the $\Delta\theta$ pulses from the gyros are accumulated in the digital computer The direction cosine matrix is updated using a 2nd order Runge-Kutta algorithm

$$C^{NB}(t_{n+1}) = C^{NB}(t_n)\left(I + [\theta x] + 5\,[\theta_1 x]\,[\theta_2 x] - \frac{3}{2}[\theta_1 x]^2 - \frac{3}{2}[\theta_2 x]^2\right)$$

where C^{NB} is the direction cosine matrix from the body to the navigational coordinate frame

$$\Delta t = t_{n+1} - t_n$$

$$\underline{\theta}_1 = \Sigma\Delta\underline{\theta} \text{ over the 1st half of } \Delta t$$

$$\underline{\theta}_2 = \Sigma\Delta\underline{\theta} \text{ over the second half of } \Delta t$$

$$\underline{\theta} = \underline{\theta}_1 + \underline{\theta}_2$$

$$[\underline{\theta} x] = \begin{bmatrix} 0 & -\theta_Z & \theta_Y \\ \theta_Z & 0 & -\theta_X \\ -\theta_Y & \theta_X & 0 \end{bmatrix}$$

The attitude drift rate W_d (deg/sec) induced by this particular choice of update algorithm is given by

$$W_d = 3\,7 \times 10^{-5}\,\frac{W^3}{f_c^2}$$

where W is the magnitude of the angular velocity vector

f_c is the frequency of the direction cosine matrix update

This equation is applicable in the case where W is essentially constant over the update interval Δt

(5) Body Rate Computation

The algorithm for extracting body rates from the gyro data is

$$\underline{W} = \begin{bmatrix} P \\ Q \\ R \end{bmatrix} = \left(-\frac{1}{2}\underline{\theta}_1 + \frac{3}{2}\underline{\theta}_2\right)\frac{1}{\Delta t}$$

where P, Q, and R, are the x, y, and z axis body frame components respectively of angular velocity $\underline{W}$, $\underline{\theta}_1$, $\underline{\theta}_2$, and Δt are as defined above This procedure fits a straight line through the angular velocity measured in the two halves of the interval Δt

6) Euler Angle Computation

The Euler angles are extracted from the direction cosines

Since

$$C^{NB} = \begin{bmatrix} \cos\theta\cos\psi & \sin\phi\sin\theta\cos\psi - \cos\phi\sin\psi & \cos\phi\sin\theta\cos\psi + \sin\phi\sin\psi \\ \cos\theta\sin\psi & \sin\phi\sin\theta\sin\psi + \cos\phi\cos\psi & \cos\phi\sin\theta\sin\psi - \sin\phi\cos\psi \\ \sin\theta & \cos\theta\sin\phi & \cos\theta\cos\phi \end{bmatrix}$$

and since from physical considerations

$$-\pi/2 < \phi < \pi/2$$

$$-\pi/2 < \theta < \pi/2$$

$$0 < \psi \leq 2\pi$$

the Euler angles are computed as follows

θ Computation

$$C_{31} = \sin\theta$$

so $$\theta = \sin^{-1} C_{31}$$

ϕ Computation

$$C_{32} = \sin\phi\cos\theta$$

$$= \sin\phi\,(1-(C_{31})^2)^{1/2}$$

so $$\phi = \sin^{-1}\left[C_{32}(1-(C_{31})^2)^{-1/2}\right]$$

Computation

$$C_{21} = \cos\theta\sin\psi$$

$$= (1-(C_{31})^2)^{1/2}\sin\psi$$

Let

$$\psi' = \sin^{-1}\left[C_{21}\ (1-(C_{31})^2)^{-1/2}\right]$$

Then

$$\psi = \psi' \quad \text{if } C_{11} \geq 0$$

$$\psi = \pi-\psi' \quad \text{if } C_{11} < 0$$

b Simplified Definition of Velocity and Attitude Sensor Error Models

The simplified velocity and attitude sensor error models are shown in Figures IV-4 and IV-5, respectively

5 Air Speed Indicator With Pitot Head

The error model for a typical airspeed sensor was developed by Bell Aerospace Company under this contract A discussion of the source and expected magnitudes of the errors in this sensor is contained in the following paragraphs

For a typical aircraft moving forward with a speed V, the air speed is determined by measurement of the static pressure of the undisturbed air p, and the total, or stagnation, pressure p_t i e , the pressure at a point on the vehicle which has been brought to rest, e g at the bellows of the air speed indicator, or at the measuring head

The relationship between the true air speed V and these pressures, assuming adiabatic conditions in a compressible medium may be given as

$$p_t = p \left\{ 1 + \frac{(\gamma - 1)}{2\gamma} \frac{\rho V^2}{p} \right\}^{\gamma/(\gamma - 1)} \tag{1}$$

where γ is the coefficient of adiabatic expansion

and ρ is the density of the air

American practice is to calibrate air speed indicators using this formula with γ as a constant and assuming International Commission for Air Navigation (ICAN) Standard Atmosphere values p_o (for p) and ρ_o (for ρ) yielding the equation

$$V_r = \left[\frac{2 \gamma p_o}{(\gamma - 1) \rho_o} \left\{ \left(\frac{p_o + \Delta_p}{p_o} \right)^{\gamma - 1/\gamma} - 1 \right\} \right]^{1/2}$$

where V_r is the rectified air speed

$\Delta_p = (p_t - p)$

Significant differences do not arise between these two formulae until sonic speeds are approached

An alternative to this equation is to directly expand equation (1) and neglecting all but the first two terms to yield

$$\Delta_p = \frac{\rho_o}{2} V_r^2 \left(1 + \frac{V_r^2}{4 c_o^2} \right)$$

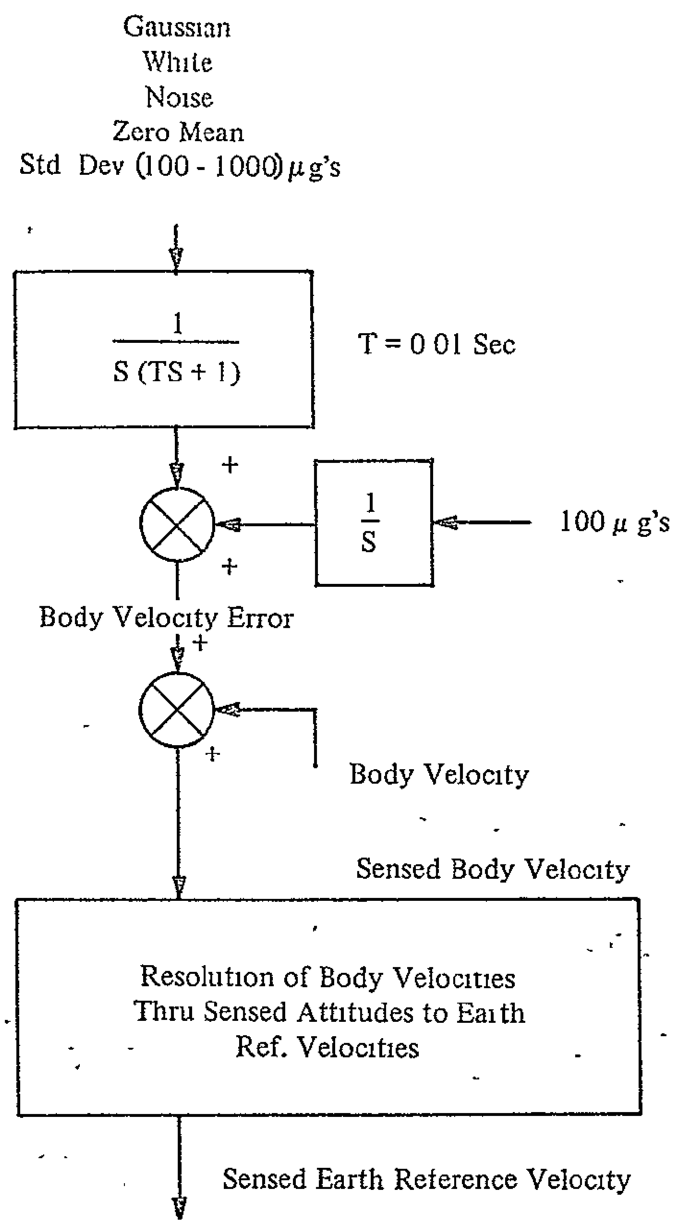

Figure IV-4 Velocity Sensor

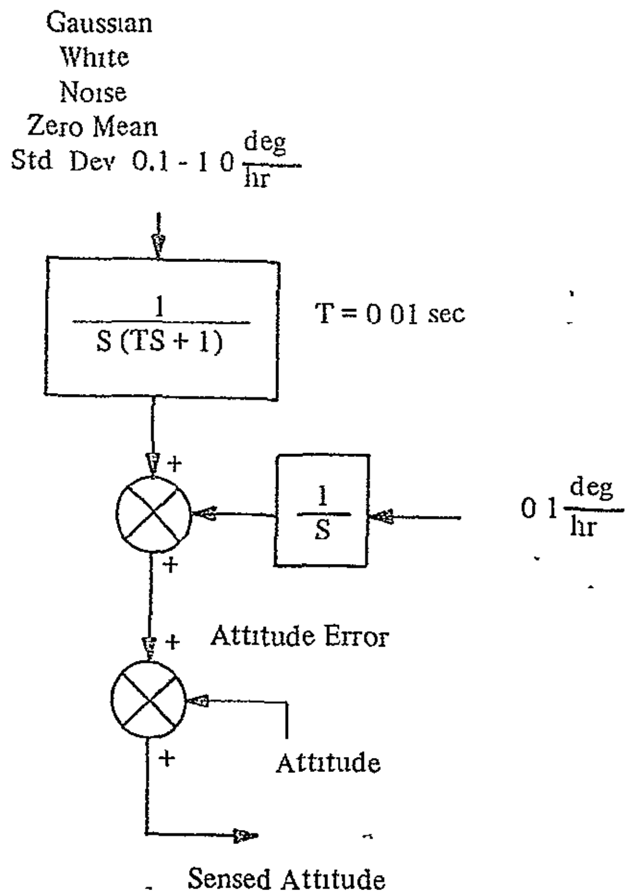

Notes: (1) Angular Rate Resolution within estimated quantization of 0 1 $\frac{deg}{sec}$

(2) Attitude quantization less than 0 01 deg should be no problem

Figure IV-5. Attitude Sensor

where c_0 is the velocity of sound in the Standard Atmosphere At low speeds the second term in this equation may be neglected and the true air speed and rectified air speed are then related by the expression related by the expression

$$\rho_0 V_r^2 \doteq \rho V^2$$

Thus to a first approximation the air speed is proportional to the square root of the difference between the pressure at the pilot head and the static pressure.

The manufacturing tolerances at normal temperatures for a typical low air speed indicator with a range of 30 to 150 knots do not exceed ±4 knots over the whole range However, when used on helicopters the downwash from the rotors increases this error substantially as speeds typically below 50 knots

In addition to the instrumental errors, errors in the total and static pressures at the measuring head, known as position errors, will occur These vary with the tape of aircraft and the pressure head installation, but with a carefully selected position, the average values can be reduced to about 3 to 4 knots

Hysteresis effects in the instrument will also contribute errors, but these will in general be small, of the order of 1 or 2 knots

Errors will also be introduced if the axis of the pilot tube does not coincide with direction of air flow The magnitude of these errors will depend on the angle of incidence, γ, of the pitot tube axis and also upon the ratio d/D where d is the diameter of the pitot aperture, and D is the overall diameter of the pitot tube For example for a ratio of $d/D \leqslant 0.3$ and angles not exceeding $\pm 10°$, the error, expressed as a percentage of the pressure difference Δp (not of the air speed) which is the operating pressure for the airspeed indicator does not exceed 1 5%, although for angles up to ±25° this error may increase to about 10%

The pitot tube is connected to the air speed indicator by means of metal tubing, usually about 3/16 in inside diameter The length of the tubing will vary with the installation, but lengths exceeding 50 feet are not uncommon Due to this length, there will be a finite pressure drop between the pitot head and the instrument bellows, and therefore the transient response of the system to pressure changes at the head position will be an exponential motion with a finite time constant τ Thus if the external pressure is suddenly decreased at time τ at a uniform rate dp/dt, the instrument pressures will, after the decay of any transient conditions, change at a similar rate, but the pressures will lag by an amount equal to τ dp/dt where τ is the time constant of the system A typical value of τ for a 50 foot length of 3/16 in diameter tubing will be about 0 2 second

Thus the accuracy of the air speed indicator is not high, but it is generally adequate for the pilot's use If this information is to be used for navigation purposes then an order of improvement in accuracy is required This is usually calculated when required, using calibration information, etc.

A mathematical error model of the airspeed indicator and pitot tube is thus illustrated in Figure IV-6,

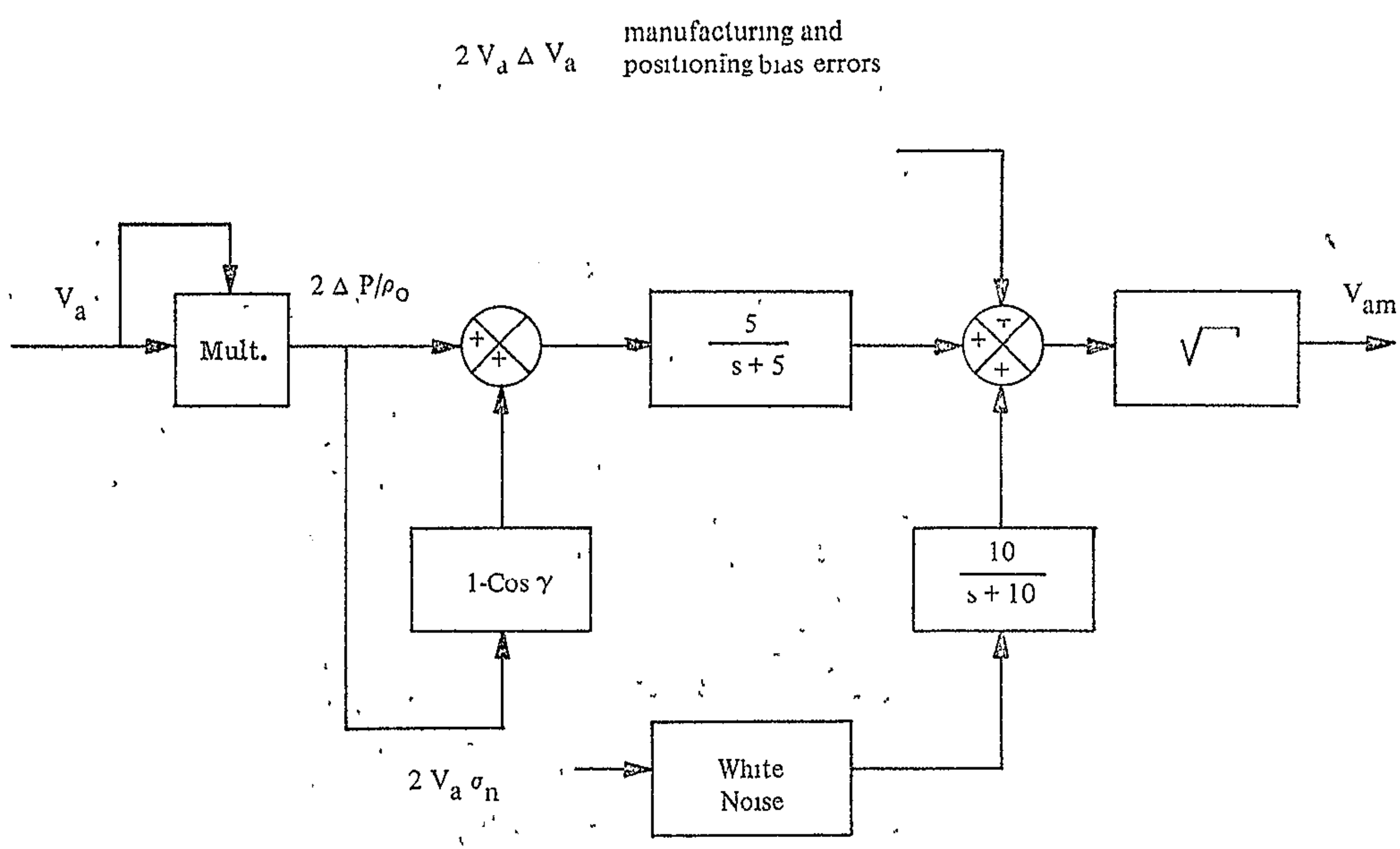

Figure IV-6 Pitot Tube Model

6 Alpha and Beta Vanes

The error model for typical Alpha Beta Vanes was developed by Bell Aerospace Company under this contract A discussion of the sources and expected magnitudes of the errors in these vanes is contained in the following paragraphs

The Alpha and Beta Vanes are simply vanes mounted on the aircraft, one in the horizontal axis, the other in the vertical axis, such that they are free to swivel and lie in the plane of the airstream The angles that these planes makes with the body axes are thus the measures of alpha, the angle of attack and Beta, the sideslip angle Since they are both identical instruments, only one needs to be described

The vane is mounted on the vehicle in the form of a "flag," its vertical "post" being free to turn in its mounting The angular position of the post relative to the body axis is measured through a synchro (which does not significantly impede the movement of the post) and the angular information transmitted back to the followup servo and pointer mechanism The instrument dynamics are such that the pointer is almost critically damped so as to avoid pointer chatter The vane itself, being virtually free mounted is influenced by air turbulence and other noise effects as well as the primary air flow, but this noise component is largely filtered out in the followup servo.

A mathematical error model of a typical vane may therefore be constructed as illustrated in Figure IV-7.

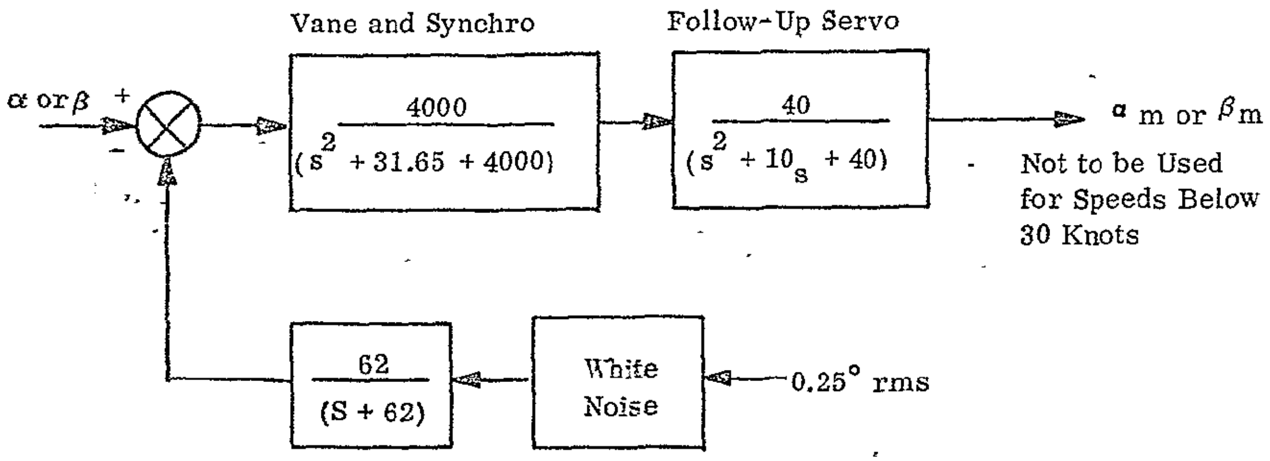

Figure IV-7. α, β Vane Model

In this figure the vane and synchro are represented by an underdamped second order transfer function to simulate a relatively free pivot The second quadratic transfer function represents the followup servo and the pointer mechanism which is much better damped and has a smaller bandwidth The errors introduced into such an instrument are usually constant at about ±0 25° and this error may be simulated by introducing a band limited noise signal as illustrated in the figure

At speeds below 30 knots (approximately) the accuracy of this instrument decreases considerably In particular the natural frequency of the Vane and Synchro decreases and the amplitude of the noise error increases Since in practice the instrument is switched out at low speeds the errors introduced below 30 knots need not be considered

7 GSN-5 Radar Model

a General

The error model for the Bell Aerospace Company GSN-5 radar system was developed by Bell under this contract A discussion of the source and expected magnitudes of the errors in this system is contained in the following paragraphs

The GSN-5 radar system as illustrated in block diagram form in Figure IV-8, is a K_a band, conical scan type employing a parabolic antenna for propagation and receiving of the radar signal The range of the target is determined by the spacings between the transmitter and corresponding reflected K_a band pulses The radar antenna is mounted on a two axis gimbal which continuously rotates as the radar automatically tracks the target A resolver unit, geared to the gimbal, determines the aircraft's position in rectangular coordinates Translation of the coordinate system from antenna to T D point is accomplished by analog summation Derivatives are also obtained by differentiation in the analog computer The resulting analog information is finally multiplexed through a 14 bit A-D converter for transmission to the vehicle via the data link (13 bits of information)

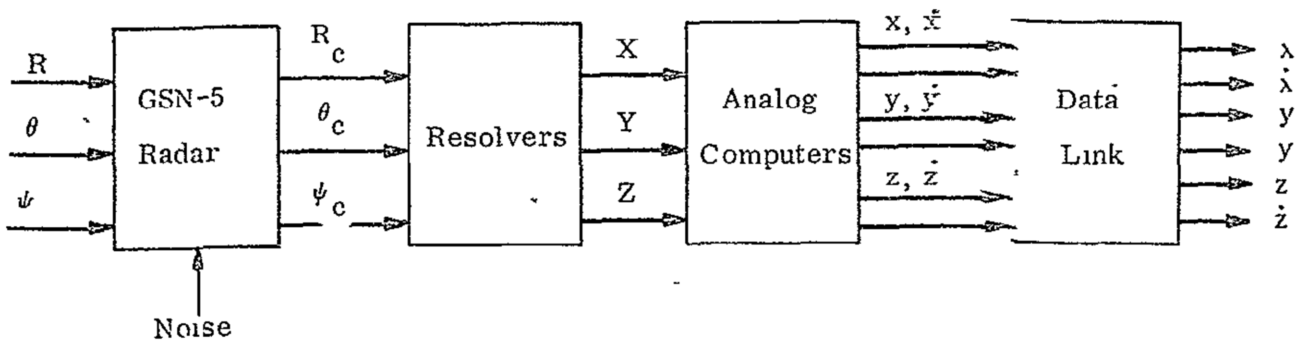

Figure IV-8 Block Diagram of the GSN-5 Radar System

Each of the blocks illustrated in Figure IV-8 will be discussed.

b GSN-5 Radar

The radar illuminates the target and, due to its scanning mechanism, forms a spin error from the reflected signal This error is electronically split into corresponding elevation and azimuth error angles. This split is not, however, perfect, so that a 10% crosstalk is assumed to remain It is assumed that no dynamic effects occur through the electronics, although a certain amount of noise is generated The resultant error signals then drive two positioning servo motor/gearbox combinations with tachometer feedback, which physically move the antenna such as to minimize these error angles The two servos involved (one for each axis) may for simulation purposes be represented by the closed loop transfer function,

$$\frac{\theta_c(s)}{\theta_e(s)} = \frac{\psi_c(s)}{\psi_e} = \frac{w_o^2}{(s^2 + 2\ \delta\ w_o + w_o^2)}$$

where θ_e is the elevation angle error, and ψ_e is the azimuth angle error The appropriate coefficients have been experimentally determined as $w_o = 50$ rads/sec, $\delta = 0\ 7$ Various nonlinear effects such as backlash, hysteresis etc , present in the position servos may safely be neglected (This is confirmed by experimentation)

The range signal is not affected by any dynamics, but is subject to electronic and system noise The various noise levels, including electronic noise, backscatter, scintillation effects, etc have been found to be approximately 0 3 milliradian rms for the elevation and azimuth angles, and is distributed uniformly over the antenna servomechanism bandwidth of 50 rads/sec The radar slant range noise content is 15 feet rms up to a range of 1500 feet and 1 percent of the range thereafter. These figures apply when the antenna is pointing fairly accurately towards the corner reflector which is positioned in the nose of the vehicle Under certain conditions, skin tracking predominates and the rms content of the noise signals will increase substantially For example, if the vehicle's orientation with respect to the antenna varies by more than approximately 15° in elevation or approximately 20° in azimuth, the radar received signal will be reduced by around 3 db so that the noise level will increase by a similar amount Further if no corner reflector is incorporated into the vehicle, the noise level can increase by 10 or 12 db The noise figures given above will also deteriorate with atmospheric conditions such as rain or snow, but at short range this effect is not considered to be too important compared to the other noise sources

Taking all of these factors into account, block diagram of the GSN-5 model may be constructed as illustrated in Figure IV-9

As far as the elevation and azimuth angles are concerned, the resulting noise spectrum will be further shaped by the positioning dynamics to finally become the desired spectrum The variable potentiometers representing the rms noise amplitude are varied according to vehicle orientation and absence of corner reflector so that the variations in noise level due to these factors are accurately modeled

c The Resolvers

The resolver unit is geared to the gimbals and translates coordinates of the aircraft's position from polar to rectangular axes There are no significant dynamic effects present in this unit and so they may be ignored. From experience, however, it has been found that since the radar unit spends most of its lifetime looking at one particular "homing" window, the resolvers tend to become a little noisier with age, especially at these particular angles This extra noise could be incorporated into the model by using logic to recognize when these offending angles are being tracked, subsequently adding this noise However, due to the other noise sources present in the system, this effect may be safely neglected

The resolution of the resolver unit is such that a quantizing error of 0 4 milliradian is introduced. This is quite a significant error, but since this error is less than the quantizing error produced by a 14-bit A-D converter. (13 bits information, one bit sign) this particular source of error will be, for convenience, translated downstream into the data link block (Figure IV-12)

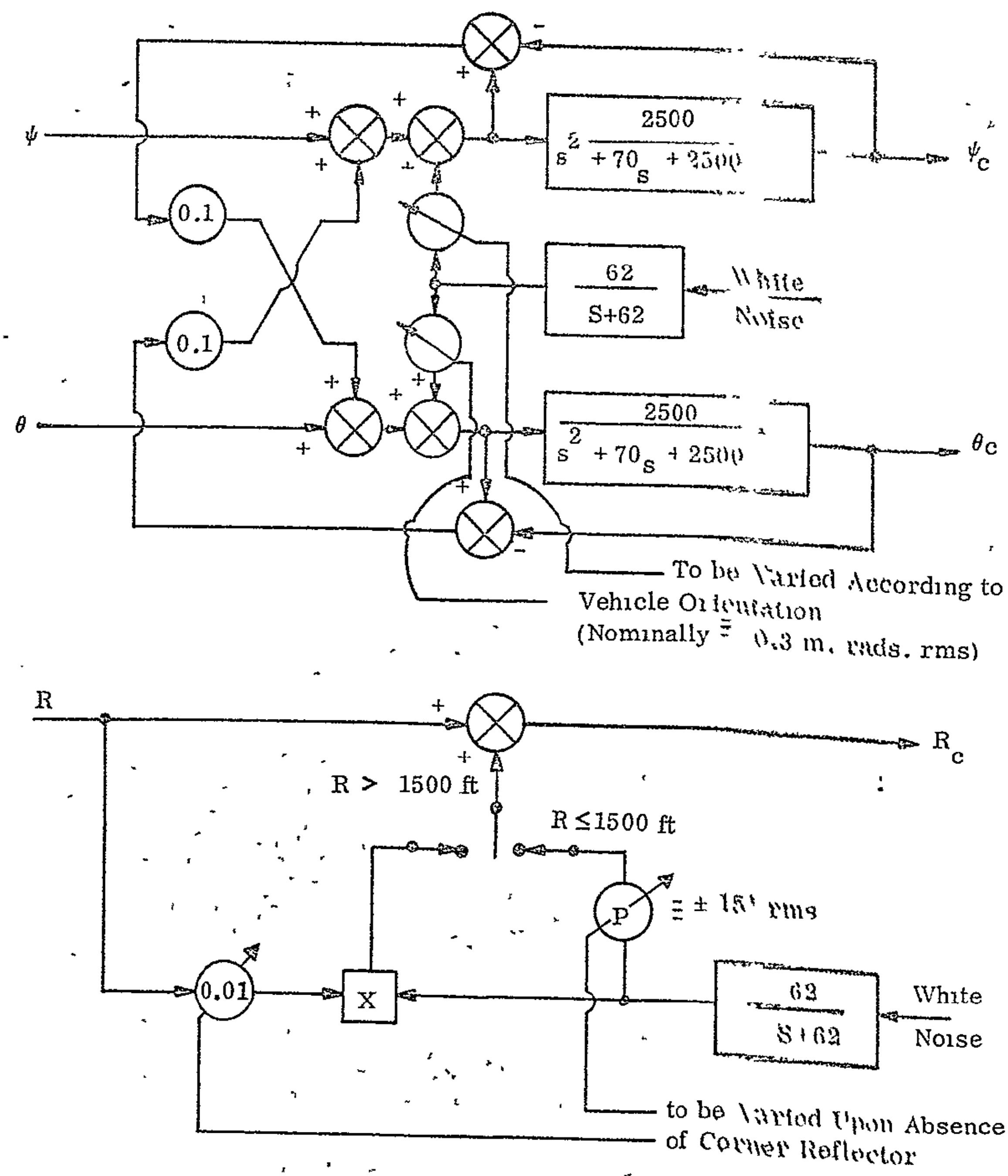

Figure IV-9. GSN-5 Radar

The resolver unit may therefore be simply simulated as illustrated in Figure IV-10

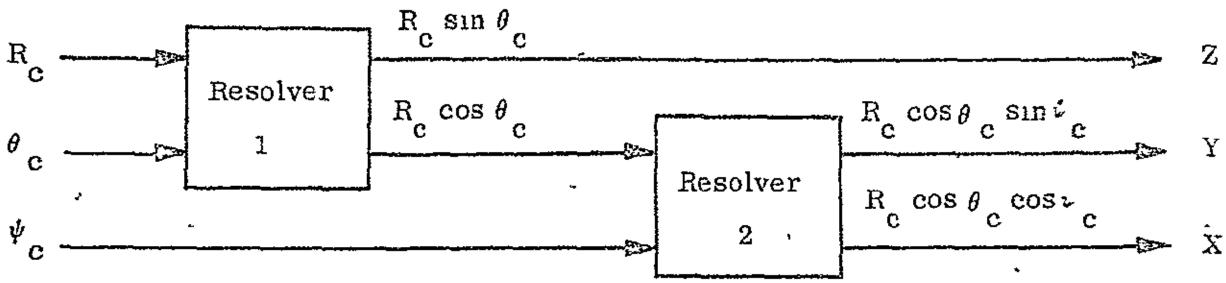

Figure IV-10 Resolver Unit

d. Analog Computer

The analog computer in the GSN-5 system is used to translate the X-Y-Z coordinate system produced by the resolver unit to the appropriate runway axes This may be simply accomplished by adding (or subtracting) the required offsets X_O, Y_O, and Z_O between the touchdown point and the antenna focus point It is normal practice to align the radar unit parallel to the runway so as to eliminate any further angular translations

The analog computer is also used to calculate the necessary derivatives in each axis These are achieved in the usual manner with 1 second filtering on the X and Z axis, and 0 5 second filtering on the Y axis It is not considered that the GSN-5 computer rates will be used but this information is included for completeness The resulting model is shown in Figure IV-11

e Data Link

The resulting information is finally multiplexed through a 14 bit A-D converter for transmission to the vehicle via the data link The converter word contains 13 bits of information and a plus sign and is accurate to within 0 017, plus or minus one half the least significant bit In addition to this error, an error also exists due to the time delay between conversions This error is equivalent to a lag of one half the sampling period The resulting block diagram of the data link error model is shown in Figure IV-12, for any particular channel This configuration completes the description of the GSN-5 radar unit model

8. Radar Altimeter - Honeywell YG7091B

The error model for a typical radar altimeter was developed by Bell Aerospace Company under this contract This model is based on specifications and flight tests on the Honeywell YG7091B radar altimeter A discussion of these and the resulting error model is discussed in the following paragraphs

The operation of the Honeywell Pulse Radar Altimeter is based upon the precise measurement of time required for an electromagnetic energy pulse to travel from the aircraft to the ground terrain, and return to the aircraft

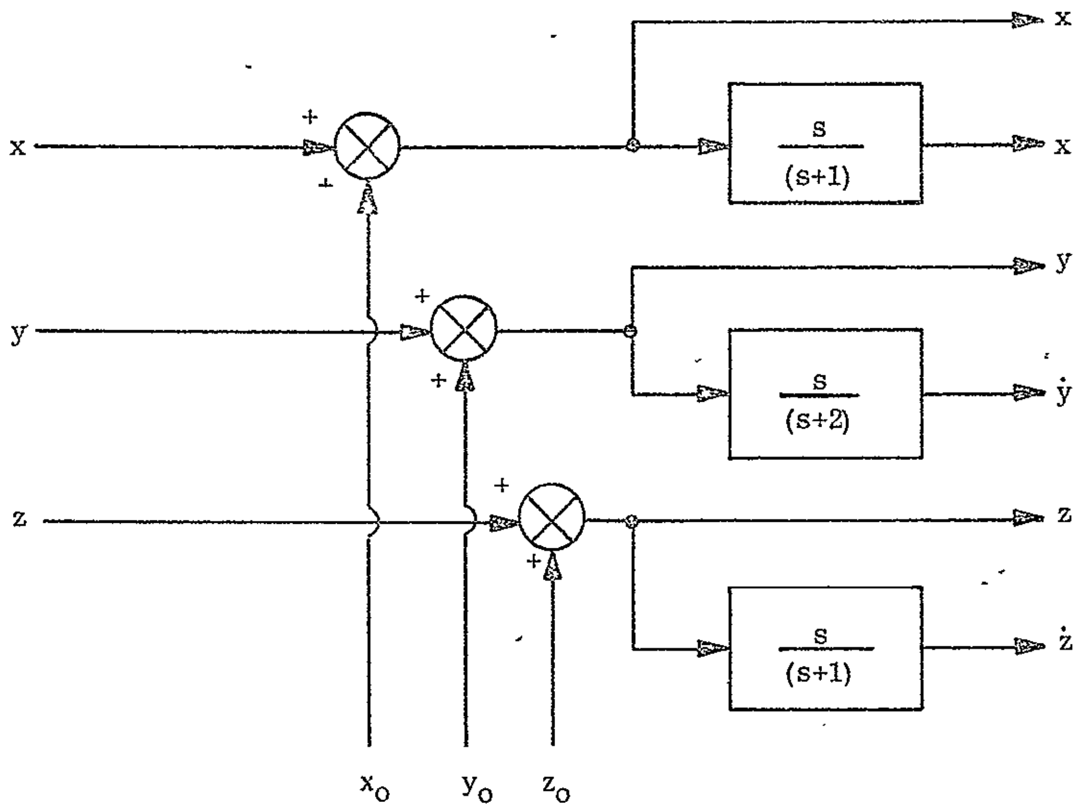

Figure IV-11 Analog Computer Model

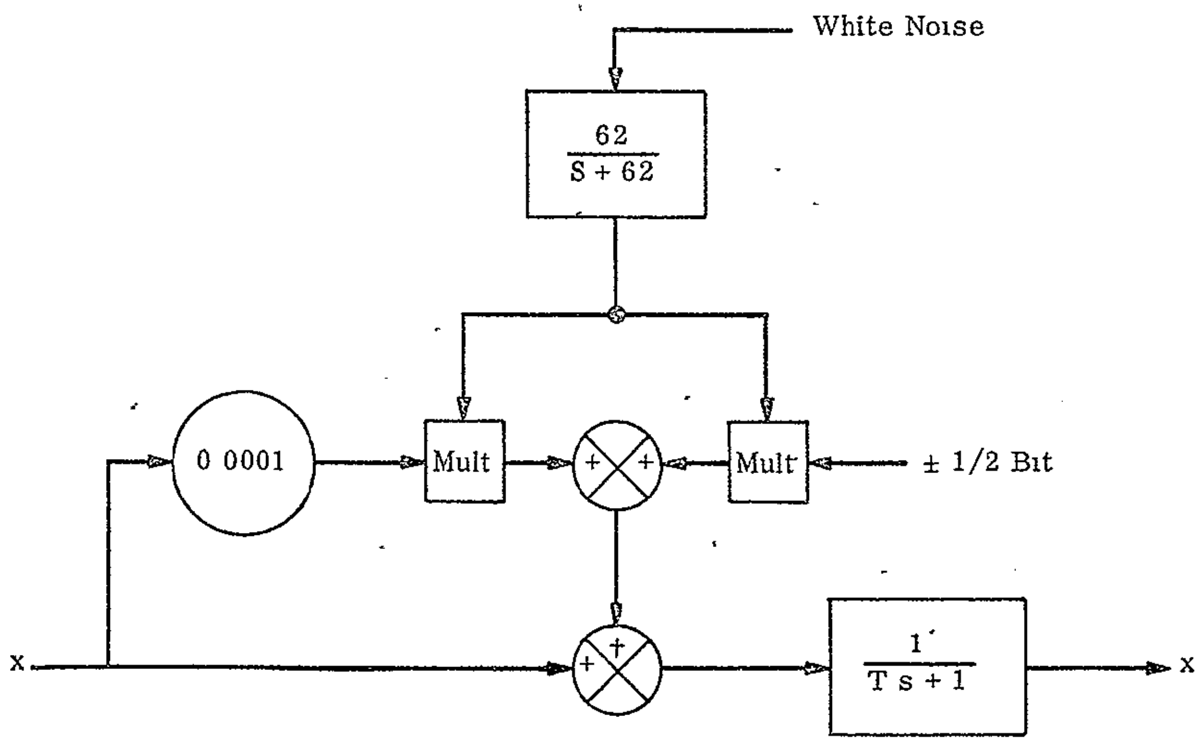

Figure IV-12 Data Link Error Model

The receiver detects the leading edge of the reflected signal After "lock on" to this signal, the receiver rejects all other signals until the next pulse is received This ensures that the closest point of contact within the radar "window" is detected The time of arrival of the pulse is compared with the time of pulse transmission, the resulting time difference being directly proportional to the required altitude

From the specifications for the YG7091B, the nominal altitude response time for a small change in altitude is 0 1 second This is defined as the time taken to reach 90% of the final steady state value The shape of this step response is indicated by flight tests taken over the flight deck of an aircraft carrier From these results it may be concluded that a transfer function that will reasonably satisfy the given data is

$$G(s) = \frac{(848 - 19\ 05s)}{(848 + 44\ 6s + s^2)}$$

which may be simplified to a first order lag with a 0 1 sec time constant without too much inaccuracy. The quoted accuracy of the radar system is (ignoring the pointer mechanism) 1 5 feet + 0 5% of altitude to the one sigma point Any antenna parallax error is considered to be generally too small to be significant and is therefore ignored The spectrum of the error signal is not known and so is assumed to be Gaussian and distributed uniformly over a bandwidth of 10 Hz This is an arbitrary choice of bandwidth A model for the radar altimeter is therefore illustrated in Figure IV-13

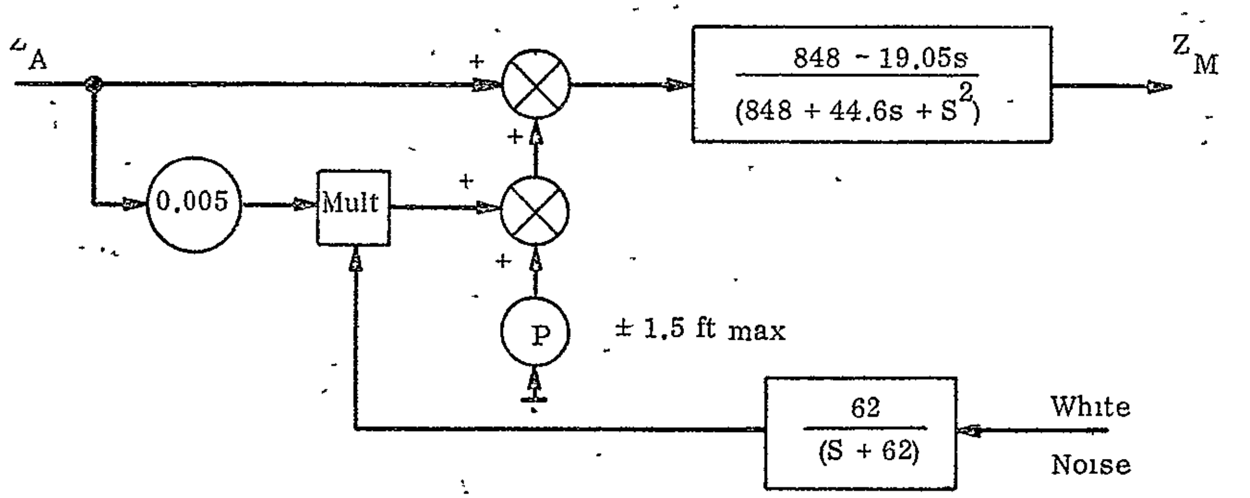

Figure IV-13 Radar Altimeter

Note that if the scale errors of the pointer mechanism are included, the total system errors increase to approximately 2 0 feet + 0 75% of altitude This is of significance for display purposes but the smaller error is valid for the automatic control functions These error values will also change depending upon the vehicle orientation For example, the YG7091B specifications state that the above accuracy will hold for pitch and roll angles to approximately ±25 degrees, and the system will still work but with decreased accuracy for pitch and roll angles to ±45 degrees This feature can be simply built in to the model of Figure III-8 by recognizing when the pitch and roll angle of the vehicle exceeds ±25 degrees and increasing the noise (or inaccuracy) levels by a factor of five (say) and by a factor of ten or more if the vehicle attitude angles exceed ±45 degrees These multiplication factors are arbitrarily chosen and may be modified

C SIMULATION MECHANIZATION

1 General Description

The simulation is a modular hybrid type with modules for the CH-46C helicopter, the flight data systems, the guidance and flight control laws, and the cockpit The helicopter module contains models for the actuator and rotor dynamics, the linearized equations of motion for the bare helicopter, the stability derivatives, and a wind model The flight data systems module contains error models for an inertial measurement unit, an airspeed sensor, a Beta vane, and the GSN-5 radar update system The guidance and flight control law module contains the digital control laws for the Digital Flight Control and Landing System The cockpit module contains the displays and controls necessary to use all the modes of operation of the Digital Flight Control and Landing System In addition to these basic modules, the simulation also contains several control modules for operating and control purposes

The simulation modules are mechanized on hybrid computing equipment shown in Figure IV-14 As shown in this figure, all of the basic modules, except for the wind model and cockpit module, are mechanized on the IBM 7090 digital computer The wind model is mechanized on a PACE231R analog computer This computer is also used to interface with the cockpit which is mechanized on a modified X-22A cockpit simulator

The simulation input/output provisions are mechanized on both the analog and digital computers For operating convenience, the simulation mode control and initial condition inputs are mechanized on the analog computer All other inputs are mechanized on the digital computer since they do not normally change from run to run The recording of all flight variables in the time domain is done on analog strip chart recorders However, digital print is used to record the initial conditions, performance index, and touchdown conditions for each run since it provides a concise record of the system performance

The necessary interface between the analog and digital modules is mechanized on Bell interface equipment. The variables and discretes which are transmitted over this equipment are also shown in Figure IV-14

In addition to the functional modules shown in Figure IV-14, a main program control module is also used to control the operation of the digital modules in real time This module is described in the following paragraphs

The helicopter simulation main program (Figure IV-15 and Table IV-15) controls the operational aspects of the digital simulation modules As shown in this figure, the program loads input data into core and performs all initial computations which can be made outside of the main simulation loop Discrete data commands are then read from the analog These include flight control mode, guidance mode, landing mode, analog mode and a group of function switches controlling input, output and termination The analog mode is tested In the IC (Initial Condition) mode, time is set to zero and all initialization is performed In the Operate mode, a test is made to determine if the pilot commanded a mode switch, in which case a flight control initialization procedure is performed The helicopter module is then entered, after which tests are made to determine whether it is time to enter the Guidance or Flight Control subroutines Guidance is normally entered 8 times per second while flight control is normally entered 32 times per second The program is set up so that both guidance and flight control will be entered on the iteration at which a mode switch is detected This insures that all initialization will occur at once In the Hold mode, all computational loops are bypassed

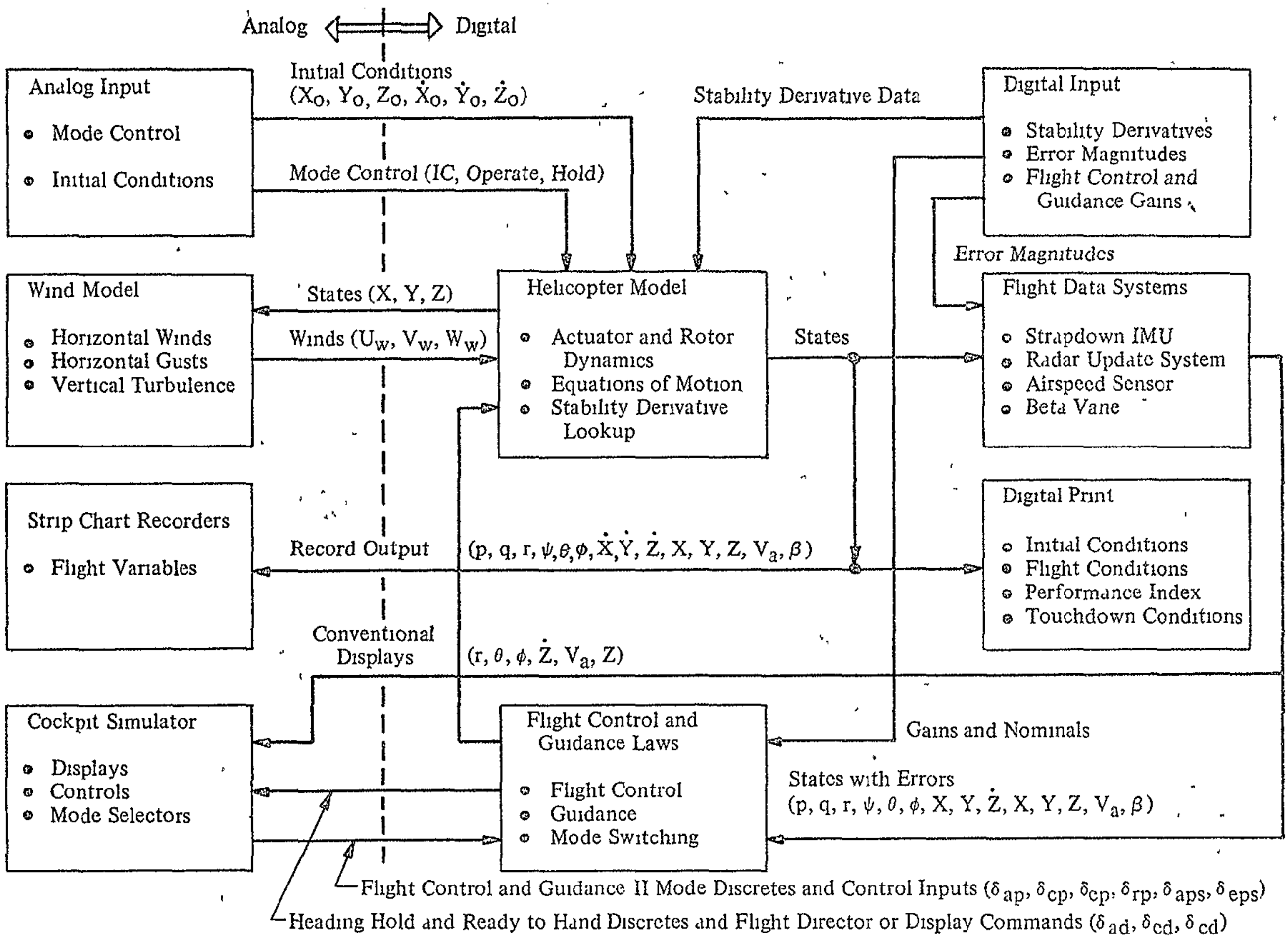

Figure IV-14 Hybrid Simulation Flow

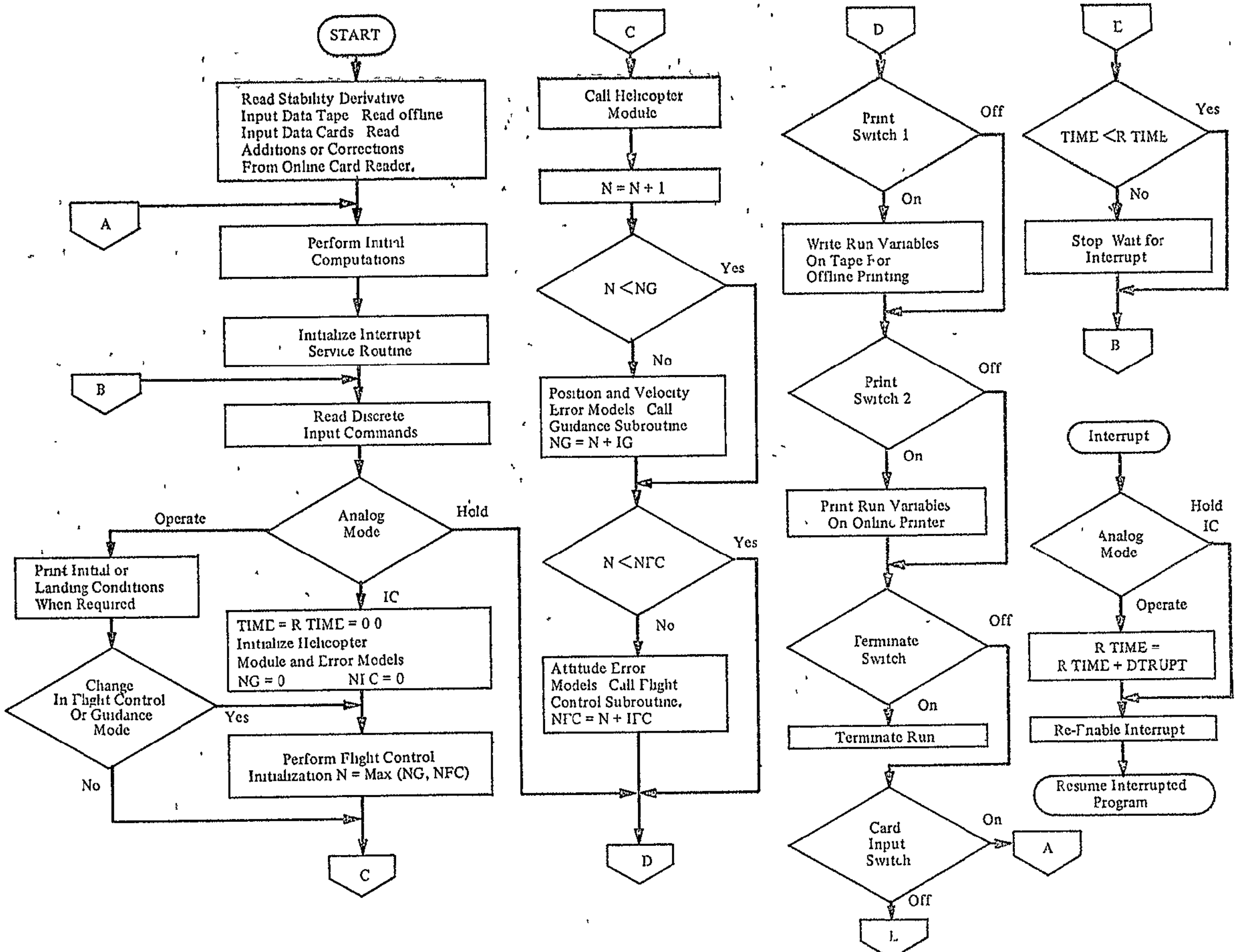

Figure IV-15. Helicopter Simulation Program

Timing is accomplished by using a real time clock which interrupts the program at a determined frequency, nominally once every 0 003 second When an interrupt is received, real time is updated in the operate mode The program then resumes at the point of interruption At the end of each iteration, real time is compared with problem time and the program halts until real time is equal to the problem time simulated on the current iteration

Several forms of printed output are available The program automatically prints on-line the initial conditions, performance index, and landing conditions for each run At any time during the run, an on-line print of key problem variables may be obtained A time history of these variables may also be recorded on tape for later offline printing In addition certain D/A outputs are always transmitted to the analog for strip chart recording and display indicators

A switch is provided to read data cards on-line if any corrections must be made while the simulation is running A terminate switch on the analog side is provided to end the program

TABLE IV-15

DEFINITION OF SYMBOLS USED IN FLOW CHART

DTRUPT	Incremental time between interrupts in seconds
IFC	Number of iterations between calls to flight control subroutine
IG	Number of iterations between calls to guidance subroutine
N	Iteration counter
NFC	Iteration when next call to flight control subroutine is to be made
NG	Iteration when next call to guidance subroutine is to be made
RTIME	Real time in seconds as computed by counting interrupts from a real time clock
TIME	Problem time in seconds as computed in helicopter module.

2 Helicopter Module

a Flow Diagram

All of the helicopter module except for the wind model, is mechanized as a subroutine on the digital computer The digital flow diagram for this subroutine is illustrated in Figure IV-16 As shown in the figure, this subroutine is divided into different sections which can be updated at different rates In the order of the frequency (from highest to lowest) at which they are updated, these sections are (1) actuator and rotor dynamics, (2) body axis equations, and (3) ANF equations and stability derivatives

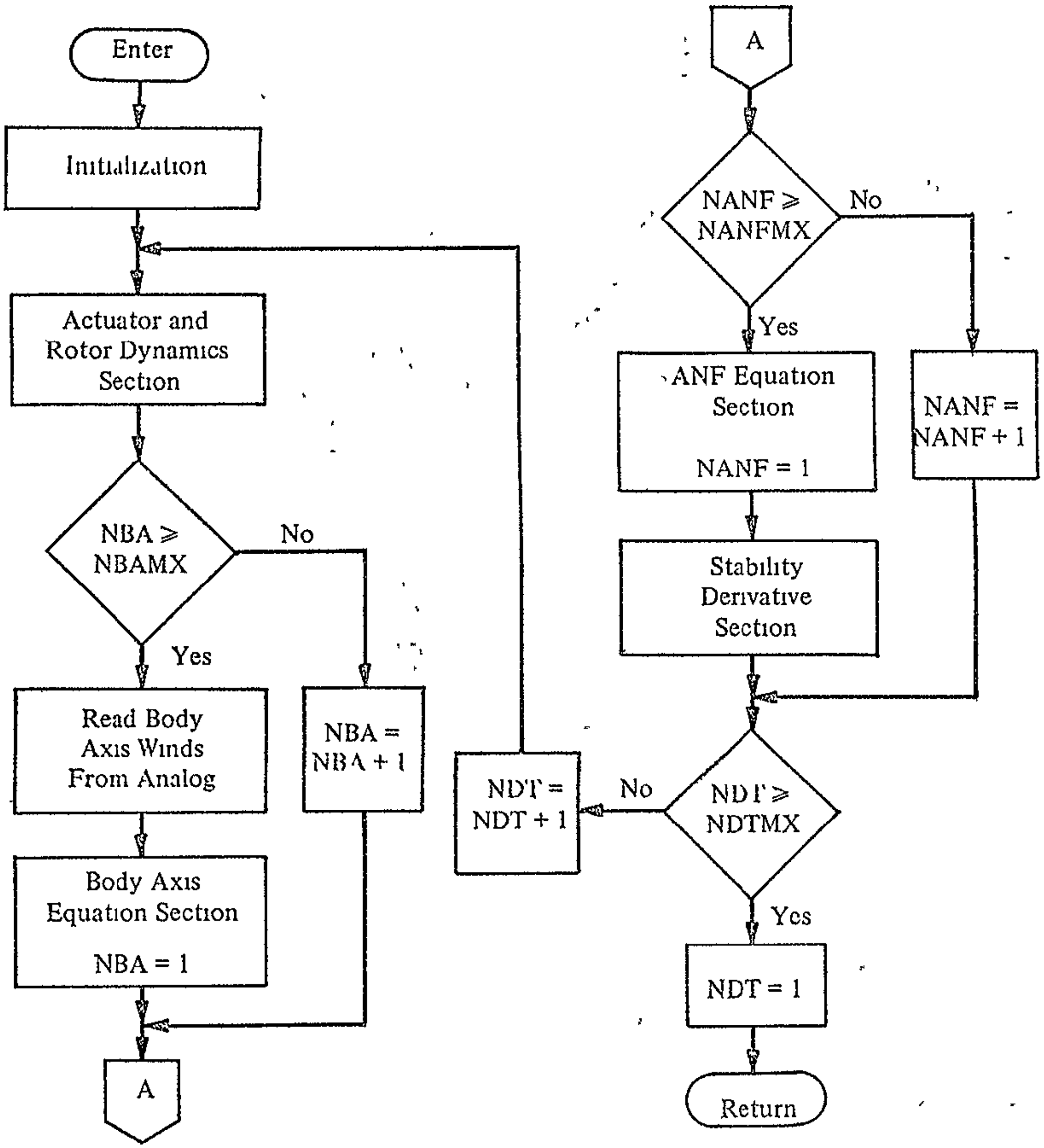

Notes
(1) Basic Entry Rate – 32 times/sec
(2) NDT = Helicopter Simulation Cycle Counter
(3) NDTMX = Number of Helicopter Simulation Cycles per Entry
(4) NBA = Body Axis Equation Counter
(5) NBAMX = Number of Helicopter Simulation Cycles Between Update of Body Axis Equations
(6) NANF = ANF Equation and Stability Derivative Counter
(7) NANFMX = Number of Helicopter Simulation Cycles Between Updates of ANF Equations and Stability Derivatives

Figure IV-16 Helicopter Module Subroutine b Actuator and Rotor Dynamics

All of the actuator and rotor dynamic equations presented in Section IV B 2 are mechanized in the simulation. The position limits on the stick inputs are mechanized in the following form.

$$\delta_{cl} = \delta_c, \text{ if } \delta_{min} \leq \delta_c \leq \delta_{max}$$

$$= \delta_{min}, \text{ if } \delta_c < \delta_{min}$$

$$= \delta_{max}, \text{ if } \delta_c > \delta_{max}$$

The second order actuator and rotor response transfer functions are mechanized by difference equations of the following form

$$\delta_{yi} = a\,\delta_{xi} + b\,\delta_{xi-1} + c\,\delta_{xi-2} + d\,\delta_{yi-1} + e\,\delta_{yi-2}$$

where: a to e are difference equation coefficients
x denotes input of transfer function
y denotes output of transfer function
i denotes current value
i–1 denotes value from first previous update
i–2 denotes value from second previous update

The difference equation coefficients are defined as

$$a = \Delta t^2/f$$
$$b = 2\,\Delta t^2/f$$
$$c = \Delta t^2/f$$
$$d = (8/\omega^2 - 2\,\Delta t^2)/f$$
$$e = (4\,\zeta\Delta t/\omega - 4/\omega^2 - \Delta t^2)/f$$
$$f = 4\,\zeta\Delta t/\omega + 4/\omega^2 + \Delta t^2$$

where Δt = update period
ω = natural frequency
ζ = damping ratio

The rate limits on the actuator are mechanized in the following form

$$\delta_y = \delta_x, \text{ if } \delta_{yi-1} - \dot{\delta}_{max}\Delta t \leq \delta_x \leq \delta_{yi-1} + \dot{\delta}_{max}\Delta t$$

$$= \delta_{yi-1} - \dot{\delta}_{max}\Delta t, \text{ if } \delta_x < \delta_{yi-1} - \dot{\delta}_{max}\Delta t$$

$$= \delta_{yi-1} + \dot{\delta}_{max}\Delta t, \text{ if } \delta_x > \delta_{yi-1} + \dot{\delta}_{max}\Delta t$$

where $\dot{\delta}_{max}$ is the maximum rate
Δt is the update period
x denotes input to rate limit
y denotes output of rate limit

The hysteresis in the mechanical linkages in each channel are mechanized as shown in Figure IV-17

The nomenclature in this figure is as follows

$\Delta\delta_H$ is the half width of the hysteresis
x denotes hysteresis input
y denotes hysteresis output

c. Body Axis Equations

The body axis equation section contains (1) the linearized 6 DOF equations for the translational and angular body axis accelerations, (2) the integration of these to obtain translational and angular body axis rates, (3) the transformation of the body axis angular rates to Euler attitude rates, and (4) the integration of these to obtain Euler attitudes These equations are mechanized directly in the form in which they are presented in Section IV B 1 A second order Adams numerical integration formula is used for all integrations The form of this formula is,

$$y_{i+1} = y_i + 1.5\dot{y}_i \Delta t - 0.5\, \dot{y}_{i-1} \Delta t$$

where $\dot{y}$ is the integration input
y is the integration output
Δt is the update period

d ANF Equations

The ANF Equation section contains the transformation of body axis velocities to ANF velocities and the integration of these to obtain ANF positions These equations are mechanized directly in the form in which they are presented in Section IV B 1 A second order Adams numerical integration formula is again used for all integrations in this section

e. Stability Derivatives Routine

This section computes the stability derivatives, nominals, and trims datums for the helicopter as functions of the flight conditions For any given helicopter weight and c g position, the equilibrium flight stability derivatives, are functions of the forward airspeed, and altitude rate, the altitude, and the rear rotor axis tilt The stability derivatives that are computed are the partial derivatives of the time derivatives of the body axis translational and angular accelerations with respect to the body axis translational and angular velocities and the rotor deflections The nominals that are computed are the reference points about which the linearized body axis equations are referenced The trim datums that are computed are the equilibrium trim positions for the rotor collective, differential collective, cyclic, and differential cyclic commands

Before this section was developed, it was first necessary to determine how to use the equilibrium stability derivative data to simulate transient flight conditions since non-equilibrium data could not be obtained Three methods of simulating non-equilibrium flight conditions were considered

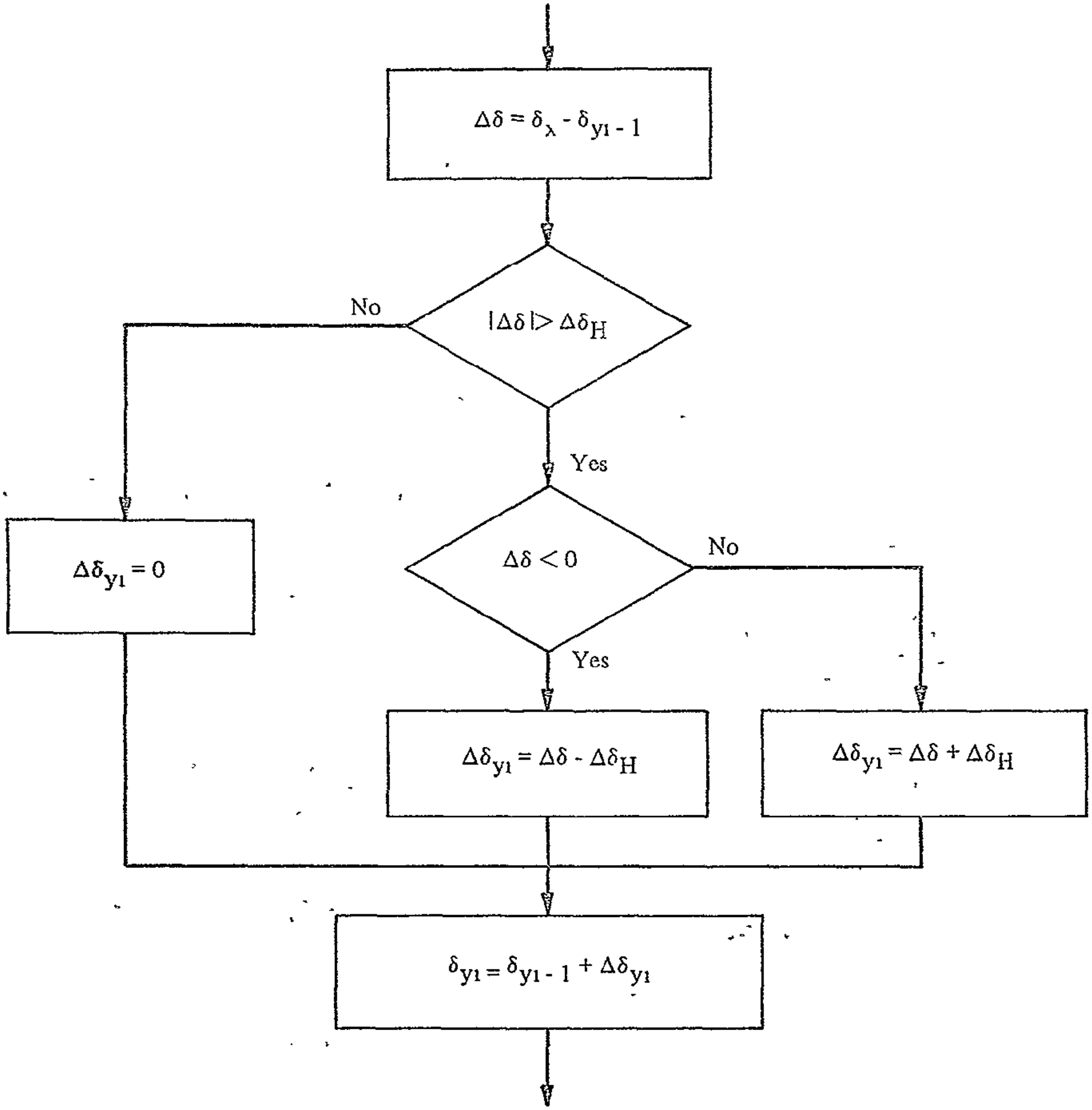

Figure IV-17 Hysteresis Mechanization

(1) Use the equilibrium d... corresponding to the current flight conditions regardless of whether they are ... ibrium conditions or not

(2) Develop a procedure ... determining the closest equilibrium conditions along a stored nominal flight ... use the equilibrium data corresponding to nominal conditions

(3) Develop a procedur... determining the closest equilibrium conditions to the current flight condit...

Although the first approa... the simplest, it can result in large errors, since the instantaneous rate of descent and velocity may ... different from the equilibrium values for the same power setting and attitude.

The second approach requ... a procedure for determining the closest equilibrium conditions for each point along a stored nom... flight However, since the nominal flight itself will involve nonequilibrium phases such as decelerat... ...ues, it became apparent that, once such a procedure is determined it could also be applied to ... al flight conditions This is the third approach, and does not have any of the disadvantages associa... ...ith operating about a fixed nominal flight As a result, the third approach was selected as the be... ...rnative

This approach requires de... ...ning the equilibrium point closest to any given instantaneous operating condition By "closest" ...eant the one whose derivatives are most nearly equal to those (unknown) derivatives which actua... ...ist at the instantaneous point

Using the equilibrium dat... equilibrium point is specified by specifying a forward velocity and a rate of descent (neglecting ... de effects) For a given velocity, an equilibrium climb rate can be specified by specifying either ... ...ective power setting or an angle-of-attack, the unspecified of these two quantities is then impl... defined by the requirement for equilibrium

Investigations indicated th... ...gle-of-attack (or vertical velocity) will have a smaller effect on the stability and control derivat... ...than collective power setting Hence, the approach selected for determining the closest equili... ...condition to a given nonequilibrium point is to use the one which would exist if angle-of-att... ...re adjusted for translational equilibrium at the instantaneous velocity and collective power settin...

The mechanization and op... ...ation of this subroutine is as follows The helicopter body axis velocities, wind components along th... ...dy axes, and pitch attitude are used to compute the forward airspeed, $V_{A/H}$, in the plane of the ... body axis

$$V_{A/H} = (U+U_W) \cos \theta + (W+W_W) \sin \theta$$

The rotor collective power setting, altitud... ...and rear rotor axis trim change are used to compute the equilibrium altitude rate, $\dot{h}_{eq}$, correspond... to the rotor collective power setting The manner in which this is done can best be described af... the procedure that is used for computing the stability derivatives, nominals, and trim datums ha... ...en described

The stability derivatives, ...nominals, and trim datums are then computed as functions of forward airspeed, the equilibrium attitud... ...corresponding to the current rotor collective power setting, attitude, and rear rotor axis til... ...do this, a two dimensional table lookup procedure with linear interpolation is first used to deter... the stability derivatives, etc as functions of the current forward airspeed and the equilibrium alti... ...rate corresponding to the current rotor collective power setting. In general,

$$C'(i) = f(V_{A/H}, \dot{h}_{eq}),$$

where $C'(i)$ is a stability derivative, etc

A one dimensional table lookup procedure with linear interpolation is then used to determine the effect of altitude on these derivatives as a function of forward airspeed

$$\partial C(i)/\partial h = f(V_{A/H})$$

$$\Delta C_h(i) = (\partial C(i)/\partial h)\, h$$

Since the pilot normally retrims the rear rotor at speeds greater than 80 knots, the effect of this trim change on the derivatives, etc is also computed by looking up the effect of the trim change on each derivative, etc at 80 knots and multiplying it by the rear rotor axis tilt, δ_{RR}, which is read from the cockpit over an A/D conversion channel

$$\Delta C_{RR}(i) = \Delta C(i)_{max} (\delta_{RR}/\delta_{RR,\,max})$$

The altitude and rear rotor trim change effects are then added to the derivatives, etc that were computed as functions of forward airspeed and equilibrium altitude rate to obtain the total derivatives, etc

$$C(i) = C'(i) + \Delta C_h(i) + \Delta C_{RR}(i)$$

The stability derivatives, nominals, and trim datums that are computed in this manner are as follows, (1) stability derivatives X_U/m, X_{δ_c}/m, X_{δ_e}/m, Z_U/m, Z_W/m, Z_{δ_c}/m, Z_{δ_e}/m, M_U/I_{YY}, M_W/I_{YY}, M_Q/I_{YY}, M_{δ_c}/I_{YY}, M_{δ_e}/I_{YY}, Y_V/m, Y_P/m, L_V/I_{XX}, L_P/I_{XX}, L_R/I_{XX}, L_{δ_a}/I_{XX}, N_V/I_{ZZ}, N_P/I_{ZZ}, N_R/I_{ZZ}, and N_{δ_r}/I_{ZZ}, (2) nominals θ_o, and (3) trim datums δ_{cro}, δ_{ero}, δ_{aro}, and δ_{rro}

In addition, the nominal pitch attitude computed by the above procedure is used along with the current forward airspeed and the equilibrium altitude rate corresponding to the current rotor collective power setting to compute the nominal body axis velocities along the x and z body axes

$$U_o = V_{A/H} \cos\theta_o + \dot{h}_{eq} \sin\theta_o$$

$$W_o = V_{A/H} \sin\theta_o - \dot{h}_{eq} \cos\theta_o$$

It is apparent at this point that the equilibrium trim datum for the rotor collective power setting, δ_{cro}, is one of variables that is computed as a function of forward airspeed and equilibrium altitude rate in the two dimensional table lookup procedure Because of this, it is possible, through a reverse lookup procedure, to enter this table with the current forward airspeed and collective power setting and determine the equilibrium altitude rate that corresponds to that collective power setting

$$\dot{h}_{eq} = f'(V_{A/H}, \delta'_{cro})$$

However, before this can be done, the altitude and rear rotor trim change effect on the rotor collective setting must be computed and subtracted from the current rotor collective setting since the table being used is for sea level, no trim change conditions

$$\partial\delta_{co}/\partial h = f(V_{A/H})$$

$$\Delta\delta_{co}/h = (\partial\delta_{co}/\partial h)\, \dot{h}$$

$$\Delta\delta_{co}/RR = \Delta\delta_{co\ max}(\delta_{RR}/\delta_{RR\ max})$$

$$\delta'_{cro} = \delta_{cro} - \Delta\delta_{co/h} - \Delta\delta_{co/RR}$$

This is the procedure that is used to compute the equilibrium altitude rate corresponding to the current rotor collective power setting in the stability derivative subroutine

3 Flight Data Systems Module

a Strapdown System

This section describes the simulation models developed for the strapdown system from data supplied by NASA-ERC on this system These error models were used during the evaluation of the Digital Flight Control and Landing System

(1) Gyro Pulses

A prime error in the accumulated attitude pulses from the pulse rebalanced gyros in the strapdown system is due to roundoff The magnitude of this error is dependent on the quantization level used and the rate at which the gyros are rebalanced If there were no other errors in these pulses, the distribution of this error would depend only on the actual magnitude and direction of change of the attitude being measured and would be a sawtooth type function for a constant attitude rate However, since the pulses will contain other errors, due to such things as vibration, that will probably be of the same order of magnitude as the roundoff error, the error after roundoff will probably be noisy and somewhat random in nature Therefore, in the simulation, this error is simulated by an evenly distributed random error of the following form (pitch axis used for example),

$$\Delta\theta' = \left(\frac{Q_{low}}{N_G}\right) (\Delta\theta')^*_{ED},\ \text{if } Q \leq Q_{low}$$

$$= \left(\frac{Q_{high}}{N_G}\right) (\Delta\theta')^*_{ED},\ \text{if } Q > Q_{low}$$

where

Q_{low} = maximum measurable attitude pulse rate at low scaling
Q_{high} = maximum measurable attitude pulse rate at high scaling
N_G = gyro rebalance rate
$(\Delta\theta')^*_{ED}$ = an evenly distributed random number with an amplitude of one

(2) Body Axis Angular Rates

In the strapdown system, the accumulated attitude pulses are numerically differentiated to obtain the body axis angular rates A typical difference equation for performing this differentiation was provided by NASA-ERC and is of the form (pitch axis used for example),

$$Q = [1\ 5\ \theta'_2 - 0\ 5\ \theta'_1]\ 2\ N_{AR}$$

where θ'_2 = pulses accumulated over second half of update period
θ'_1 = pulses accumulated over first half of update period
N_{AR} = update rate of angular rate computation

From this difference equation, it can be seen that the noise error in the accumulated gyro pulses will cause a noise error in the computed angular rates that will be of the following form

$$\Delta Q_N = [1\ 5\ \Delta\theta'_2 - 0\ 5\ \Delta\theta'_1]\ 2\ N_{AR}$$

This error is computed in this manner in the simulation It is then added to the angular rates to form the angular rates that are used in the flight control laws

$$P_{FC} = P + \Delta P_N$$

$$Q_{FC} = Q + \Delta Q_N$$

$$R_{FC} = R + \Delta R_N$$

(3) Euler Angles

In the strapdown navigational system, the accumulated gyro pulses are also integrated to update the direction cosine matrix for the Euler angles. The appropriate terms in this matrix are then inversely resolved to obtain the Euler angles A typical numerical integration procedure (second order Runge-Kutta) for updating the direction cosine matrix was provided by NASA-ERC and is of the following form

$$C^{NB}_{n+1} = C^{NB}_{n} \left(1 + [\theta'_x] + 5[\theta'_1 x][\theta'_2 x] - 1\ 5\ [\theta'_1 x]^2 - 1\ 5\ [\theta'_2 x]^2\right)$$

where C^{NB} = direction cosine matrix
$[\theta'_1 x]$ = matrix summation of attitude pulses over first half of update period
$[\theta'_2 x]$ = matrix summation of attitude pulses during second half of update period

$$[\theta'_x] = \begin{bmatrix} O & -\theta_z & \theta_y \\ \theta_z & O & -\theta_x \\ -\theta_y & \theta_x & O \end{bmatrix}$$

This integration procedure was analyzed for error propagation and it was found that the rms value of the noise error propagated through all terms is only about 5% greater than that propagated through the $[\theta'_x]$ term alone Therefore, for simulation purposes, only this term is considered It was further found that the resulting noise error in the direction cosine matrix transforms into a noise error in the Euler angles through the normal Euler rate transformation. In the simulation, this error is computed as,

$$\Delta\psi_N = (\Delta\theta' \sin\phi + \Delta\psi' \cos\phi)/\cos\theta$$

$$\Delta\theta_N = \Delta\theta' \cos\phi + \Delta\psi' \sin\phi$$

$$\Delta\phi_N = \Delta\phi' + \Delta\psi_N \sin\theta$$

In addition to the noise error in the Euler angles, there is also a drift error which results from the propagation of the errors in the accumulated attitude pulses and from errors in the integration procedure itself In the simulation, this error is computed as (pitch axis used for example)

$$\Delta\theta_D = (k_D\, Q^3/N_{DC}{}^2)/s$$

where k_D = drift constant,
N_{DC} = update rate of direction cosine matrix integration

The noise and drift errors are then added to the Euler angles to obtain the angles that are used in the flight control laws

$$\psi_{FC} = \psi + \Delta\psi_N + \Delta\psi_D$$

$$\theta_{FC} = \theta + \Delta\theta_N + \Delta\theta_D$$

$$\phi_{FC} = \phi + \Delta\phi_N + \Delta\phi_D$$

(4) Body Axis Accelerations

The error model for the accelerometers was provided by NASA-ERC and consists of Gaussian white noise shaped through a 100 radian/sec filter In the simulation, this noise error is being represented simply by a normally distributed random number of the following form (longitudinal acceleration used for example)

$$\Delta\dot{U}_N = \sigma_N\, \Delta\dot{U}^*_{ND}$$

where σ_N = standard deviation
$\Delta\dot{U}^*_{ND}$ = normally distributed random number with mean of zero and standard deviation of one

The 100 rad/sec filter is not included since this error is generated at a rate that excludes frequencies greater than 100 rad/sec

(5) Body Axis Velocities

In the strapdown system, the sensed accelerations are integrated to obtain the body axis velocities For a typical trapezoidal numerical integration method, the noise error in the sensed accelerations will be propagated through the integration into an error in the body axis velocities in the following manner (longitudinal velocity used for example)

$$\Delta U_N = 0.5\,(\Delta\dot{U}_{N/n} + \Delta\dot{U}_{N/n-1})/N_v + \Delta U_{N/n-1}$$

where N_v = update rate of velocity integration

A drift error is also computed as,

$$\Delta U_D = \Delta \dot{U}_D / s,$$

where $\Delta \dot{U}_D$ = drift rate

The noise and drift errors are then added to the body axis velocities to obtain the body axis velocities that are used in the flight control laws

$$U_{FC} = U + \Delta U_N + \Delta U_D$$

$$V_{FC} = V + \Delta V_N + \Delta V_D$$

$$W_{FC} = W + \Delta W_N + \Delta W_D$$

(6) Inertial Velocities

In the strapdown system, the body axis velocities are transformed into inertial velocities through an Euler resolution This resolution is of the form

$$\begin{bmatrix} \dot{X} \\ \dot{Y} \\ \dot{Z} \end{bmatrix} = \begin{bmatrix} C\psi\, C\theta & C\psi\, S\theta S\phi - S\psi C\phi & C\psi\, S\theta C\phi + S\psi S\phi \\ S\psi C\theta & S\psi\, S\theta S\phi + C\psi C\phi & S\psi S\theta C\phi - C\psi S\phi \\ -S\theta & S\phi C\theta & C\theta C\phi \end{bmatrix} \begin{bmatrix} U \\ V \\ W \end{bmatrix}$$

From this transformation, it can be seen that the errors in both the body axis velocities and Euler angles will be propagated into errors in the inertial velocities For small angle approximations on pitch and roll, the errors in the inertial velocities are of the form

$$\Delta \dot{X}_E = C\psi \Delta U_E - S\psi \Delta V_E + (C\psi\theta + S\psi\phi)\, \Delta W_E$$
$$- (US\psi + VC\psi + W(S\psi\theta - C\psi\phi)\, \Delta\psi_E + WC\psi\Delta\theta_E + WS\psi\Delta\phi_E$$

$$\Delta \dot{Y}_E = S\psi \Delta U_E + C\psi \Delta V_E + (S\psi\theta - C\psi\phi)\, \Delta W_E$$
$$+ (UC\psi - VS\psi + W(C\psi\theta - S\psi\phi)\,)\, \Delta\psi_E + WS\psi\Delta\theta_E - WC\psi\Delta\phi_E$$

$$\Delta \dot{Z}_E = -\theta \Delta U_E + \phi \Delta V_E + \Delta W_E - U\Delta\theta_E + V\Delta\phi_E$$

These errors are computed in this manner in the simulation They are then added to the inertial velocities to obtain the inertial velocities that are used in the flight control laws

$$\dot{X}_{FC} = \dot{X} + \Delta \dot{X}_E$$

$$\dot{Y}_{FC} = \dot{Y} + \Delta \dot{Y}_E$$

$$\dot{Z}_{FC} = \dot{Z} + \Delta \dot{Z}_E$$

(7) Inertial Positions

In the strapdown system, the inertial positions are obtained by integrating the inertial velocities For a typical trapezoidal numerical integration method, the noise error in the inertial velocities will be propagated through the integration into noise errors in the inertial velocities in the following manner (longitudinal position used for example)

$$\Delta X_N = 0.5\,(\Delta \dot{X}_{N/n} + \Delta \dot{X}_{N/n-1})/N_P + \Delta X_{N/n-1}$$

where N_P = update rate of position integration

The drift error in the inertial velocities will also be propagated through the integration into drift errors in the inertial positions in the following manner (longitudinal position used for example)

$$\Delta X_D = \Delta X_{D/n-1} + 0.5\,(\Delta X_{D/n} + \Delta \dot{X}_{D/n-1})/N_P$$

These equations are used to compute the noise and drift errors in the inertial positions in the simulation These errors are then added to the inertial positions to obtain the positions that are used in the guidance laws

b Radar Update System

In the airborne system, the inertial position data from the strapdown system is updated by a precision GSN-5 radar system This reduces the errors in the updated positions to those in the radar information at the update points This is simulated by resetting the initial conditions ($\Delta X_{D/n-1}$, $\Delta Y_{D/n-1}$, and $\Delta Z_{D/n-1}$) on the inertial position drift error integrators to the errors that exist in the radar information at the update points A specified number of discrete updates per flight are simulated and these occur as a function of range Therefore, instead of computing the radar errors on line in the simulation, they are computed off line and stored in a table for several discrete range points Whenever the range, $|X|$, in the simulation first becomes equal to or less than a stored update value, the initial conditions on the inertial position drift error integrators are set equal to the stored radar position errors

If $|X| \leq X_1$,

$$\Delta X_{D/n-1} = \Delta X_{R1}$$

$$\Delta Y_{D/n-1} = \Delta Y_{R1}$$

$$\Delta Z_{D/n-1} = \Delta Z_{R1}$$

The initial conditions on the integrators are set only once when an update point occurs and then are allowed to integrate up until the next update point is reached

In the airborne system, the radar information will gradually be blended with the strapdown system information when an update occurs to prevent sharp discontinuities This is simulated by rate limiting the updated inertial position errors from the integrators as follows (longitudinal position used for example)

$$\Delta X_{D\,max} = \Delta X_{D/n-1} + \dot{X}_{max}\,\Delta t$$

$$\Delta X_{D\,min} = \Delta X_{D/n-1} - \dot{X}_{max}\,\Delta t$$

$$\Delta X_{DU} = \Delta X_{D/n-1}, \text{ if } \Delta X_{D\,min} \leq \Delta X_{D/n-1} \leq \Delta X_{D\,max}$$

$$= \Delta X_{D\,max}, \text{ if } \Delta X_{D/n-1} > \Delta X_{D\,max}$$

$$= \Delta X_{D\,min}, \text{ if } \Delta X_{D/n-1} < \Delta X_{D\,min}$$

$$\Delta X_{DU/n-1} = \Delta X_{DU}$$

c Airspeed Pitot Tube

From the error model presented for the pitot tube in Section IV B 5 , it can be seen that the final noise error in the sensed airspeed is always about ±3 knots at speeds greater than about 50 knots regardless of the magnitudes of the individual errors that make up this final noise error Below this speed, the final noise error increases due to the downwash effect of the rotors but its magnitude is primarily a function of forward airspeed As a result of this, the final noise error in the sensed forward airspeed is computed in the simulation. The equations used for this are

$$\Delta V_{a/N} = \sigma_{Va}\,\Delta V^*_{a/ND}, \quad V_a > 50 \text{ knots}$$

$$= \sigma_{Va}\left(1 + k_{\sigma/V}(50 - V_a)\right)\Delta V^*_{a/ND}, \quad V_a \leq 50 \text{ knots}$$

where σ_{Va} = standard deviation
$k_{\sigma/V}$ = effect of airspeed on standard deviation
$\Delta V^*_{a/ND}$ = normally distributed random number with zero mean and standard deviation of one

In the simulation this error is generated at a rate that approximates the 10 rad/sec filter shaping that is included in the error model

In addition, when the helicopter is at an angle of attack or sideslip angle, a bias error will exist in the sensed airspeed since the axis of the pitot tube will not be aligned with the velocity vector In the simulation, this bias error is computed as,

$$\Delta V_{a/B} = -0.5(1 - \cos\tau)\,V_a,$$

where τ = the total angle of incidence between the pitot tube axis and the velocity vector

These errors are then added to the computed airspeed to obtain the airspeed that is used in the flight control laws

$$V_{a/FC} = V_a + \Delta V_{a/N} + \Delta V_{a/B}$$

d Sideslip (β) Vane

From the error model that was developed for the "β" vane during the first quarter and presented in the first quarterly report, it can be seen that the final noise error in the sensed sideslip is always about ±0 25° for speeds greater than about 30 knots Since this covers the range over which it is planned to use the "β" vane in the flight control laws, the sideslip error in the simulation is represented simply by a normally distributed random number with a standard deviation of 0 25° Again, this error is generated at a rate that approximates the 62 rad/sec filter shaping that is included in the error model

4 Guidance and Flight Control Module

This section contains the guidance and flight control laws described in Section III These are mechanized in a form that is functionally identical to that presented in the Final Flight Control and Guidance Software documents and, therefore, will not be repeated here

5 Cockpit Module

A cockpit simulator is incorporated into the total simulation of the helicopter The cockpit panel display and control functions are patterned after the CH-46C helicopter

The cockpit simulator consists of three units, the cockpit, the electronic cabinet, and the hydraulic unit The cockpit stick and pedal controls have hydraulic force opposition There is pitch and roll trimming for the stick and yaw trimming for the pedals The hydraulic feel forces may be varied from the control panel of the electronic cabinet A collective stick is provided that has a controllable drag adjustment

The cockpit display layout is shown in Figure IV-18 The airspeed is shown in knots from -40 to +160 The heading indicator is in degrees from -180 to +180 The flight path angle is calibrated from +40 to -20 degrees The angle of attack meter also ranges from +40 to -20 degrees The attitude reference indicator will show +60 to -60 degrees of pitch and +60 to -60 degrees of bank The turn rate meter will show a maximum of 1 minute turn The vertical and horizontal bars of the indicator display command or velocity errors The scope display of the cockpit is used to display X, Y position by a variable positioned dot The altimeter is a standard aircraft instrument The vertical speed meter is scaled in feet per second

A push button control display is attached to the right side of the cockpit panel There are eight modes of operation selectable from the display. These are

1.	SAS	5	VEL 2
2	ATT 1	6	VEL 3
3.	ATT 2	7	AUTO
4	VEL 1	8.	LAND

A sidearm controller has been added to the cockpit for investigation of the velocity modes The sidearm controller is a NASA 3-axis unit obtained from Houston for another NASA program

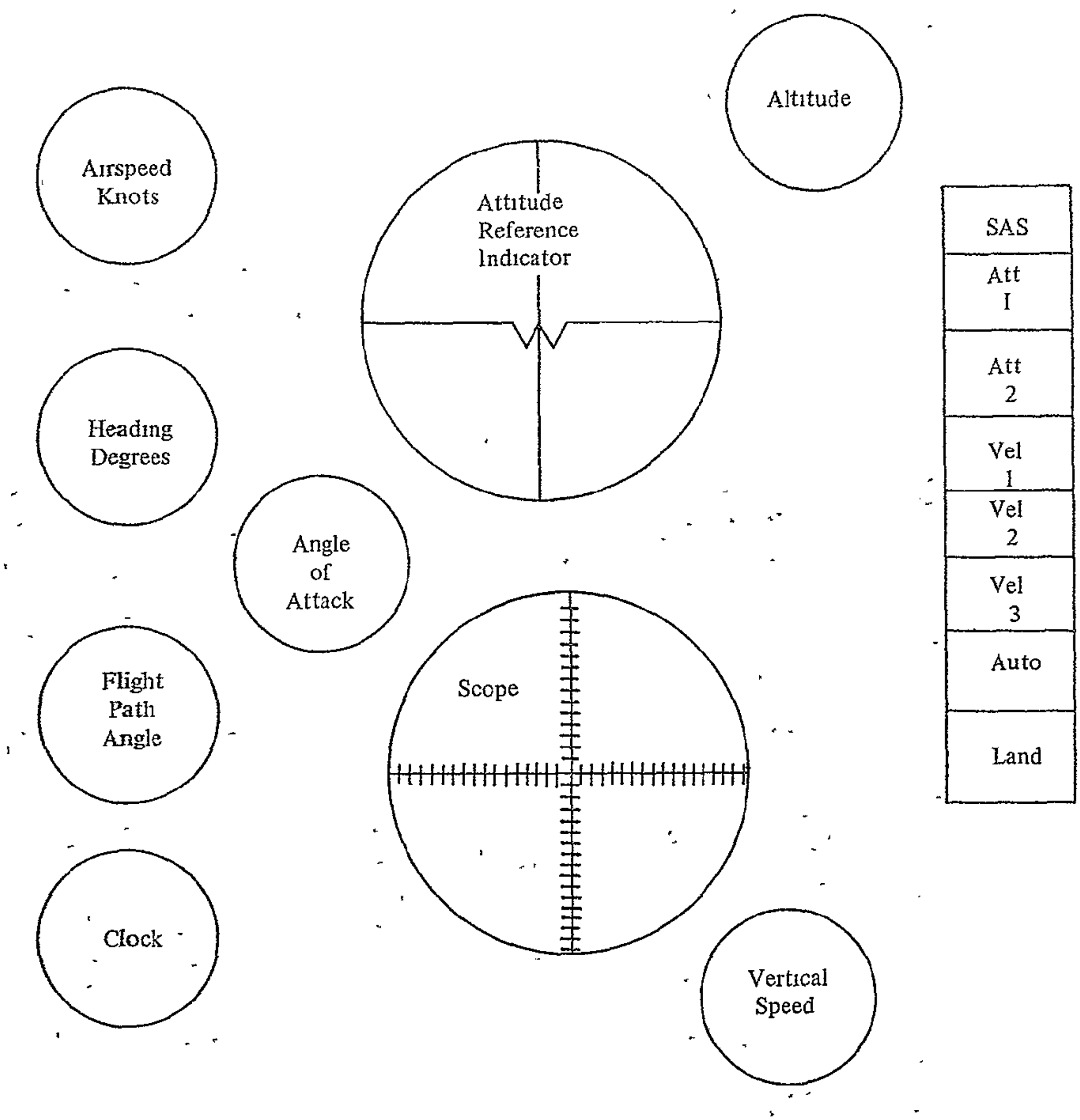

Figure IV-18 Cockpit Displays

V RESULTS OF EVALUATION

A GENERAL

The evaluation criteria used are discussed in Section III B 1 e After optimization of the pilot's controls sensitivities and the scaling of the FDI display, a test procedure was set up Table V-1 shows the initial conditions which were employed with all modes Table V-2 shows additional initial conditions used with the AUTO, VEL 1 and ATT 2 modes These modes were singled out for additional testing with 30 knot winds and the full amplitude of wind gusts (see Data Base in Section IV) because they were the most flyable modes

After indoctrination in the cockpit routine and instrumentation, and several familiarization runs by the pilot, any small discrepancies noted by the pilot were corrected, before the beginning of the final or "official" piloted runs

The pilot operated the simulator in each mode, subject to the initial offsets and wind conditions listed in Tables V-1 and 2 The profile of the fixed path, which the pilot was directed to fly is discussed in Section III C Each run was repeated twice and the results were averaged to obtain a numerical value of the Performance Index (PI), touchdown velocity ($\dot{Z}_{TD}$), forward velocity ($\dot{X}_{TD}$), lateral velocity (Y_{TD}) and radial error (R_{TD}) for the respective mode and initial condition After each run, the pilot numerically rated the handling qualities during the simulated flight, based on the Cooper rating scale discussed in Section III B 1 e A sample computer printout of initial conditions, the operational mode, landing conditions, and PI, obtained after each run, is shown in Figure V-1

The simulator was operated in the AUTO mode with the pilot in the seat During the preliminary optimizing, the pilot was directed to supply stick inputs during the AUTO runs, to evaluate the feasibility of pilot assists during AUTO landings This feature was deleted from the program, after it appeared that the PI was being degraded by pilot inputs and the philosophy was adopted that switching to a manual mode was preferable to mixing AUTO and manual inputs

B DATA COMPILED

Table V-3 lists the forward speed, $\dot{X}_{TD}$, lateral speed, Y_{TD}, sink rate, $\dot{Z}_{TD}$, radial offset error, R_{TD}, and the roll angle, ϕ, observed at touchdown Defining a good landing as $|X_{TD}| < 3$ ft/sec, $|\dot{Y}_{TD}| < 3$ ft/sec, $Z_{TD} < 5$ ft/sec (note 3 ft/sec was programmed desired value), $|\phi| < 2\,5°$, $R_{TD} < 30$ ft, Table V-3 shows

1 $|\dot{X}_{TD}| > 3$ ft/sec

one case	ATT 1	Condition 8
one case	SAS	Condition 8

2 $|Y_{TD}| > 3$ ft/sec

two cases	SAS	Condition 8, 14

(Continued on page V-5)

TABLE V-1
FLIGHT TEST CONDITIONS – ALL MODES

Run Number Condition	Initial Conditions		Winds		
	Y	ψ	Velocity (knots)	Direction	Gusts
1	0	0	0	0	No
2	0	0	0	0	Yes
3	0	0	15	0°	Yes
4	0	0	15	90°	Yes
5	0	0	15	180°	Yes
6	1000	0	0	0	No
7	1000	0	15	0°	Yes
8	1000	0	15	90°	Yes
9	1000	0	15	180°	Yes
10	0	30°	0	0	No
11	0	30°	0	0	Yes
12	0	30°	15	0°	Yes
13	0	30°	15	90°	Yes
14	0	30°	15	180°	Yes

TABLE V-2
ADDITIONAL FLIGHT TEST CONDITIONS – AUTO, VEL 1, AND ATT 2 MODES

Run Number Condition	Initial Conditions		Winds		
	Y	ψ	Velocity (knots)	Direction	Gusts
15	0	0	30	0°	Yes
16	0	0	30	90°	Yes

* *

INITIAL CONDITIONS

THETA	-	2.320	PHI	-	-0.000	PSI	-	0.067
P	-	0.000	Q	-	0.007	R	-	0.000
U	-	135.181	V	-	-0.159	W	-	5.463
UWIND	-	-0.177	VWIND	-	0.140	WWIND	-	-0.159
X	-	-10012.576	Y	-	0.000	Z	-	-443.001
XDOT	-	135.292	YDOT	-	0.000	ZDOT	-	-0.011

FLIGHT CONTROL MODE - SAS

LANDING CONDITIONS

TIME	-	158.066	RTIME	-	184.270			
THETA	-	9.492	PHI	-	-0.795	PSI	-	-5.953
P	-	0.425	Q	-	-2.423	R	-	0.474
U	-	0.124	V	-	-0.973	W	-	4.354
UWIND	-	-0.226	VWIND	-	0.177	WWIND	-	-0.171
X	-	-59.839	Y	-	-13.121	Z	-	-13.609
XDOT	-	0.750	YDOT	-	-0.989	ZDOT	-	4.291

PERFORMANCE INDEX - 0.0846

* *

Figure V-1 Sample Computer Output

TABLE V-3

TOUCHDOWN CONDITION DATA

Run Condition No	Mode	$\dot{X}_{TD}$ (ft/sec)	$\dot{Y}_{TD}$ (ft/sec)	Z_{TD} (ft/sec)	R_{TD} (ft)	ϕ (deg)
1	AUTO	0 94	0 01	3 89	17 1	0 14
	VEL 1	0 88	-0 025	2 85	9 4	0 07
	VEL 3	0 68	-0 11	3 12	15 4	-0 06
	ATT 2	-0 31	-0 88	1 15	3 2	-0 30
	ATT 1	0 96	-0 62	4 05	19 6	-1 89
	SAS	0 33	-0 25	4 00	16 5	-0 06
2	AUTO	1 5	0 03	3 88	16 63	0 04
	VEL 1	0 71	-0 63	2 9	17 0	0 17
	ATT 1	1 5	0 55	3 87	22 1	0 27
	SAS	1 01	-0 09	4 25	7 1	0 88
3	AUTO	0 80	0 02	3 11	8 46	0 07
	VEL 1	1 93	1 11	5 06	21 8	-0 42
	VEL 3	1.18	-1 0	2 25	9 96	0 37
	ATT 2	1 19	-0 25	3 25	13 08	0 09
	ATT 1	-0 50	-0 95	4 25	20 9	0 50
	SAS	-2 20	0 60	4 9	15 8	0 76
4	AUTO	1 29	0 02	2 68	21 2	0 04
	VEL 1	0 10	0 55	2 7	10 19	1 80
	VEL 3	0 72	-1 23	2 37	13 6	0 70
	ATT 2	0 28	-0 85	2 35	11 7	0 69
	ATT 1	1 42	1 04	2 9	14 05	1 00
	SAS	0 09	-2 33	4 63	18 8	0 07
5	AUTO	1 54	-0 7	3 69	6 6	-0 1
	VEL 1	0 5	-0 5	3 62	7 2	0 35
	VEL 3	0 35	-0 65	3 6	13 3	0 03
	ATT 2	0 64	-0 61	3 36	13 8	-0 35
	ATT 1	1 53	-0 33	4 4	9 7	0 18
	SAS	0 42	-0 45	4 7	9 04	0 29
6	AUTO	1 02	-0 03	4 0	30 6	-0 08
	VEL 1	0 40	0 39	2 75	17 9	-0 43
	VEL 3	0 09	-0 57	3 0	12 1	-0 10
	ATT 2	0 64	0 85	3 5	11 2	-0 17
	ATT 1	1 29	-0 02	3 9	18 1	0 0
	SAS	0 55	0 05	3 89	14 2	0 41
7	AUTO	1 02	-0 12	3 20	33 7	-0 10
	VEL 1	0 05	0 60	3 75	7 2	0 03
	VEL 3	0 71	0 24	3 9	14 3	-0 20
	ATT 2	1 62	0 35	3 84	11 8	0 10
	ATT 1	2 25	-0 15	4 63	18 0	-0 03
	SAS	0 94	-0 53	4 44	18 5	-0 81
8	AUTO	1 14	0 73	4 16	15 1	0 24
	VEL 1	0 95	1 04	4 25	13 9	1 08
	VEL 3	1.30	0 79	4 0	13 2	0 72
	ATT 2	0 91	1 38	3 4	12 1	1 22
	ATT 1	8 16	0 30	3 94	17 5	0 10
	SAS	-40 87	-22 48	3 23	53 7	-10 41
9	AUTO	1 07	-0 05	5 07	16 6	-0 15
	VEL 1	-0 81	-1 07	6 27	16 4	-0 97
	VEL 3	1 96	-0 31	5 12	3 3	[illegible]
	ATT 2	-0 40	-0 73	5 45	11 8	[illegible]
	ATT 1	0 97	-1 53	4 7	15 2	-1 46
	SAS	-1 20	-2 55	5 16	9 04	-0 54
10	AUTO	1 32	-0 01	4 09	17 39	-0 15
	VEL 1	1 63	-0 98	4 13	17 4	0 15
	VEL 3	1 22	-0 26	3 6	12 3	-0.07
	ATT 2	1 25	0 65	4 15	17 4	-0 13
	ATT 1	1 82	0 88	3 42	18 1	0 20
	SAS	1 74	0 13	3 46	20 4	-0 44
11	AUTO	1 26	-0 02	3 48	14 99	-0 06
	VEL 1	0 95	-0 49	3 5	11 5	0 46
	VEL 3	1 18	-0 28	3 52	13 9	0 13
	ATT 2	2 0	-0 06	3 9	16 6	0 17
	ATT 1	1 0	0 29	3 80	14 3	0 28
	SAS	1 33	0 16	4 34	11 2	0 73
12	AUTO	1 04	-0 13	3 05	14 32	0 25
	VEL 1	2 0	-0 53	3 61	18 1	0 18
	VEL 3	2.2	-0 50	3 49	6 94	0 12
	ATT 2	1 69	0 60	4 82	13 9	-0 08
	ATT 1	1 64	0 38	3 53	21 8	-0 23
	SAS	1 10	0 32	3 69	12 9	0 37
	VEL 2	0 50	-0 22	5 84	17 2	0 12
13	AUTO	1 67	-0 07	4 37	14 5	0 01
	VEL 1	1 02	0 31	3 63	15 5	1 05
	VEL 3	1 45	0 86	3 81	17 5	0 76
	ATT 2	0 98	0 21	3 59	17 44	0 63
	ATT 1	1 16	0 94	3 53	14 9	0 42
	SAS	1 39	0 22	3 77	18 4	0 66
	VEL 2	0 42	0 06	4 09	17 9	0 12
14	AUTO	1 05	0 07	4 23	17 04	0 06
	VEL 1	0 63	0 51	5 17	16 03	0 49
	VEL 3	1 46	0 33	2 20	17 6	0 18
	ATT 2	1 41	0 24	3 15	13 1	0 45
	ATT 1	2 01	-1 05	3 95	11 55	-0 48
	SAS	-2 09	3 77	5 68	15 5	0 32
15	AUTO	0 87	0 18	4 90	17 05	0 12
	VEL 1	1 13	0 65	3 80	10 68	-0 50
	ATT 2	1 93	-0 30	5 25	10 6	-0 22
16	AUTO	1 79	0 64	4 34	7 51	-0 39
	VEL 1	1 76	1 81	4 0	21 81	0 63
	ATT 2	-0 40	-2 13	5 7	18 5	2 34

3 $\dot{Z}_{TD} > 5$ ft/sec

one case	AUTO	Condition 9
three cases	VEL 1	Condition 3, 9, 14
one case	VEL 3	Condition 9
three cases	ATT 2	Condition 9, 15, 16
		(note 15, 16 are high gust, 30 knot winds)
one case	VEL 2	Condition 12

4 $|\phi| > 2.5°$

one case	SAS	Condition 8

5 $R_{TD} > 30$ ft

two cases	AUTO	Condition 6, 7
one case	SAS	Condition 8

In reviewing these failures, all were marginal failures within the given definition of a good landing, except ATT 1, Condition 8 where the forward speed was 8 2 ft/sec, VEL 1, Condition 9 where the sink speed was 6 3 ft/sec; and SAS Condition 8 which was very poor in almost all categories The two cases of AUTO landing slightly beyond 30 ft appear surprising and suggests a 14 foot system bias existed (see Table V-4)

Table V-3 has been reduced to show the essential statistics of the data Table V-4 shows the average value and the standard deviation (rms deviation from the average) of X_{TD}, Y_{TD} and Z_{TD} Reviewing this tends to confirm the belief that a system bias of 14 ft in X existed due to tolerances in forward speed for the LAND condition

Table V-5 lists the average and the rms value of the Performance Index (PI) under the various flight conditions and for the different modes

Review of the results shown in Tables V-3, 4, 5 indicates that the AUTO mode is best and SAS the poorest in terms of performance The pilot was capable of adapting to all modes and the performance criteria indicate little to choose between any of the manual modes except SAS SAS exhibited a tendency to get away from the pilot which was considered dangerous This point clearly showed up in the Cooper rating

Table V-6 lists the consensus Cooper rating for the modes The velocity modes which used the stick were preferred by the pilot with the ATT 2 mode following ATT 2, it should be remembered, is still a velocity control on the collective stick VEL 3 was the mode using the side arm controller and some problems were experienced The only available side arm controller was a bang-bang design with a relatively heavy spring load The pilot had to hold this off-center at an uncomfortable elbow angle for prolonged periods while the VEL 3 velocity trimming integrator caught up Though his performance was about as good as in the other velocity modes, the pilot's discomfort led him to give it a lower Cooper rating

TABLE V-4
MEAN TOUCHDOWN CONDITIONS

Mode	Run Conditions	X_{TD} (ft)		Y_{TD} (ft)		Z_{TD} (ft/sec)	
		avg	rms	avg	rms	avg	rms
AUTO	1-14	14 1	4 7	0 4	11 3	3 8	0 6
VEL 1	1-14	13 2	4 5	2 1	3 5	3 9	1 0
VEL 3	1-14	11 4	3 4	2 2	4 2	3 4	0 8
ATT 2	1-14	12 6	3 6	0 2	1 9	3 5	1 0
ATT 1	1-14	16 5	3 5	1 6	8 0	3 9	0 5
SAS	1-14	14 3	4 1	0 2	1 2	4 3	0 7
VEL 2	12-13	17 2	0.9	2 7	2 1	4 9	1 1
AUTO	15-16	6 0	1 4	7 7	8 9	4 6	0 2
VEL 1	15-16	16 2	5 6	1 7	0 2	3 9	0 1
ATT 2	15-16	14 5	3 9	0 1	0 3	5 4	0 2

TABLE V-5
PERFORMANCE INDEX MEANS

Mode	Run Conditions	PI avg	PI RMS
AUTO	1-14	0 04	0.01
VEL 1	1-14	0 08	0 03
VEL 3	1-14	0 09	0 04
ATT 2	1-14	0 09	0 07
ATT 1	1-14	0 09	0 06
SAS	1-14	0 12	0 05
VEL 2	12-13	0 09	0 03
AUTO	15-16	0 05	0 02
VEL 1	15-16	0 10	0 05
ATT 2	15-16	0 09	0 04

TABLE V-6

COOPER RATING

Mode	Rating
VEL 1	2
VEL 2	2
ATT 2	3
VEL 3	4
ATT 1	4
SAS	8

An observation with respect to the SAS mode must be noted Though the pilot managed to make numerous successful landings with SAS, his Cooper rating of the mode was very low and it was evident that the pilot work load was very high The success in achieving landings suggested that it might serve as a backup emergency mode This hypothesis was tested and is false The pilot's success depended on early adaption A number of tests were made where the pilot started in one of the other manual modes and the SAS mode was suddenly switched in The drastic change in work load (CR 2 to CR 8) resulted in an excessive readaptation time during which the pilot essentially lost the vehicle. It is concluded that SAS without attitude hold cannot be used as a backup mode

The data presented in Tables V-3 through V-6 tested the control system and the pilot's ability to follow the displays They were essentially performed with idealized sensors simulated The effect of errors was determined by 18 runs (2 each, 15 knot winds of Table V-1) in the AUTO mode with the sensor error models simulated This gives the additional errors which must be root-sum-squared with the previous numbers to obtain the composite system performance These are listed in Table V-7 The principal conclusion to be reached is that total performance is affected as follows

a Modified PI = $\sqrt{(PI)^2 + (0\ 08)^2}$
where PI is the "no instrumentation errors" PI
Note that in all cases the Modified PI is still very satisfactory

b Z_{TD} no change

c Total X_{TD} error will be almost entirely due to instrumentation and not pilot or FCS. Since this number is large (45 ft), the error model indicates more frequent update is required

d Total Y_{TD}, same comments as for c above but with a magnitude less than one-half as large

TABLE V-7

ERROR MODEL AUTO

PI avg	0 09	ft/sec
PI rms	0 02	ft/sec
Z_{TD} avg	3 8	ft/sec
Z_{TD} rms	0 62	ft/sec
X_{TD} avg	-45	ft
X_{TD} rms	10 5	ft
Y_{TD} avg	-19	ft
Y_{TD} rms	5	ft

Since the instrumentation error results are based on the error and update model, these results could have been easily modified to attain any degree of accuracy and, therefore, these results were simply used to determine the instrumentation accuracies required for FCS inputs

C SUMMARY OF EVALUATION CONCLUSIONS

1 Primitive SAS, defined as SAS with body rate feedback and no attitude hold, is not suitable as a flight mode or as a backup mode

2 The velocity modes are the best manual modes

3 The side arm controller required human factors engineering but did well enough to suggest that Conclusion 2 is valid

4 Attitude control, with altitude hold, and velocity control on the collective, is approximately equivalent to the velocity modes

5. Command displays are capable of enabling the pilot to fly the profile in any mode

6 The principal system error was excessive dispersion from the touchdown point due almost entirely to instrumentation errors This is readily corrected by increased update frequency and better blending algorithms and has no bearing on the FCS design

VI RECOMMENDATIONS FOR FUTURE STUDIES

A GENERAL

The development of the hybrid simulation has proven to be an excellent tool for the evaluation of guidance and control laws applicable to V/STOL type vehicles Results have been obtained, as has been discussed in previous sections of this report, which are now ready for further evaluation in forthcoming flight test programs To supplement these flight tests there are additional studies and analyses which can and should be performed which would take advantage of the available simulation and would provide continuing inputs for the tests with the CH-46C as well as inputs for flight test with other V/STOL's such as the X-22A and/or XC-142 These studies represent areas of investigation which are a logical extension of the work accomplished and/or areas where time did not permit full optimization under the present contract Conversely, the results of the flight test program should be used to upgrade the simulation to enhance its fidelity to the actual vehicle performance and, thereby, permit continued use of the simulator to evaluate new concepts The recommended studies are given below and discussed in the following subsections

- B. Approach Profiles
- C. Displays
- D. Computation Simplification
- E. Other Control Modes
- F. Simulation of Other V/STOL Vehicles
- G. Examination and Evaluation of Performance Criteria

B. APPROACH PROFILES

In the present contract a landing profile, as described in Section III C, was used to evaluate the guidance and control laws However, there may be other profiles which may be easier to fly, provide better obstacle clearance, with better fuel economy For example, the final portion of the present approach profile which calls for a hover at 50 ft prior to descent to the pad is very costly in fuel consumption to a V/STOL type of airframe such as the XC-142 or the X-22A Some of the other types of profiles which should be considered and evaluated are as follows

1. Fixed Glide Path to the Touchdown Point

For this type of glide path the aircraft flies level until glide slope intercept and then flies "down the glide slope" to touchdown Speed is reduced at a constant rate so as to attain zero ground velocity at touchdown. In the lateral plane, guidance would be provided as in the present system including turn into the wind The advantage of this profile is flying simplicity, economy of fuel, guidance law simplicity and guidance sensor simplicity Glide slopes in the range of 6° to 30° could be included in the investigation

2 Segmented Glide Path

As a modification to the above, a segmented glide path could be used wherein the vehicle would approach initially on a high glide in the range of 15-30° and then phase into a shallow glide path on the order of 6° to a touchdown This would have the advantage of good obstacle avoidance coupled with the good stability and ease of flying close to the ground associated with the shallower glide slope The range at which switchover occurs and the technique for smoothly changing glide slopes would be part of the investigation

3 Exponential or Recomputing Flight Path

The flight profiles described above are fixed in space with respect to the touchdown point Another type of profile which can be generated involves the recomputation of an exponential flight path to touchdown based on the vehicle's instantaneous states and the desired states at touchdown This could have the advantage of ease of flying in a turbulent or high wind shear environment

4 Modifications to Present Flight Profile

There are modifications to the present flight path which could be made to enhance overall performance These include increasing the glide slope from 6° to a higher value and decreasing the hover altitude from 50 ft to some lower value

It should be noted that some flight profiles may be more compatible with different flight control modes. Therefore, it may even be possible to optimize separately for each mode However, performance criteria in terms of such factors as pilot workload, fuel consumption and dispersion in vehicle state at touchdown under the constraints of turbulence and wind shear have to be established

C DISPLAYS

The cockpit simulation used an ARU-2B/A flight director indicator in conjunction with a cathode ray tube (CRT) situation presentation for the manual flying and monitoring modes This is essentially an extrapolation of what constitutes good control information from fixed wing experience Repeated simulation and flight tests are required to reveal shortcomings in display layouts or to the displayed information This could be quite time consuming On the other hand, the application of display theory which has been developed in recent years in conjunction with the hybrid simulation could lead to a more optimum arrangement

To obtain a good balance between pilot workload and precision, a compromise is required between purely director type or purely status type of displays Although directors have been shown to improve flying precision, there is also a strong requirement for status information The pilot needs this to assure himself that the primary system is working and for backup in case of director system failure Therefore, situation and director display arrangements which will provide information for efficient control while minimizing pilot's scanning workload need to be investigated The type of information and symbols to be used and methods for integrating situation and directors are included in the above

The scope of the study would include but not be limited to the following

(1) Detailed study of required display parameters
(2) Use of standard instruments supplemented with range-to-go information
(3) ILS display versus CRT
(4) Investigation of other types of flight directors including hovering flight director
(5) Perspective type of presentations and/or contact analog

It is recommended that the analytical theory of display/control systems be used to synthesize various arrangements as described above which are applicable to approach and landing and to utilize the cockpit simulation to evaluate pilot workload and performance

D COMPUTATION SIMPLIFICATION

The computation algorithms and sampling rates as presented in the software package have been shown to be satisfactory during the piloted simulation from a noise and display-flicker point of view To determine whether the computational requirements for the airborne digital computer can be further reduced it is recommended that studies be conducted in two areas

1 Sampling Rates

The SAS and attitude control laws use update rates of 32 times/sec while the attitude command, velocity command and velocity control laws use rates of 8 times/sec An investigation through additional analysis and simulation is suggested to determine whether the above rates can be substantially reduced without affecting control performance This is particularly the case for the manual modes Included in the above are the rates at which input variables are sampled, control and guidance laws computed, and rates at which data are outputted to the displays In particular, with regard to the display, there are other hardware techniques which can be utilized to reduce undesirable needle motion without imposing undue requirements on the digital computer The study would include all the various guidance and control modes

2. ISU Updating

A relatively simple updating and/or blending algorithm was utilized for the simulation There may be other algorithms which may be more efficient either from a computation point of view or, from an update frequency point of view It is desirable that updates be accomplished on an infrequent basis so that a sensor such as the GSN-5 could provide service to many vehicles on final approach It is, therefore, recommended that a detailed study consisting of both analysis and simulation to synthesize a more optimum filter be conducted The analysis would use digital-filter technology to formulate concepts for the update or blending filter These would then be compared using the hybrid simulation to select the best one

It is recognized that the update frequency and blending algorithms are heavily tied in with the error model of the ISU or its equivalent and these must be studied together

E OTHER CONTROL MODES

The present simulation has shown the inherent capability of the system to perform either manual or automatic approaches to a touchdown on a landing pad However, under the stress of an actual approach and landing in IFR conditions the pilot workload may be excessive for some of the manual modes To relieve this condition a technique called split-axis control can be employed In this situation the pilot manually controls one channel (such as pitch), while an automatic system or even the copilot controls the other The pilot's display scanning and control activity are essentially cut in half and his overall performance is expected to improve Such procedures are also beneficial from a flight safety point of view It permits the need for only limited pilot takeover when a partial failure of the automatic flight control has occurred

An important consideration in the use of automatic flight control during approach and landing is the question of pilot confidence and acceptance In a technique called "force wheel steering" the pilot is afforded the capability of introducing maneuvering command inputs into the autopilot in the coupled modes This technique is accomplished by generating signals as a function of pilot applied forces and by introducing these force signals into the outer loops of the flight control system This technique has been tested and evaluated by the Air Force for fixed wing aircraft with very promising results It permits the pilot to become an integral part of an automatic flight control system. The present study did not indicate any benefits from mixing pilot inputs with the automatic mode. The modifications required to enable a successful mix are recommended as a future study item

F. SIMULATION OF OTHER V/STOL VEHICLES

Although the guidance and control technology being developed is applicable to V/STOL vehicles, the present hybrid simulation was developed around the CH-46C parameters It is desirable to determine whether the guidance and control laws are applicable with minor modifications to V/STOL vehicles- It is, therefore, recommended that a study be performed to design a computer model such that the characteristics of the various V/STOL airframes can be switched from one to another and to determine whether the present hybrid simulation can be modified to accommodate this computer mode This would essentially give the hybrid simulation a Variable Stability System capability Quick comparisons of vehicle types under automatic or manual flight control can then easily be made Such a system would compliment the flight test programs of such VSS aircraft as the X-22A

G. EXAMINATION OF EVALUATION AND PERFORMANCE CRITERIA

As discussed in Section III B and demonstrated in Section V, the specification of performance criteria is, to a large extent, an art This is particularly true of pilot opinion A mathematical model combining performance and pilot opinion is required Idealy a combination of the two with a model of the "standard" pilot is desired. In this way a large number of runs could be made in evaluating systems by simulator and arriving closer to the optimum before actually introducing a pilot to the program